NASA CR-54333
AVCO RAD SR 65-44

SECOND QUARTERLY PROGRESS REPORT

RESISTOJET RESEARCH AND DEVELOPMENT - PHASE II

by

Richard R. John and Dean Morgan

prepared for

NATIONAL AERONAUTICS AND SPACE ADMINISTRATION

January 20, 1965

CONTRACT NAS 3-5908

Technical Management
NASA Lewis Research Center
Cleveland, Ohio
Electric Propulsion Office
Henry Hunczak

RESEARCH AND ADVANCED DEVELOPMENT DIVISION
AVCO CORPORATION
Wilmington, Massachusetts

NASA CR-54333
AVCO RAD SR 65-44

SECOND QUARTERLY PROGRESS REPORT

RESISTOJET RESEARCH AND DEVELOPMENT - PHASE II

by

Richard R. John and Dean Morgan

prepared for

NATIONAL AERONAUTICS AND SPACE ADMINISTRATION

January 20, 1965

CONTRACT NAS 3-5908

Technical Management
NASA Lewis Research Center
Cleveland, Ohio
Electric Propulsion Office
Henry Hunczak

RESEARCH AND ADVANCED DEVELOPMENT DIVISION
AVCO CORPORATION
Wilmington, Massachusetts

NOTICE

This report was prepared as an account of Government sponsored work. Neither the United States, nor the National Aeronautics and Space Administration (NASA), nor any person acting on behalf of NASA:

A.) Makes any warranty or representation, expressed or implied, with respect to the accuracy, completeness, or usefulness of the information contained in this report, or that the use of any information, apparatus, method, or process disclosed in this report may not infringe privately owned rights; or

B.) Assumes any liabilities with respect to the use of, or for damages resulting from the use of any information, apparatus, method or process disclosed in this report.

As used above, "person acting on behalf of NASA" includes any employee or contractor of NASA, or employee of such contractor, to the extent that such employee or contractor of NASA, or employee of such contractor prepares, disseminates, or provides access to, any information pursuant to his employment or contract with NASA, or his employment with such contractor.

Requests for copies of this report should be referred to

National Aeronautics and Space Administration
Office of Scientific and Technical Information
Attention: AFSS-A
Washington, D.C. 20546

ABSTRACT

19265

Experimental results are presented on the transient propulsion performance of a 10 watt fast heat-up resistojet which operates in the thrust range of from 100 to 500 micropounds. The resistojet consists of a thin-wall tubular heating element with a 5 mil throat diameter exit nozzle. Engine performance data have been obtained with a direct force measurement thrust stand. A single axis resistojet attitude control system to be evaluated on the air bearing test bed at the NASA, Lewis Electric Propulsion Test Facility is described. The resistojet ACS contains an ammonia propellant feed system, control logic and power conditioning test packages, a position sensor, and three nominal 10 watt resistojet engines. Two of the engines are for attitude control and one of the engines is for station keeping. The resistojet ACS has been completely fabricated and will be evaluated at NASA, Lewis during the next quarter.

AUTHOR

CONTENTS (Cont'd)

CONTENTS

ILLUSTRATIONS

CONTENTS (Concl'd)

ILLUSTRATIONS (Cont'd)

ILLUSTRATIONS (Cont'd)

ILLUSTRATIONS (Concl'd)

TABLES

SUMMARY

The overall objective of this program is to carry out research and development on both pulsed and continuous resistojet thrustors for operation from 5 to 5000 watts. Work is currently being concentrated on the development of 5 to 50 watt thrustors suitable for the attitude and orbit control of satellites in the 500 to 1000 pound class.

During the past quarter program emphasis has been directed to the development of a fast heat-up resistojet thrustor for operation with ammonia in the thrust range from 10^{-4} to 10^{-3} lbs, and to the development of a single axis resistojet attitude control system (ACS) for evaluation on the air bearing at the NASA, Lewis Electric Propulsion Test Facility.

Engine performance data has been obtained with a direct force measurement thrust stand for both cold and hot engines. The fast heat-up resistojet engine was operated with a propellant feed system such that the propellant flow was choked across the exit nozzle throat. As energy is added to the gas flow, the engine chamber pressure and thus the thrust remains essentially constant, and the propellant flow rate is decreased. Preliminary results obtained using a 20 mil diameter molybdenum heater indicate that at the 3×10^{-4} lb thrust level the engine specific impulse could be more than doubled (70 to 150 seconds) with less than 15 watts input power. A vapor deposited tungsten engine was thermally cycled 40,000 times without failure. The fast heat-up resistojet thus continues to hold considerable promise for attitude and orbit control of satellites in the 500 to 1000 lb class.

A single axis resistojet attitude control and station keeping system has been designed, developed and constructed for evaluation on the air bearing attitude control system test bed located at the NASA, Lewis Electric Propulsion Test Facility. The air bearing attitude control system test bed has a moment of inertia about the vertical axis of about 30 slug-ft^2. The test bed is completely isolated from the laboratory and is self-contained. Power is supplied by on-board batteries, and communication from the test bed will be accomplished by means of a telemetry system. The overall purpose of the initial resistojet ACS test will be to hold the test bed to $\pm$ 0.5 degree for extended time periods, and thereby demonstrate the feasibility of the resistojet concept for application to an ACS.

The single axis resistojet attitude control system contains an ammonia feed system, control logic package, power conditioning package and a position sensor. The system contains three 10 watt fast heat-up resistojet engines; two of the engines will be required for attitude control and one for possible station keeping applications. The system contains 8 input command channels and 24 output information channels. The control logic circuitry contains an electronic network for estimating vehicle angular rate from the angular position output of the sensor;

the control logic is therefore based on both vehicle angular position and angular rate. The resistojet ACS will be evaluated at the NASA, Lewis Electric Propulsion Test Facility during the next quarter.

I. INTRODUCTION

This is the second Quarterly Progress Report submitted under contract NAS 3-5908, entitled Resistojet Research and Development - Phase II. This report covers the period 1 October 1964 through 31 December 1964.

A. PROGRAM OBJECTIVES

The overall objectives of this program are to pursue research and development of electrothermal thrustors of the resistance type in the power range from 5 watts to 5 kilowatts. Both pulsed and continuous operation of the thrustor are to be explored. During the second quarter attention has continued to be focused on resistojets operating in the 5 to 50 watt input power level. The possible application of the low power, fast heat-up, resistojet to the attitude control and station keeping of a nominal 500-pound synchronous satellite is being explored. A laboratory single axis resistojet attitude control system (ACS) has been designed, developed and constructed. The resistojet attitude control system includes breadboard propellant feed, power conditioning, control logic, sensor and engine packages. The objective of this phase of the program is to demonstrate the feasibility of a resistojet ACS on the air bearing facility at the NASA Lewis Research Center.

B. PROGRAM ORGANIZATION

This program originates from the Electric Propulsion Office of the NASA Lewis Research Center. Mr. Henry Hunczak is Project Manager for the NASA Lewis Reserach Center. The Project Director at Avco RAD is Dr. R. R. John. Other participants in this research and their areas of principle contribution are: Drs. S. Bennett, A. Tuchman, and D. Morgan and Mr. W. Huss, Thrustor and Test System Design and Development; Mr. C. Stewart, Thrustor Heat Transfer; Mr. J. T. Smith, Materials Development; Messrs. R. Coulombre, P. Bergstrom, and J. Vullo, System Design for the single axis tests.

C. PROGRAM SCHEDULING

This is the second Quarterly Progress Report, and summarizes technical progress under contract NAS 3-5908. Data on contract costs and manpower have been previously submitted in Monthly Letter Reports 4 (10 November), 5 (10 December) and 6 (10 January).

A paper resulting from this program entitled, 'Experimental Propulsion Performance of a Low Power Pulsed Resistojet' by S. Bennett, W. Huss, R. R. John, and A. Tuchman, was presented at the AIAA 2nd Aerospace Sciences Meeting held in New York, January 25-27, 1965.

II. RESISTOJET ENGINE DEVELOPMENT

A. INTRODUCTION AND BACKGROUND

Considerable interest has recently been shown in the application of electric propulsion to the attitude control and station keeping of earth satellites.[1-4] Systems considered have included the full range of electric thrustors from the relatively low specific impulse electrothermal engines[1,2] to the high specific impulse ion engines.[3,4] The simplest of the electric thrustors is the resistojet. In this device electrical energy is transferred to thermal energy by passage of the working fluid over an electric heating element; the thermal energy is, in turn, converted into kinetic energy by expansion of the heated working fluid through a conventional nozzle. Experimental results have been presented in the literature[5,6] on the performance of continuous flow resistojets which operate in the power range from 1 to 25 kilowatts and which have direct application to the primary propulsion of space vehicles, e.g. satellite raising. It is the purpose of the present study to obtain experimental data on the performance of pulsed resistojets which operate in the power range from 5 to 50 watts and which have direct application to orbit and attitude control of earth satellites and other space vehicles.

There are two basic concepts for the pulsed, low power resistojet thrustor[7]. These are thermal storage and fast heat-up. Schematic diagrams of the two thrustor types are shown in figure 1.

The thermal storage pulsed resistojet consists of a refractory heater element with a high heat capacity. Power is continuously supplied to the heater element and only the propellant flow is pulsed. The heat capacity of the thermal storage unit is sufficiently great that the temperature of the heater element remains essentially constant during short propellant pulses. The advantages of the thermal storage concept include no thermal cycling, minimum time delay between the input signal and resulting impulse bit, and constant power input which reduces system complexity. A complete satellite attitude control and station keeping system will probably contain ten or more engines. If the engines are thermal storage resistojets they will all have to be continuously supplied with electrical energy. The main disadvantage of the thermal storage engine for attitude control and station keeping is thus the high average system power consumption and the resulting large system weight[7].

The fast heat-up resistojet consists of a light-weight heater element with a low thermal heat capacity. The heater element of the typical fast heat-up engine shown in figure 1 consists of a thin-walled high temperature metal tube with an integral exit nozzle. The working fluid passes through the electrically-heated tube and out of the engine through the exit nozzle. In the fast heat-up thrustor both the power and propellant flow are pulsed. In contrast to the thermal storage device the heat capacity of the fast heat-up unit is held to a minimum.

The primary advantage of the fast heat-up engine is that the input electric power does not have to be supplied continuously, and thus there is a relatively low average system power consumption. Disadvantages include the necessity for thermal cycling and the existence of a delay time between the input signal and the time at which the thrustor is at operating temperature.

During the first quarter of the present program[7] experiments and preliminary systems analysis were carried out on both the thermal storage and fast heat-up units at power levels from 5 to 50 watts. The average power level for an attitude control and station keeping for a 500 pound was estimated to be nearly an order of magnitude lower for a system based on the fast heat-up resistojet concept than for a system based on the thermal storage concept. Based on these results attention during the past quarter has been directed to the design and development of a fast heat-up resistojet thrustor.

The discussion of resistojet engine development is divided into the following sections:

1. Measurement of Engine Propulsion Performance
2. Description of Experimental Fast Heat-Up Resistojet Thrustor
3. Heater Performance
4. Engine Propulsion Performance

B. MEASUREMENT OF ENGINE PROPULSION PERFORMANCE

1. Thrust Measurement

A critical tool for the determination of thrustor performance is a thrust stand for the accurate determination of the engine thrust versus time response. For the experiments presently in progress the thrust stand must have a lower sensitivity limit of about 10 micropounds (or about 5 dynes).

The thrust stand designed for this application[7] is based on a simple wire-in-tension technique and is shown in figure 2. The engine system horizontal mounting plate is supported by four wires in tension. The wires are, in turn, connected to a heavy surrounding aluminum ring which is itself shock mounted by means of long springs. The engine thrust axis is vertical.

Application of thrust by the engine results in a motion of the horizontal mounting plate with respect to the aluminum ring until a displacement is reached such that the vertical component of tension in the four supporting wires provides a restoring force equal to the thrust. The displacement is directly measured by a linear differential transducer. During the past

A. THERMAL STORAGE RESISTOJET THRUSTOR

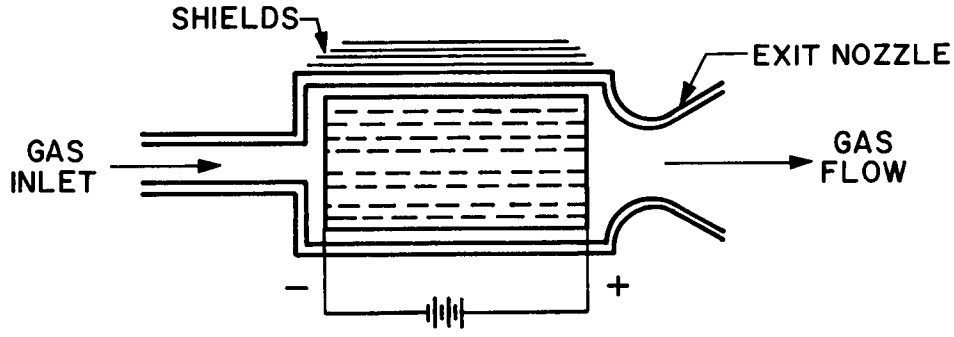

CHARACTERISTICS

(1) CONTINUOUS POWER
(2) HIGH THERMAL STORAGE CAPACITY
(3) HIGH AVERAGE SYSTEM POWER CONSUMPTION

B. FAST HEATUP RESISTOJET THRUSTOR

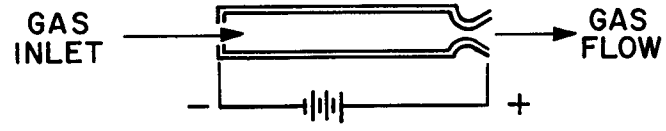

CHARACTERISTICS

(1) PULSED POWER
(2) LOW THERMAL STORAGE CAPACITY
(3) LOW AVERAGE SYSTEM POWER CONSUMPTION

65-1192

Figure 1 PULSED RESISTOJET CONCEPTS

quarter the original displacement transducer (Sanborn 581-25-1) which had a minimum displacement capability of 3×10^{-7} inches was replaced with a transducer with a minimum displacement capability of 10^{-7} inches. Static calibration is performed by adding weights to the horizontal mounting plate.

The thrust stand motion is easily analyzed by analogy with a mass-loaded string[7], yielding the results

$$F \alpha \frac{yT}{L} \tag{1}$$

where F is the applied thrust, L the length of a support wire, T the tension in a support wire, and y the measured displacement, and,

$$\nu \alpha \sqrt{\frac{T}{ML}} \tag{2}$$

where ν is the natural frequency of oscillation of the thrust stand and M is the mass of the engine system and the horizontal mounting plate.

As the tension-to-length ratio in the support wires is increased, the natural frequency of the thrust stand rises; however, a larger thrust is required to produce a given thrust stand displacement. The natural frequency of oscillation of the thrust stand decreases with increase in mass of the engine system. The relation between minimum measurable thrust and thrust stand natural frequency is shown in figure 3 for a minimum measurable displacement of 10^{-7} inches and a thrust stand system weight of 2 pounds.

The noise level currently observed is of the order of 50 micropounds so that thrust measurements down to 100 micropounds are reliable. Efforts are presently underway to improve the thrust stand mounting and it is anticipated that the lower sensitivity limit of the stand can be reduced to 10 micropounds. The present thrust stand basically has an open-loop displacement measurement system; preliminary investigations are underway on the potential advantages which might accrue to a closed loop system.

A typical thrust-time oscilloscope trace is shown in figure 4. The thrust pulse is of one second duration and 900 micropounds amplitude. The background noise for this particular trace is about plus or minus 100 micropounds; as indicated above, this value has recently been reduced to plus or minus 50 micropounds and further improvements are anticipated. The pulse rise and fall times are substantially less than 0.10 second so that the thrust pulse for this particular trace is essentially square.

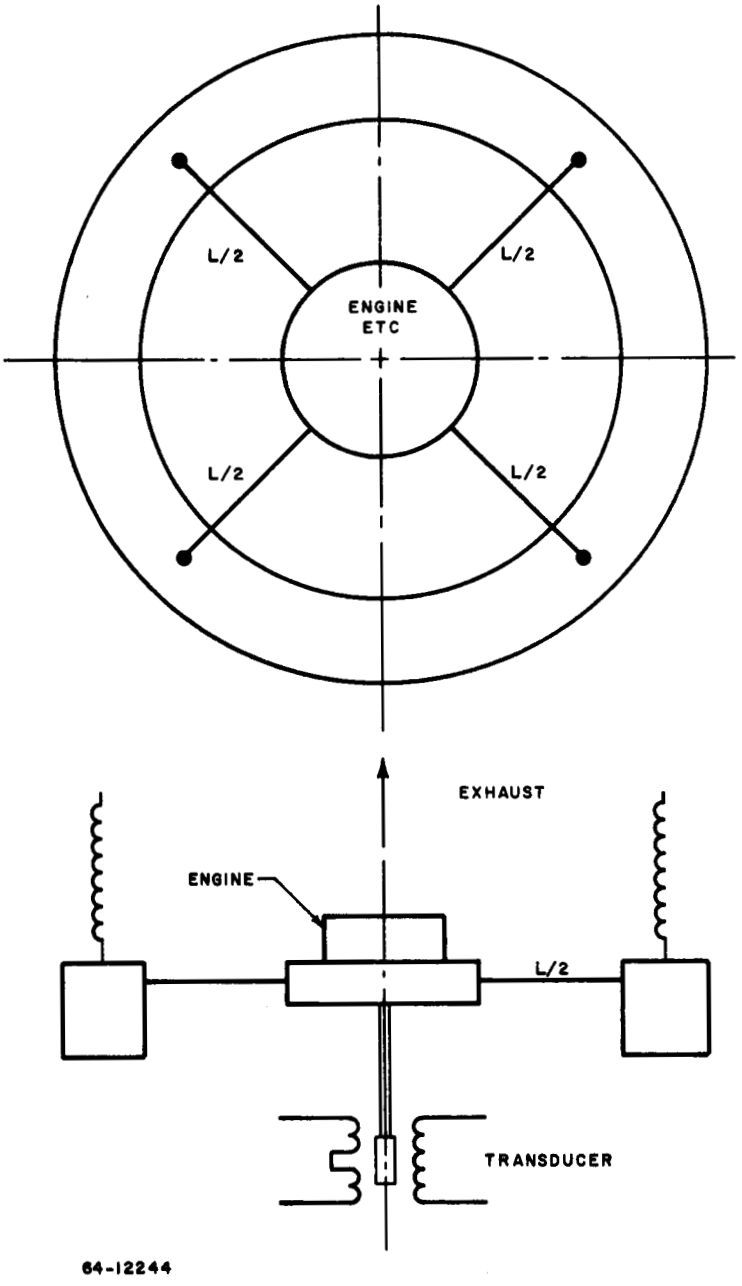

Figure 2 WIRE-IN TENSION THRUST STAND

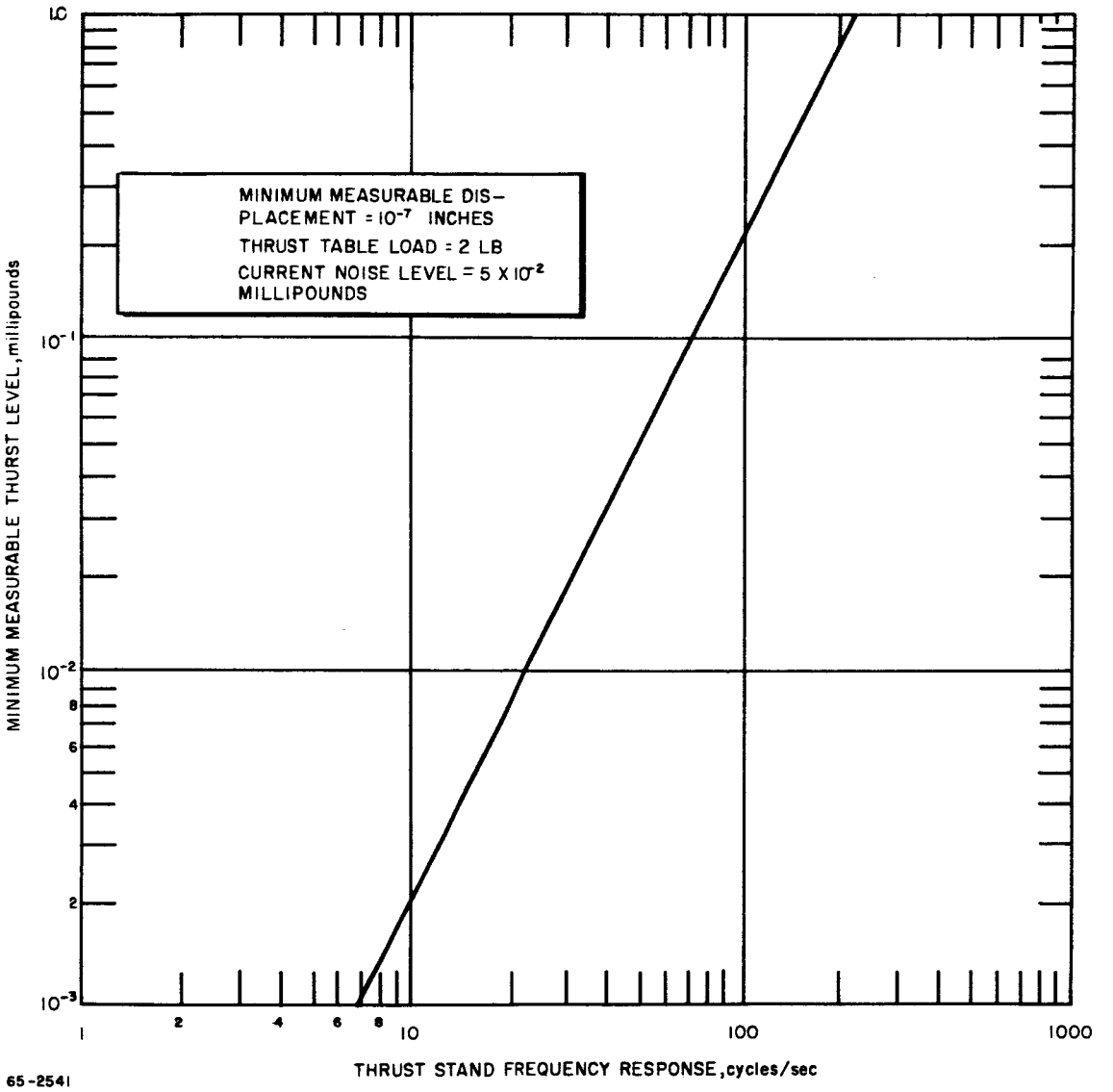

Figure 3 MINIMUM MEASURABLE THRUST LEVEL VERSUS THRUST STAND FREQUENCY RESPONSE

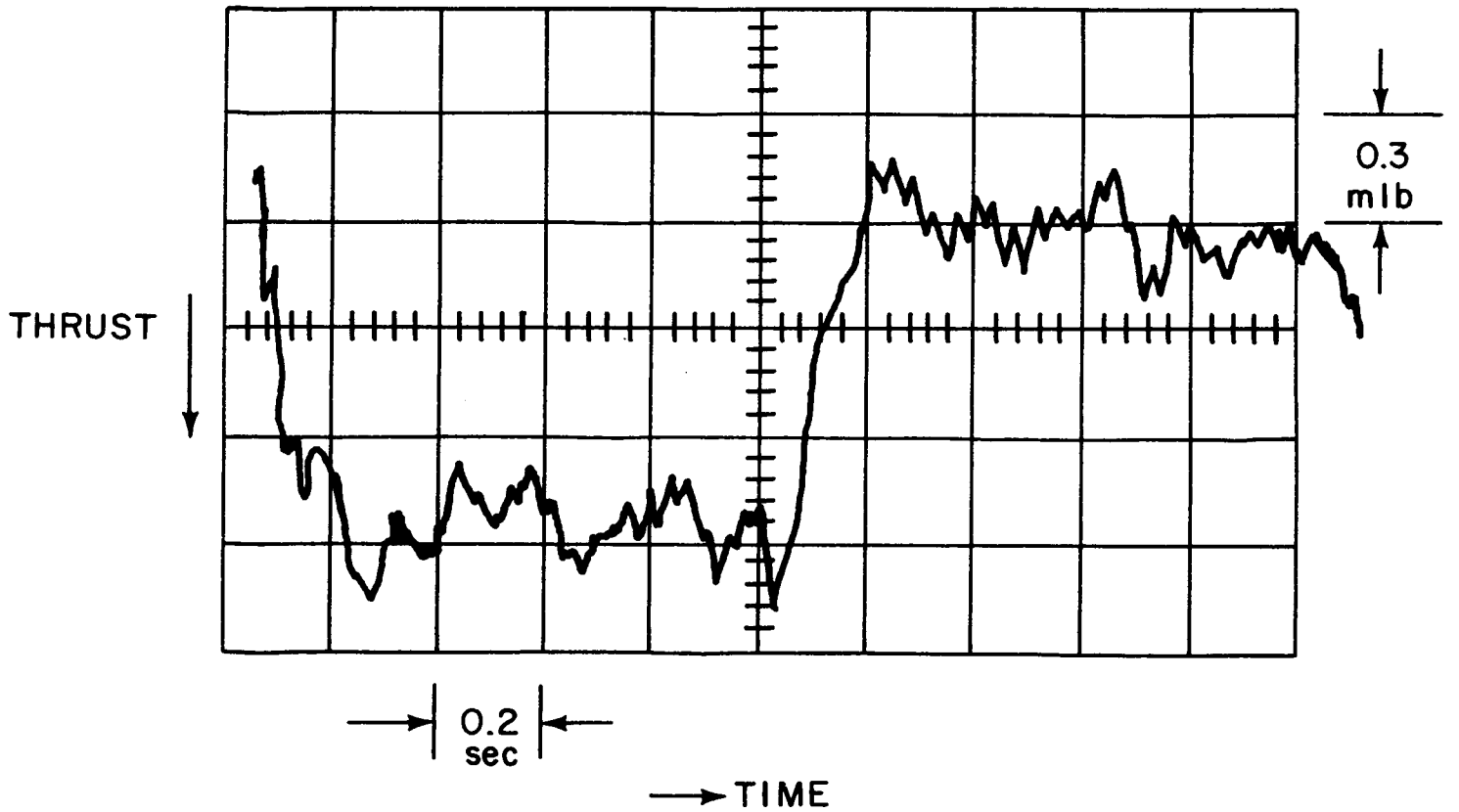

Figure 4 THRUST VERSUS TIME OSCILLOSCOPE TRACE

2. Mass Flow and Power Input Measurement

The propellant mass flow through the engine is of the order of 1 to 10 micro-lb/sec. The mass flow is measured using a differential pressure transducer and a low pressure drop orifice located upstream of the resistojet engine. See figure 7. The technique which has been used to calibrate the orifice is based on measuring the pressure rise in a known volume. The bell jar containing the thrustor and thrust measurement system is evacuated to about 1 micron and then isolated from the pump. Propellant is allowed to flow for a period of time usually chosen as 100 seconds. The pressure in the bell jar is measured and the known bell jar volume, pressure rise, and flow time are used to determine the mass flow rate. Typically the pressure rise is of the order of several hundred to several thousand microns and thus readily measured.

Engine electrical input power is obtained as direct current from a set of storage batteries. Current and voltage are measured with precision meters. Control is obtained by means of a rheostat.

C. DESCRIPTION OF THE EXPERIMENTAL FAST HEAT-UP RESISTOJET THRUSTOR

1. Engine Configuration

A schematic of an experimental fast heat-up thrustor configuration of the type which will be used in the single axis air bearing test at NASA, Lewis is shown in figure 5, and a photograph of the unit is presented in figure 6. The prototype engine consists of a solenoid type gas valve, a pressure transducer, a heating element, and an exit nozzle. The heating element is surrounded by a concentric support tube; the support tube is electrically connected to the nozzle end of the heater element through four support tabs. The support tube is, in turn, separated from the main engine body by an electric insulator. The engine power connections are located respectively on the heater support tube and on the main engine body.

2. Engine Propellant Feed System

A schematic of the propellant feed system is shown in figure 7. The resistojet gas inlet, located upstream of the solenoid gas valve, is connected to a constant pressure or essentially infinite gas reservoir. Referring to figure 7 in the case of a propellant which can be stored as a liquid e. g. ammonia, the reservoir tank pressure is held at a constant value by means of the pressure regulator located between the liquid and gaseous ammonia reservoirs. The liquid reservoir could, of course, easily be replaced by a gas or subliming solid reservoir. During a typical run the power is turned on and the heater element is brought up to temperature; after the element has been brought to temperature and while the power is still

on , the propellant valve is opened and the propellant is heated as it passes through the tubular heater element and out through the exit nozzle.

It is important to distinguish between the flow system shown in figure 7 and the flow system shown in figure 8. The system in figure 8 was used in the initial heater experiments described in the first quarterly report[7].

In the initial heater experiments, which were carried out with the flow system shown in figure 8, the propellant flow was choked across the flow metering orifice. The pressure upstream of the flow metering orifice and the area of the flow metering orifice were such that the propellant flow rate was independent of the energy added downstream of the critical flow orifice. Energy addition in the heater tube thus results in an increase in engine chamber pressure and thrust level but the flow rate remains unchanged. The pressure build-up time in this system was found to be excessive; further, and probably more important, the thrust level varied markedly during a typical power-on pulse.

In the flow system shown in figure 7 the propellant flow was choked across the exit nozzle throat; the metering orifice area was larger than the exit nozzle area. In this case, the engine chamber pressure was constant and the mass flow variable as energy was added to the gas passing through the tubular heat exchanger. Thus, for the constant chamber pressure case, the addition of energy to the gas flowing through the heater has the same effect on the propellant flow rate as would be obtained by reducing the nozzle throat area. For this mode of operation the thrust level remains essentially constant and the mass flow is reduced as energy is added to the gas stream.

3. Engine-Heat-Up and Electrical Characteristics

An important parameter in the design of the fast heat-up resistojet is the response time of the heater element or the time that the heater element requires to come to operating temperature. The response time of the heater element can be obtained from an expression of the form $\tau_{heatup} = M C_p \Delta T / P_{input}$ where M is the mass of the heater element, C_p is the specific heat of the heater material, ΔT is the required temperature rise, and P_{input} is the input power. A heat-up time of the order of 1 second is required to hold the power-on duty cycle for the individual engines in a 500 pound satellite resistojet attitude control system to about 5 percent[7]. Assuming a ΔT of 1000 °K, specific heat of 0.10 cal/ °C gm, and a power input of 10 watts or 2.4 cal/sec the required thrustor mass is of the order of $M = \tau_{heatup} P_{input} / C_p \Delta T$ = (1 sec) (2.4 cal/sec) / (0.10 cal/ °C gm) (1000 °K) = 24×10^{-3} grams. Thus, the required thrustor mass for a fast heat-up resistojet at the 10 watt power level is of the order of tens of milligrams.

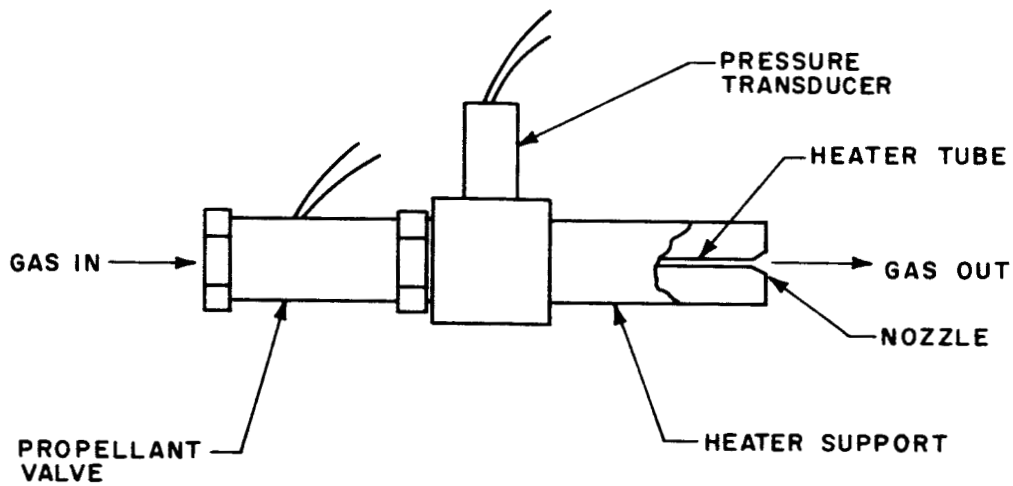

65-2542

Figure 5 SCHEMATIC OF AN EXPERIMENTAL FAST HEAT-UP THRUSTOR CONFIGURATION

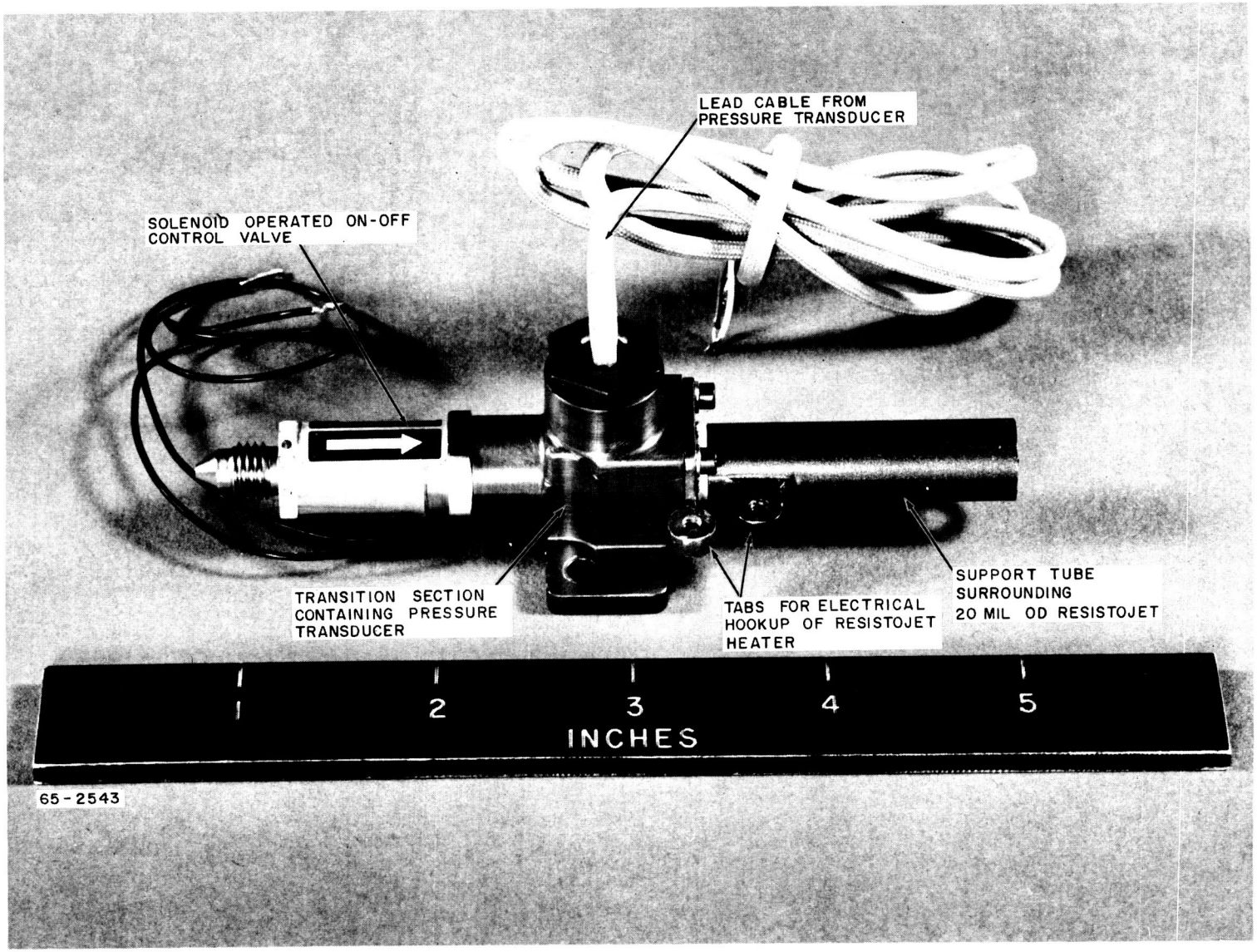

Figure 6 PHOTOGRAPH OF AN EXPERIMENTAL FAST HEAT-UP THRUSTOR

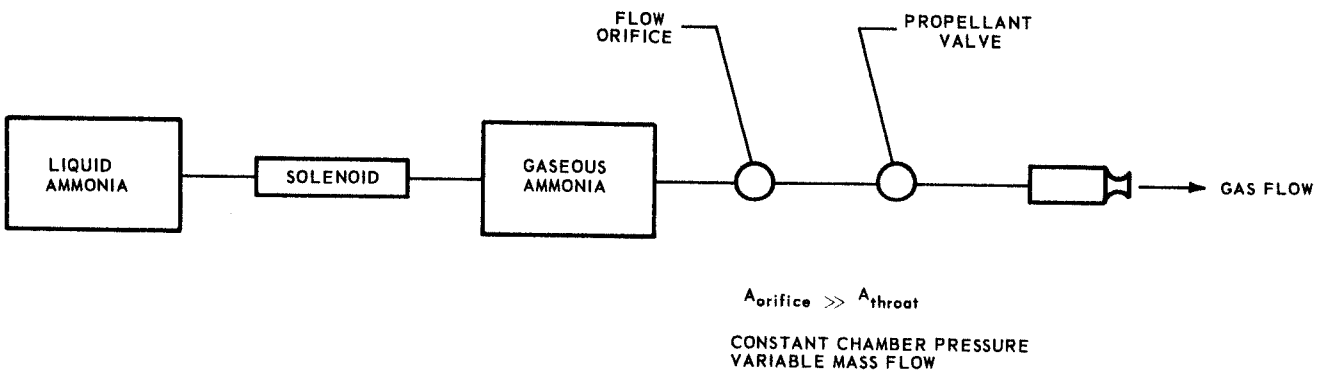

Figure 7 SCHEMATIC DIAGRAM OF A CONSTANT PRESSURE VARIABLE MASS FLOW PROPELLANT FEED SYSTEM

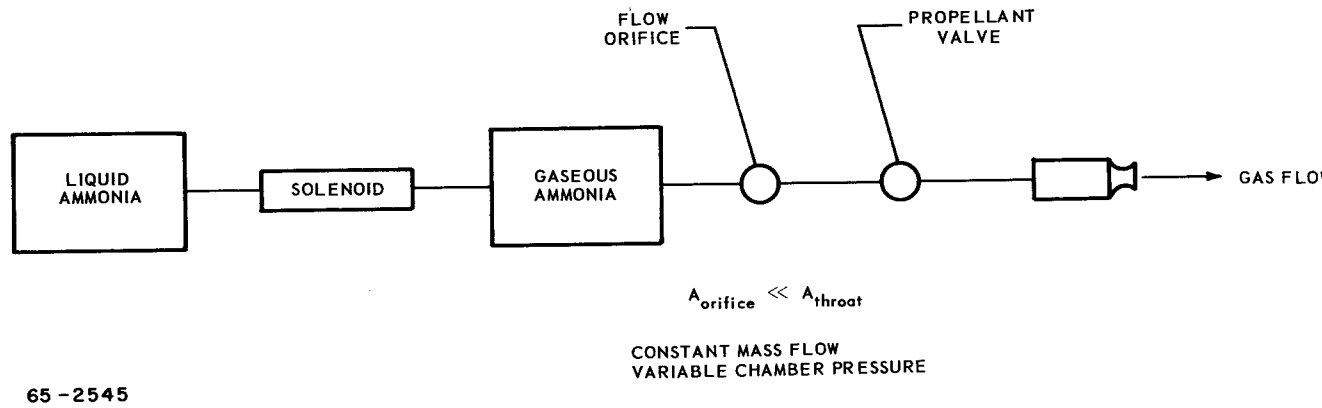

Figure 8 SCHEMATIC DIAGRAM OF A CONSTANT MASS FLOW VARIABLE PRESSURE PROPELLANT FEED SYSTEM

The need for keeping the thrustor mass to a minimum is further emphasized by the results on heater resistance presented in table I. Estimates are presented of the cold and hot resistances of a typical resistojet. The resistances in this table are based on a heater tube length of 1 inch and an inside diameter of 14 mils with wall thickness as given. It is noted that the heater resistance level is relatively low (order of 0.10 to 1 ohm) and that the cold resistance is significantly lower than the hot resistance. Further the ratio of hot to cold resistance is strikingly sensitive to heater material varying from nearly 15 to 1 for tungsten to only 2 to 1 for stainless steel. The combination of low resistance and wide variation in resistance between hot and cold flow must be integrated with the power conditioning equipment. This area is currently under investigation. Clearly, however, the resistance of the engine connections must be held to a minimum and the output of the power conditioner must be closer to constant power rather than constant current.

4. Propellant Selection

Initial program emphasis has been on ammonia as the working fluid because of potential ease of storage for long duration missions. It is to be stressed, however, that the only real limitation on working fluid selection is that the working fluid be compatible with the heater material. Other propellants can be used equally well as resistojet propellants. Table II presents the results of thermochemical calculations on the idealized frozen flow performance of a series of potential low molecular weight propellants.

5. Fast Heat-Up Resistojet Operating Variables

To summarize, for constant pressure (variable mass flow) operation, and a fixed configuration, there are five basic operating variables: a) Engine reservoir pressure; b) Engine power input; c) Engine heat-up time; d) Engine solenoid valve on-time; and e) Propellant.

The engine reservoir pressure is fixed by the setting on the regulator located between the main propellant supply and the gas reservoir upstream of the engine. In the case of liquid propellant storage the gas reservoir pressure must, of course, be a value less than the vapor pressure of the propellant at the nominal propellant supply temperature. For storage of the propellant as a solid the gas reservoir tank and regulator can, in some cases, be eliminated and the engine connected directly to the supply tank. The engine thrust level is directly proportional to the gas reservoir pressure level, and thus variation of engine reservoir pressure permits a direct control over engine thrust level.

The engine power input, to a first order, permits control over the propellant flow rate at constant engine thrust level. Increase in the engine power input increases the temperature of the gas flowing through the engine;

TABLE I

RESISTANCE OF TYPICAL RESISTOJET

(t = wall thickness, I. D. = 14 mils, length = 1 inch)

Resistance in Ohms

A. Cold Resistance (20°C)

Material	t = 7 mils	t = 3 mils	t = 1 mil
Tungsten	0.0047	0.014	0.046
Tungsten -26% Rhenium	0.027	0.076	0.26
Rhenium	0.017	0.048	0.16
Molybdenum	0.0049	0.014	0.048
Stainless Steel	0.041 - 0.066	0.12 - 0.18	0.40 - 0.63

B. Hot Resistance for Uniform Temperature

Material	Maximum Operating Temp., °C	t = 7 mils	t = 3 mils	t = 1 mil
Tungsten	2500	0.068	0.20	0.68
Tungsten -26% Rhenium	2300	0.082	0.24	0.82
Rhenium	2300	0.094	0.27	0.91
Molybdenum	1950	0.059	0.17	0.58
Stainless Steel	1100	0.099 - 0.12	0.29 - 0.35	0.97 - 1.2

TABLE II

IDEAL PROPULSION PERFORMANCE OF POTENTIAL
RESISTOJET WORKING FLUIDS

	Liquid		Solid								Gas			
Temp., °K	Ammonia NH_3 - 1 atm		Ammonium Sulfide $(NH_4)_2S$-1/2 atm		Ammonium Hydrosulfide NH_4HS - 1/2 atm		Ammonium Carbamate $NH_4CO_2NH_2$-0.1 atm		Ammonium Carbonate $(NH_4)_2CO_3$-0.05 atm		Hydrogen H_2 - 1 atm		Nitrogen N_2 - 1 atm	
	$(I_{sp})_{ideal}$	(M)avg	$(I_{sp})_{ideal}$	(M)avg	$(I_{sp})_{ideal}$	(M)avg	$(I_{sp})_{ideal}$	(M)avg	$(I_{sp})_{ideal}$	(M)avg	$(I_{sp})_{ideal}$	(M)avg	$(I_{sp})_{ideal}$	(M)avg
298	113	17.032	98	22.71	92	25.55	92	26	95	24	296	2.016	80	28.02
500	185	9.267	152	14.05	139	17.41	132	21.83	134	20.91	389	2.016	105	28.02
1000	274	8.518	228	13.63	210	17.04	214	15.62	216	16.02	558	2.016	156	28.02
1500	347	8.516	290	13.47	267	16.48	270	15.61	274	16.01	706	2.016	197	28.02
2000	411	8.510	342	12.79	316	15.22	320	15.59	324	15.98	840	2.014	231	28.02
2500	470	8.425	392	12.27	360	14.48	366	15.19	371	15.37	961	1.991	260	28.02

$(I_{sp})_{ideal}$ = sec^{-1}

(M)avg = average molecular weight

VAPOR PRESSURE AT 65 °F

A. Liquid

NH_3	115 psia

B. Solid

$(NH_4)_2S$	7.0 psia
NH_4HS	6.4 psia
$NH_4CO_2NH_2$	1.2 psia
$(NH_4)_2CO_3$	0.60 psia

the gas temperature increase, in turn, decreases the flow rate. The maximum attainable gas temperature is limited by the temperature capability of the heater and by the required input power. The weight saving in propellant must, of course, be balanced against the weight of the required resistojet power supply.

The engine heat-up time is the time required for the engine to come to operating temperature. The heat-up time must be held to a minimum, e.g. 1 second, in order to hold the average power consumption of the resistojet attitude control system to a minimum. The required heat-up time is a function of the heater mass and heater resistance. In order to keep the heater warm up time at a minimum it is necessary to closely match the design of the power conditioning equipment with the wide anticipated variation in heater resistance between cold and hot flow.

The engine solenoid valve on-time is established by control logic considerations.

Finally, propellant selection is based on a variety of considerations including ease of storage and handling, weight of tankage, and material compatibility. It is important to note that the fast heat-up resistojet concept is not limited to ammonia but can be applied to a variety of propellants and is not dependent on the storage state, i.e. gas, liquid, or solid.

D. ENGINE HEATER PERFORMANCE

A preliminary series of tests have been obtained on a molybdenum tubular heating element using the constant pressure (variable mass flow) propellant feed system which is shown in figure 7. The tubular heating element is 1.25 inches long, has a nominal inside diameter of 12 mils (12×10^{-3} inches) and a nominal outside diameter of 20 mils. The nozzle throat diameter is 5 mils, and the nozzle exit to throat area ratio is 10 to 1. Measurements have been made of both heater performance and propulsion performance. The heater performance is presented in this section and the propulsion performance is included in the following section. It is stressed that the performance results are preliminary, and that no effort has been made to establish either optimum heater dimensions or nozzle shape.

The range of experimental operating variables used to establish the performance of the molybdenum heater element are summarized in table III. Current was brought to the heating element by means of electrical connections located at the thrustor base and in the nozzle exit plane.

During the course of the test series measurements were made of engine chamber pressure, power input, maximum engine exterior temperature, propellant flow rate, and thrust level. The engine chamber pressure was measured with a pressure transducer, the power input with a dc voltmeter and ammeter, the

engine temperature with an optical pyrometer, the propellant flow rate with a calibrated orifice, and finally the thrust level with the thrust stand described in a preceding section.

Figure 9 presents a plot of measured ammonia flow rate as a function of electric input power measured across the engine terminals. As indicated previously the engine chamber pressure is held essentially constant; the flow is choked across the exit nozzle throat and is not choked across the flow metering orifice. As heat is added to the gas flowing through the engine the gas density is decreased and the mass flow is decreased. Referring to figure 9 for cold flow the ammonia flow rate is 6.6×10^{-6} lbs/sec; on the other hand at 10 watts input power the flow rate is reduced to 3.2×10^{-6} lbs/sec and at 25 watts the flow rate is reduced further to 1.9×10^{-6} lbs/sec. Thus, as explained previously, for constant chamber pressure the addition of energy to the gas flowing through the heater has the same effect on the propellant flow rate as would be obtained by reducing the nozzle throat area.

From continuity considerations the mass flow through a sonic orifice is given by an expression of the form $\dot{m} \sim P_c A_t \sqrt{M_c/T_c}$ where $\dot{m}$ is the propellant flow, P_c is the chamber pressure, A_t is the throat area, T_c is the gas stagnation temperature in the chamber and M_c is the mean molecular weight in the chamber. The ratio of mass flow when the chamber is running cold $\dot{m}_1$ to the mass flow when the chamber is running hot $\dot{m}_2$ is given by, for constant pressure operation, $\dot{m}_1/\dot{m}_2 \sim \sqrt{T_{c,2}\, M_{c,1}/T_{c,1}\, M_{c,2}}$. The temperature molecular weight ratio $T_{c,2}\, M_{c,1}/T_{c,1}\, M_{c,2}$ can be considered as a thermodynamic property of the working fluid. Measurement of the ratio of engine mass flows at constant chamber pressure for hot and cold flow can thus lead to a reasonable estimate of gas stagnation temperature and stagnation enthalpy without knowledge of the engine throat area or nozzle orifice coefficient. It is assumed, of course, that the ammonia has been dissociated into nitrogen and hydrogen.

Figure 10 presents a curve of gas stagnation temperature as estimated from the continuity considerations presented above as a function of maximum observed engine temperature. The observed engine temperature is a 'true' temperature based on a pyrometer brightness temperature and an estimated value of the molybdenum spectral emissivity at 0.65 micron. For fixed chamber pressure, as indicated previously, increase in engine temperature corresponds to a decrease in a propellant flow rate. As the engine temperature is increased and accordingly the flow rate is decreased the estimated gas temperatures and observed engine temperature tend to approach each other.

Figure 11 presents a plot of electric power input to the thrustor and power input to the propellant as a function of maximum observed thrustor temperature. The power input to the propellant is equal to $\dot{m}\, h_c$ where, $\dot{m}$ is the propellant flow rate and h_c is the gas stagnation enthalpy estimated from the continuity equation. The electric power input to the engine which is not transferred to the working fluid is either radiated from the engine surface or conducted away

to the engine support structure. Referring to figure 11, it is noted that the power difference between the power to the engine and power to the gas increases markedly with increase in engine temperature. This observed increase in power loss is probably due to the increase in radiation from the engine exterior surface.

Figure 12 shows a plot of the ratio of the power to the gas to power to the engine as a function of maximum observed engine surface temperature. The trend of the results, as might be anticipated, is the same as that in figure 11. The heater efficiency is about 80 percent at an engine temperature of 1100 °K and falls to about 25 percent at 2200 °K. Again the fall off in heater efficiency can most logically be attributed to the increase in radiation losses at the higher engine temperatures.

Elementary laminar heat transfer considerations* suggest that the heat transfer per unit length of a hollow tube is independent of tube diameter[7]. Thus, assuming that the gas temperature and the heater temperature are nearly equal, a reasonable heat transfer design value for the small tubular heater is 2 to 3 watts/cm; this value is probably quite insensitive to tube diameter as long as the flow is laminar.

The present heat transfer results are, within the accuracy of the experiments, in substantial agreement with the heat transfer results obtained in the first quarterly report[7] using the constant mass flow (variable chamber pressure) propellant feed system.

The electric to gas power energy conversion efficiency, assuming negligible heat conduction through the ends of the heater element, is given by an expression of the form

$$\epsilon_t = \frac{Q_{conv,x}}{Q_{conv,x} + \epsilon\sigma T^4 \pi D} = \frac{1}{1 + \dfrac{\epsilon\sigma T^4 \pi D}{Q_{conv,x}}} \qquad (3)$$

It is to be stressed that this expression is only semi-quantitative and is based on the assumption that the heat transfer surface can be characterized by a heat transfer value, $Q_{conv,x}$, and a mean radiation temperature, T. Nevertheless the general form of the thermal efficiency relation does indicate that in order to obtain a high thermal efficiency it is necessary that the heater diameter, D, and thus the ratio $\epsilon\sigma T^4 D/Q_{conv,x}$ be held as small as possible. At a fixed heater diameter, D, the heater efficiency will fall off with increase in heater temperature, T.

* The heat transfer coefficient for fully developed flow within a tube is given by $h D/k \cong 4$ where h is the heat transfer coefficient, D the tube diameter, and k the mean thermal conductivity of the gas. The total heat transfer per unit length of heater element is given by $Q_x \cong \pi Dh \Delta T$ where ΔT is the mean temperature differential between the heater and the gas flow. Therefore, $Q_x \cong 4\pi k \Delta T$, or the heat transfer per unit length is independent of tube diameter.

TABLE III

OPERATING VARIABLES FOR THE EXPERIMENTAL MOLYBDENUM FAST HEAT-UP THRUSTOR

Variable	Range
Heater Current	0 to 15 amperes
Heater Voltage	0 to 2.0 volts
Heater Power	0 to 30 watts
Heater Resistance (at Operating Temperature)	0.10 to 0.15 ohms
Ammonia Flow	2 to 7 x 10^{-6} lbs/sec

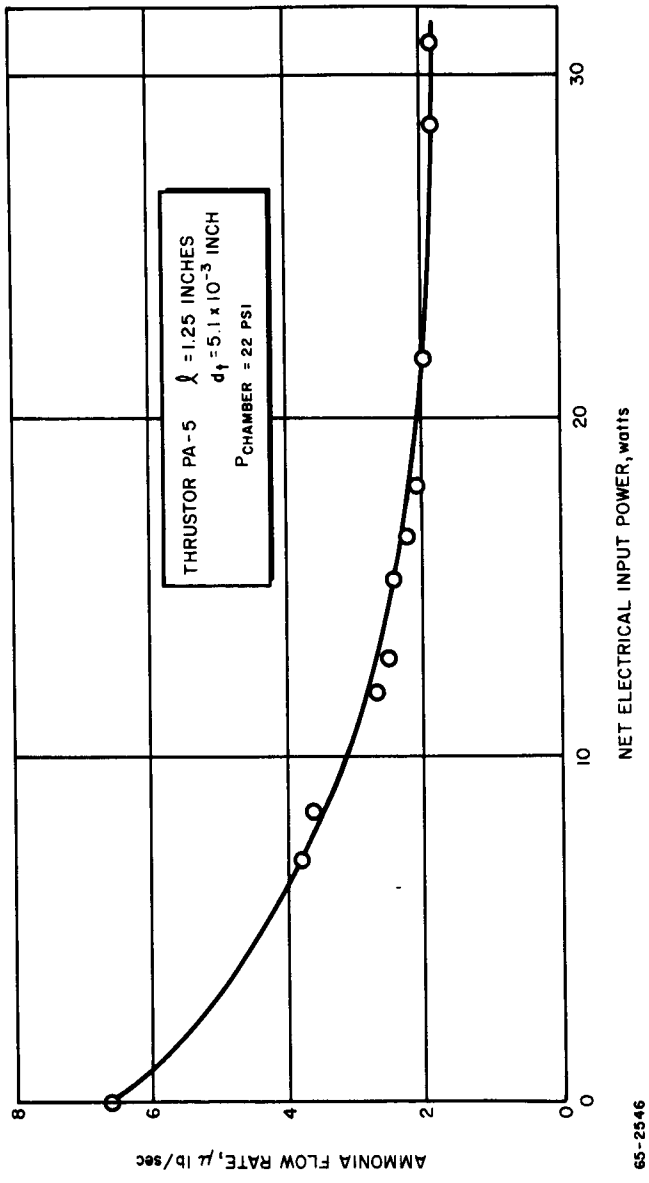

Figure 9 AMMONIA FLOW RATE VERSUS NET ELECTRICAL INPUT POWER

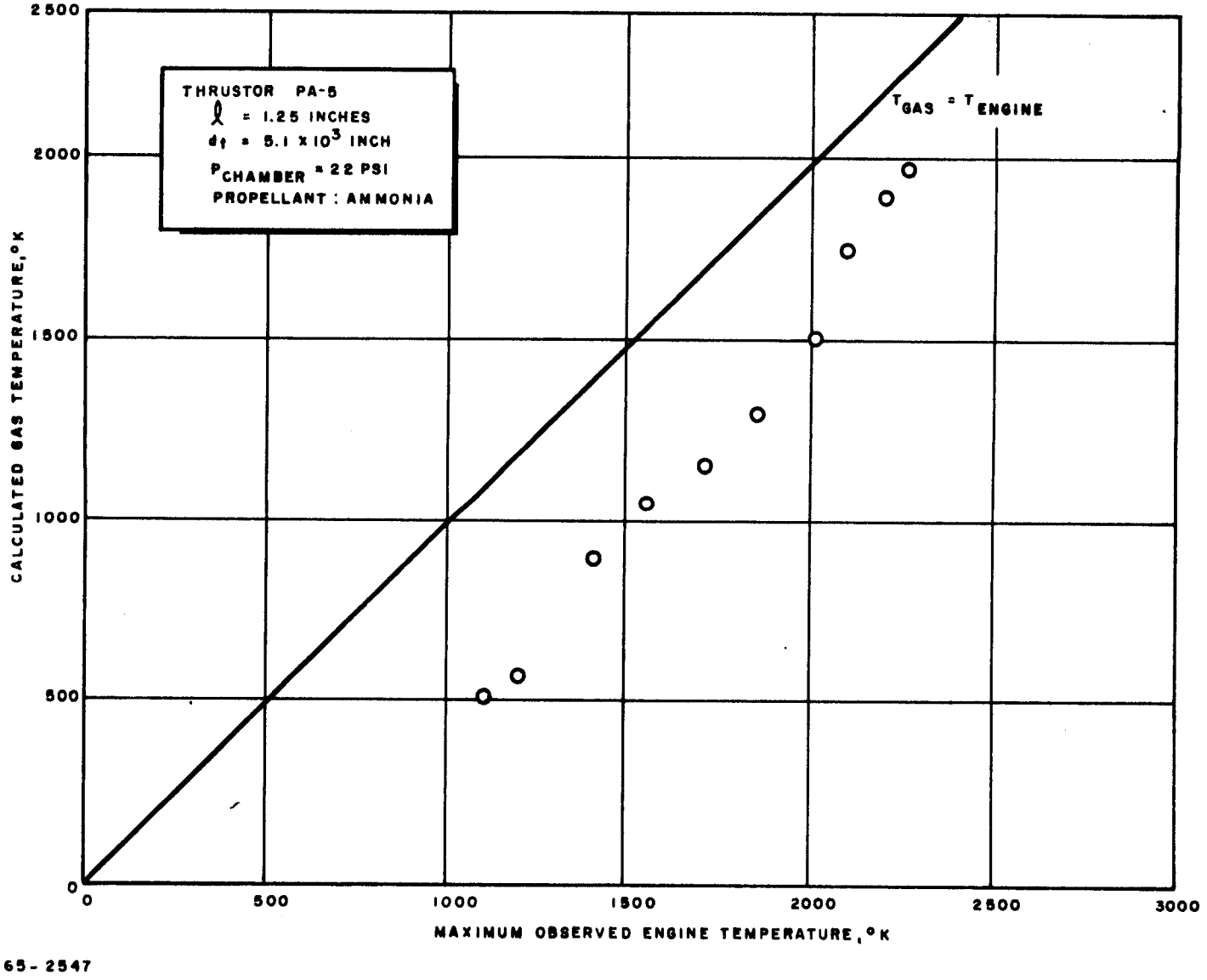

Figure 10 GAS TEMPERATURE VERSUS MAXIMUM ENGINE TEMPERATURE

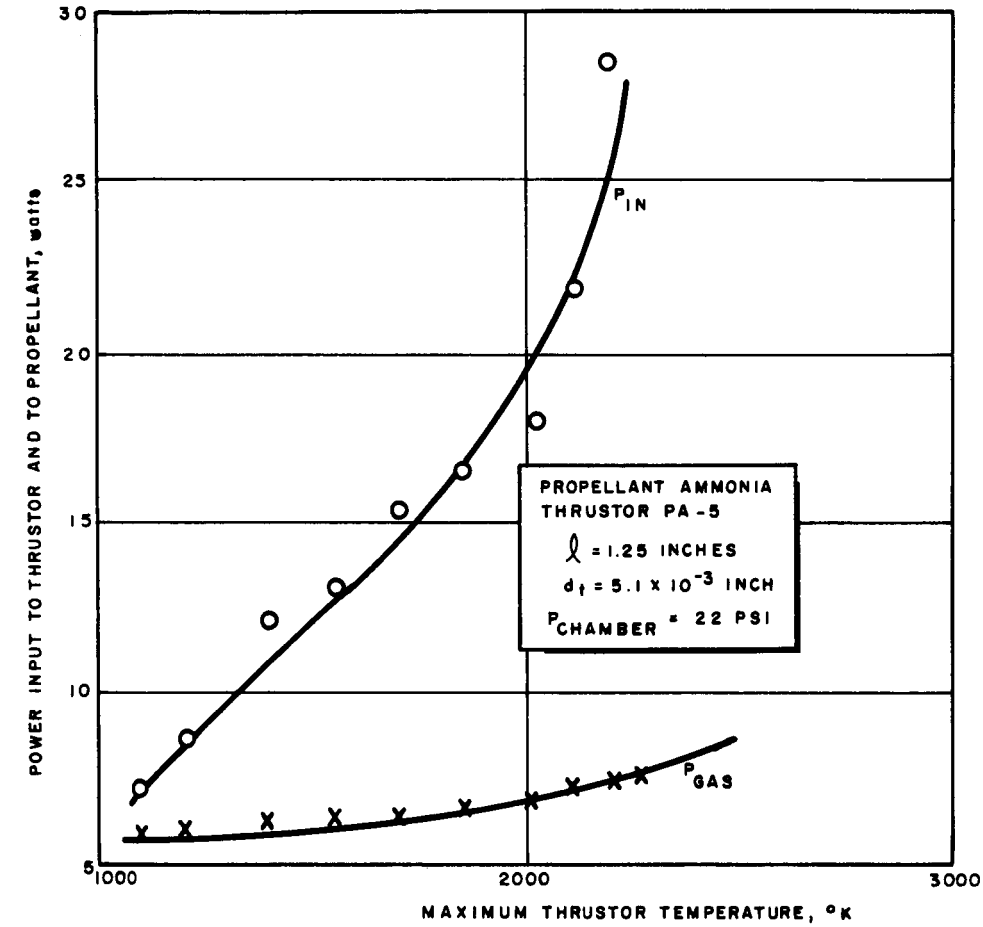

Figure 11 ELECTRICAL INPUT POWER AND POWER TO PROPELLANT VERSUS MAXIMUM THRUSTOR TEMPERATURE

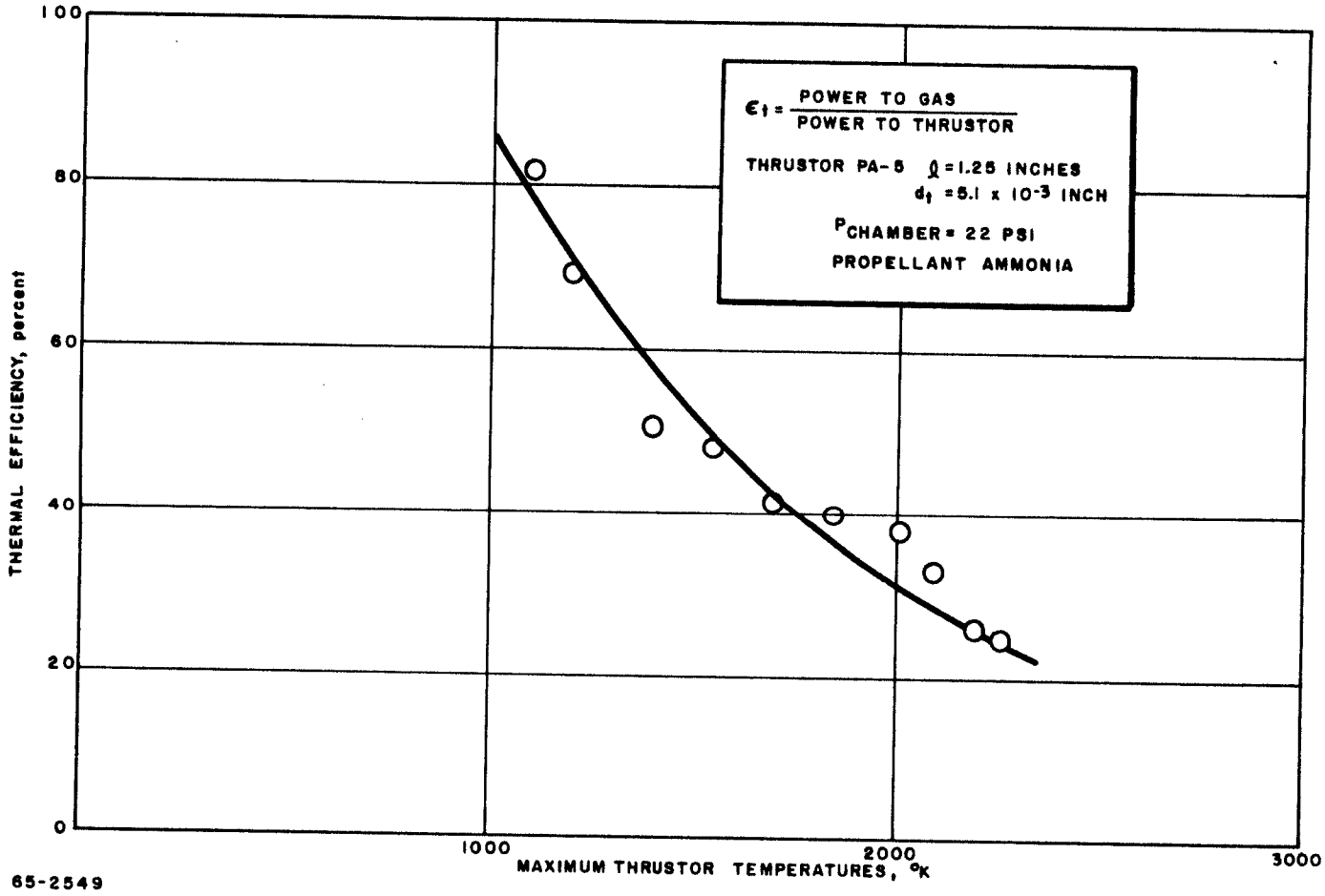

Figure 12 THERMAL EFFICIENCY VERSUS MAXIMUM OBSERVED THRUSTOR TEMPERATURE

Table IV presents estimates of the thermal efficiency of a 20 mil (5.1×10^{-2} cm) heater element; the heater emissivity is 0.50; and the convective heat transfer rate is 3 watts/cm. A comparison of the measured and estimated values of the thermal efficiency is presented in figure 13. It is noted that the general form of the results is quite similar to that predicted by elementary theory. Further, and probably somewhat fortuitously, the predicted and measured values of the heater efficiency are remarkably similar.

Figure 14 presents estimated values of the heater thermal efficiency for heater tubes ranging in diameter from 10 to 50 mils. The heater emissivity was again assumed constant at 0.50 and the convective heat transfer coefficient was assumed constant at 3 watts/cm. As anticipated the heat thermal efficiency falls off with increase in temperature and with increase in heater diameter.

E. RELIABILITY OF POTENTIAL HEATER MATERIALS

Thrustor performance data have been obtained with stainless steel and molybdenum heater elements. Major problem areas include engine fabrication and thermal cycling capability. Extended thermal cycling (10,000 cycles) appears to be no problem for stainless steel (m.p. 1500 °C) but is a serious problem[7] for molybdenum (m.p. 2620 °C) which has a higher temperature capability. To extend the upper temperature range of the heater element an effort has been made to fabricate the basic heater-nozzle structure from vapor deposited tungsten. This technique appears quite promising and it appears possible to fabricate tungsten heater elements with a wall thickness of only 1 to 2 mils.

In order to check the thermal cycling capability of the vapor-deposited tungsten, a sample tube of the material (25 mil inside diameter, 3 mil wall thickness, 3/4 inch long) was cycled through a typical resistojet heating cycle 40,000 times. The tube was placed in a 1 micron vacuum for the test. The ammonia flow entered from each end of the tube and passed out through an orifice at the tube center. The interior pressure was about 1 atmosphere. The operating cycle was: Power On - (No Flow) 0.8 second; Power On - (With Flow) 1.0 second; Power Off - 2.2 seconds. During the power on, no flow, phase, the tube was heated to 2200 °K. This temperature was maintained during the power on with flow phase after which the power was turned off and the tube cooled before beginning the next cycle. The heater was thermally cycled 40,000 times.

At the completion of the test, visual examination indicated no apparent changes in the sample. Photomicrographs of the wall cross section before and after the test were prepared at 500X and indicated that there was a change in crystal structure. The material, however, appeared structurally sound, and the structural changes which did occur evidently do not affect the integrity of the material. Additional testing will be carried out in the next quarter to provide data at different temperature levels and at a greater number of cycles.

TABLE IV

ESTIMATED THERMAL EFFICIENCY OF A 20 MIL RESISTOJET HEATER

Mean Temperature T, °K	Radiation Flux $\epsilon\sigma T^4$, watts/cm^2	Radiation Power Qrad, watts/cm	Convection Power Qconv, watts/cm	Thermal Eff. ϵ_t
1000	2.83	0.48	3.0	0.87
1500	14.3	2.24	3.0	0.57
2000	45.3	6.70	3.0	0.29
2500	110.2	17.60	3.0	0.15

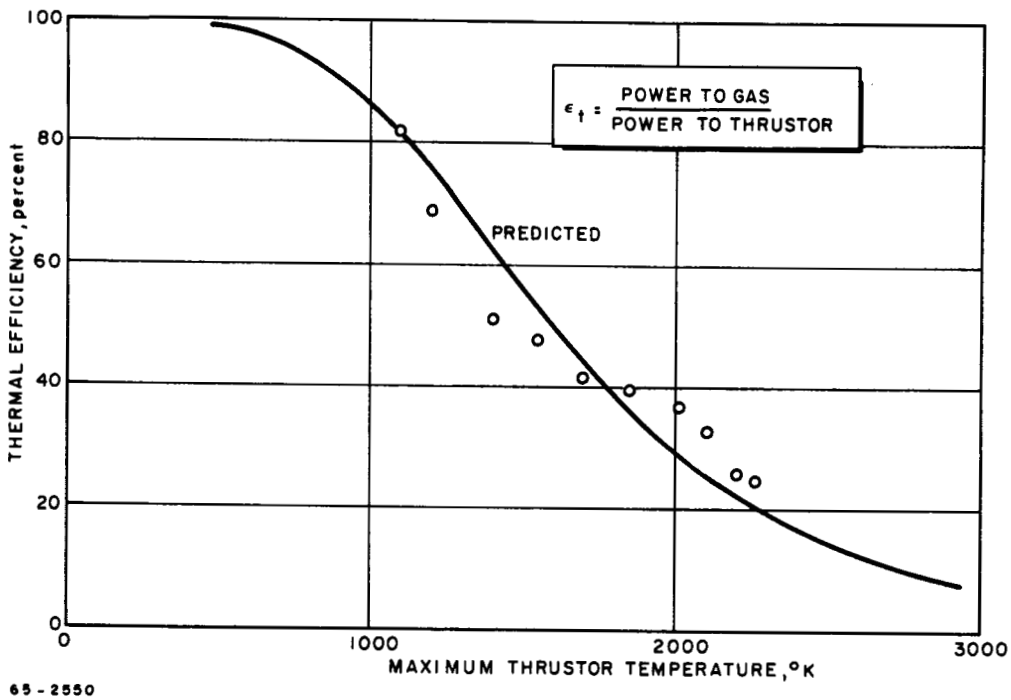

Figure 13 COMPARISON OF ESTIMATED AND OBSERVED THERMAL EFFICIENCY VERSUS MAXIMUM OBSERVED THRUSTOR TEMPERATURE

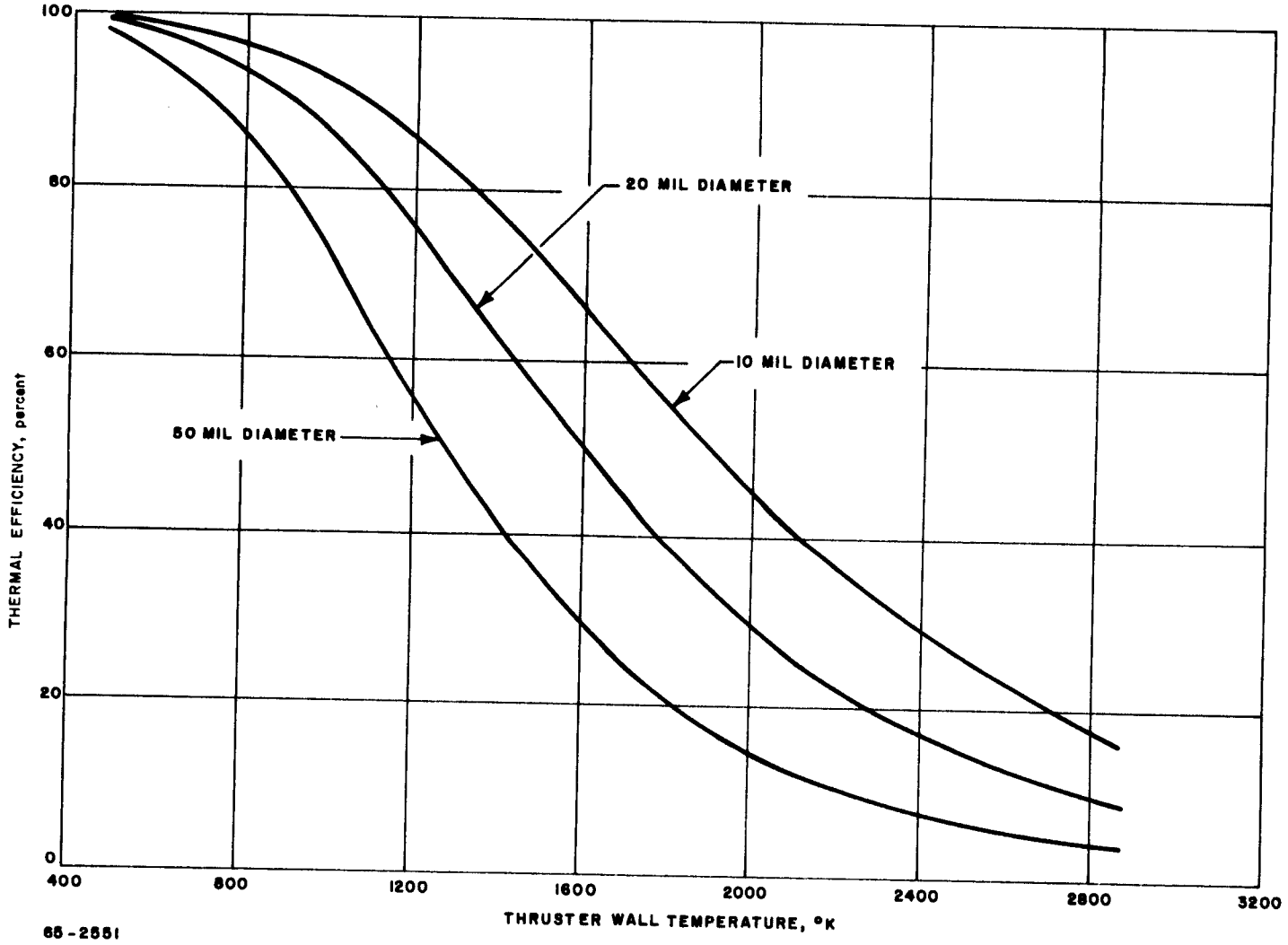

Figure 14 ESTIMATED VALUES OF THE HEATER THERMAL EFFICIENCY VERSUS HEATER TEMPERATURE AND HEATER DIAMETER

F. ENGINE PERFORMANCE

1. Measurement of Engine Specific Impulse

In the first quarterly report[7] thrust stand thermal drift problems made it impossible to obtain reliable engine thrust data in hot flow. The hot flow measurements were deduced from the cold flow measurements by assuming that the product of thrust coefficient, C_F , and throat area, A_T , in hot and cold flow measurements were identical. During the past quarter the thrust stand thermal drift problem has been essentially eliminated by reducing the thrustor on-time. The thrust results in the first quarterly[7] were essentially based on continuous thrust measurements, whereas, the results which are presented below are based on transient measurements.

The engine specific impulse, I_{sp} , is defined as the ratio of the impulse bit $\int F\,dt$ to the propellant consumption during the impulse bit $\int \dot{m}\,dt$. During the present experiments the impulse bit period was of the order of 1 second. The values of the impulse bit were in the range from 0.30 to 0.50×10^{-3} lb-sec and were obtained by integrating the thrust stand displacement transducer oscilloscope traces. Similarly the total propellant consumption during the thrusting period was established by integrating the oscilloscope trace of the differential transducer located across the flow metering orifice. Values of the specific impulse obtained in this manner as a function of estimated gas temperature are shown in figure 15. Superimposed on the experimental results are values of the ideal frozen flow specific impulse for a nozzle with an infinite area ratio and a nozzle with an area ratio of ten. The maximum measured specific impulse is close to 200 seconds and corresponds to a gas temperature of 2000 °K. Ideally, the inviscid solution for a nozzle area ratio of ten and a temperature of 2000 °K corresponds to a specific impulse of 325 seconds. There is clearly a wide discrepancy between the predicted and observed results which can be attributed to the effects of viscosity.

Figure 16 presents estimated values of the engine thrust defined as $\int F\,dt / \int dt$, (where the integrals are taken over the pulse length) as a function of power input. The reservoir pressure has been held constant at 22 psia. The thrust level, as indicated previously, is relatively insensitive to input power level; the observed fall off in thrust with increase in power input may be due to increase in gas viscosity (and thus increase in friction loss) at the higher gas temperatures.

Figure 17 shows the variation of specific impulse with electrical power input again at a fixed pressure level. The increase in specific impluse with power input falls off rather markedly at the higher input power levels. In fact there is little change in specific impulse as the electric input power is

increased from 20 to 30 watts. The decrease in mass flow (see figure 9) due to the increase in power input is to a large extent counterbalanced by the decrease in thrust level (see figure 16); thus, above 20 watts input power the specific impulse remains nearly a constant. The input power is primarily going into radiation. The largest proportional increase in specific impulse with input power occurs between 0 to 15 watts probably corresponding to the dissociation of ammonia into its constituents hydrogen and nitrogen.

Finally, figure 18 shows the overall energy conversion efficiency defined as the ratio of thrust power to electric plus cold gas power as a function of electric power input. The overall energy conversion efficiency falls off with increase in electric input power as might be expected from the preceding results. It is important to note, however, that the real parameter of interest, apart from system reliability, is system weight. An increase in propellant specific impulse from 50 to 150 seconds can result in a potential propellant weight saving of 150 pounds for the three year attitude control and station keeping of a 500 pound satellite; the weight penalty for a 20 watt solar power system is only 5 pounds. Thus, although the overall energy conversion efficiency of the electric propulsion is low the potential propellant weight saving over a cold gas system due to the increase in engine specific impulse is substantial.

2. Nozzle Behavior

In the case of conventional rocket nozzles where the thrust is measured in hundreds or thousands of pounds reasonable approximations for the nozzle coefficient can be obtained from inviscid flow theory[8]. In the case of thrustors in which the thrust levels are of the order of micropounds the nozzles must either operate at low pressure or with very small throats. In either the case of low pressure operation or small throats, viscosity effects are probably large enough such that conventional nozzle theory, based on inviscid flow, would not provide adequate estimates of thrust level and specific impulse.

Very little systematic information is available in the literature on the behavior of micropound thrust nozzles except for some work by Tinling[9] of NASA, Ames on water vapor jets. In the experiments on water vapor jets Tinling found an empirical correlation between specific impulse and mass flow rate. The measured specific impulse normalized by the theoretical value for isentropic flow was obtained for a wide range of nozzle area ratios, e.g., 1 to 1 and 100 to 1, and nozzle throat areas, e.g., 7 to 30 mils. The normalized values of specific impulse were found to correlate, in a band which is about 10 percent of the theoretical impulse in width, only as a function of mass flow rate independent of the absolute value of the throat area ratio or throat size. Tinling's results are summarized in figure 19. Superimposed on these values are those obtained in our present experiments. It is noted that the normalized specific impulse values fall within the scatter of Tinling's data.

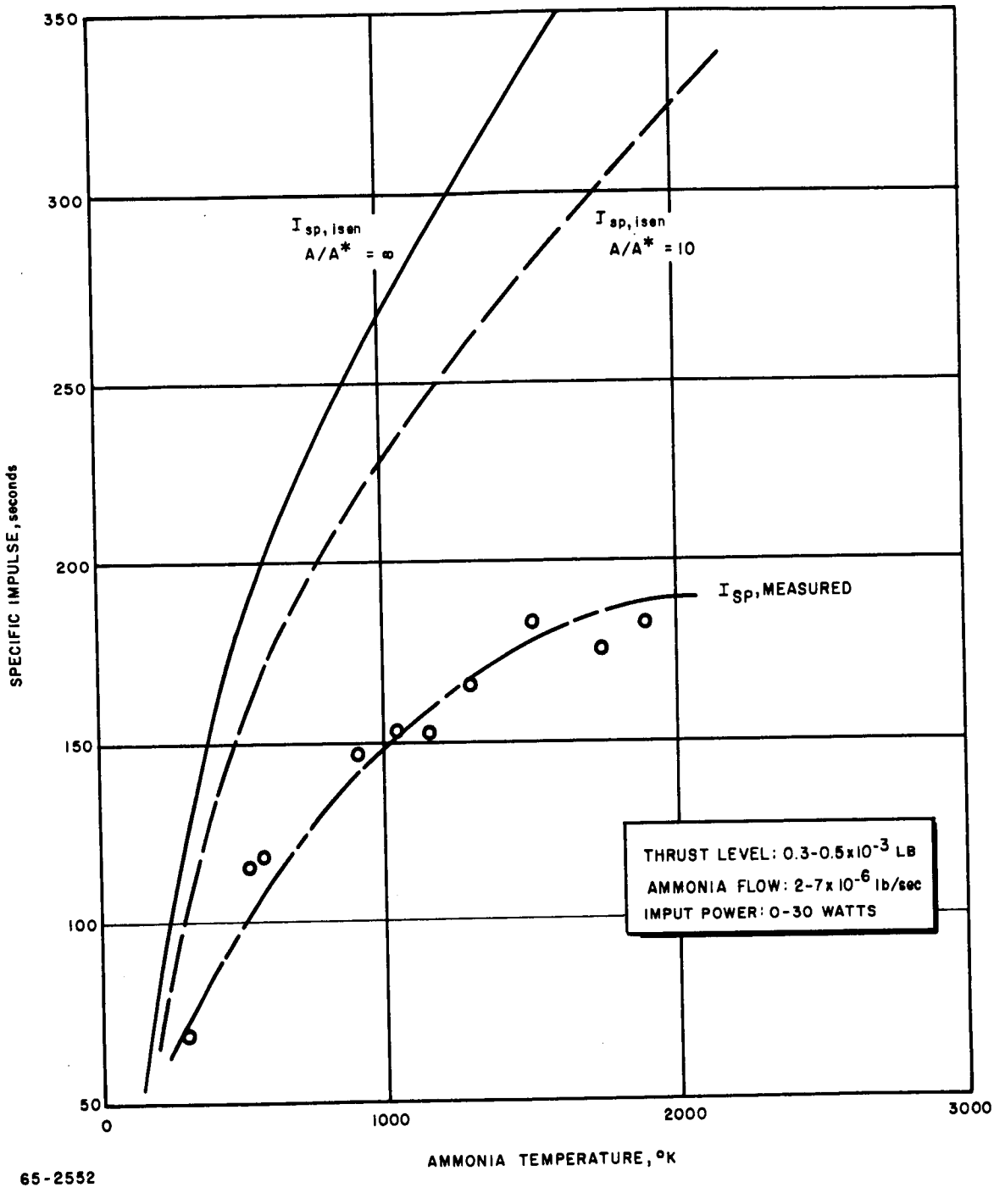

Figure 15 MEASURED ENGINE SPECIFIC IMPULSE VERSUS ESTIMATED GAS TEMPERATURE

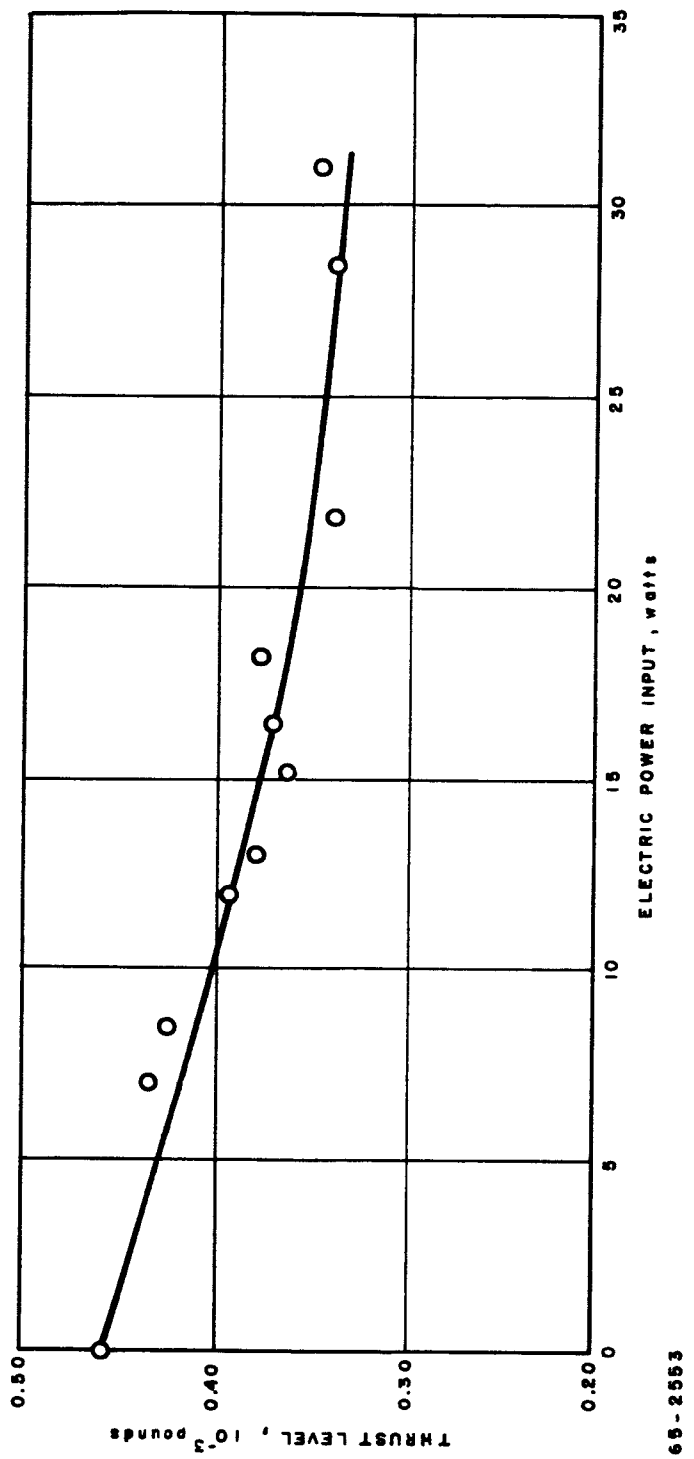

Figure 16 MEASURED ENGINE THRUST VERSUS POWER INPUT

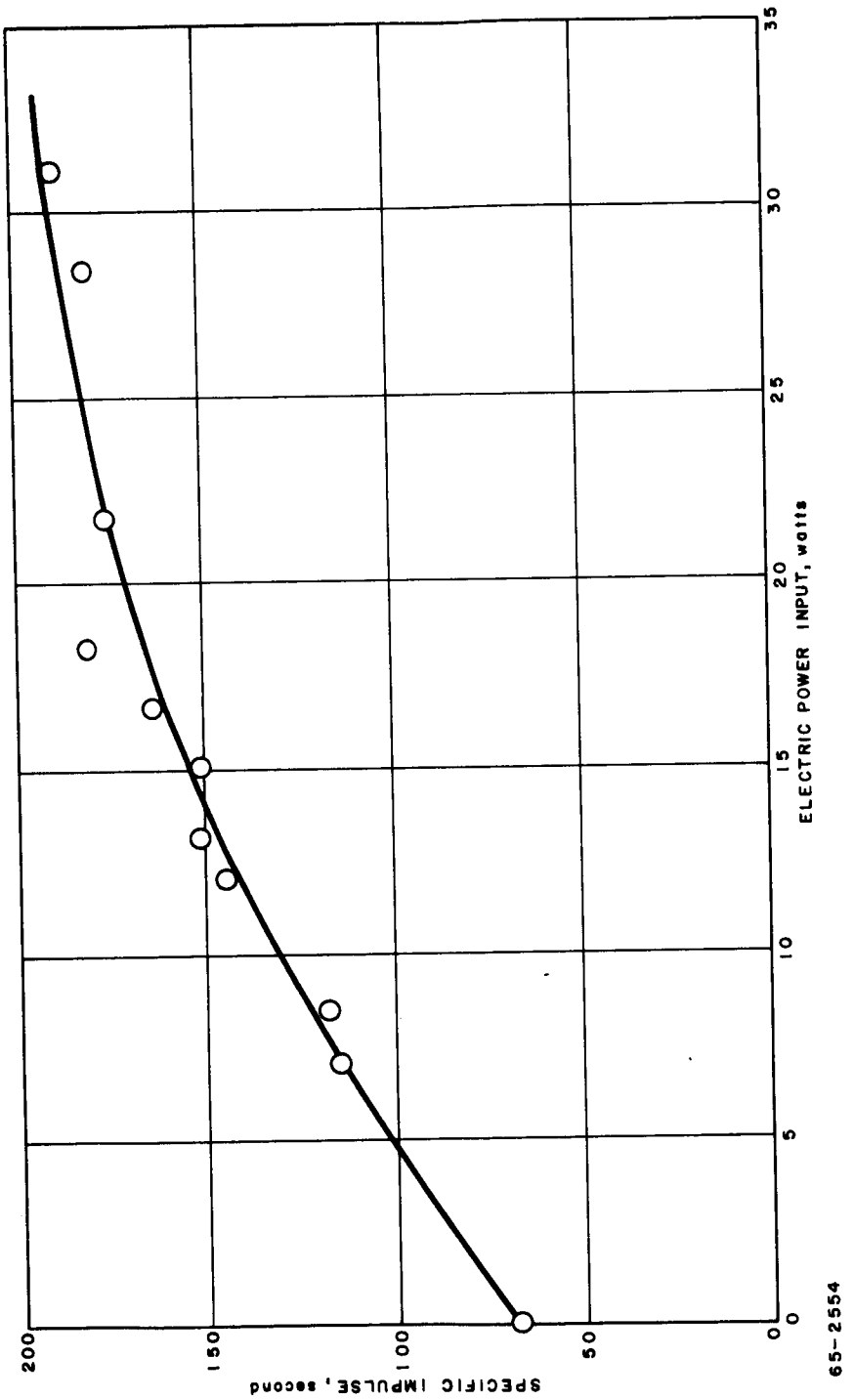

Figure 17 MEASURED ENGINE SPECIFIC IMPULSE VERSUS POWER INPUT

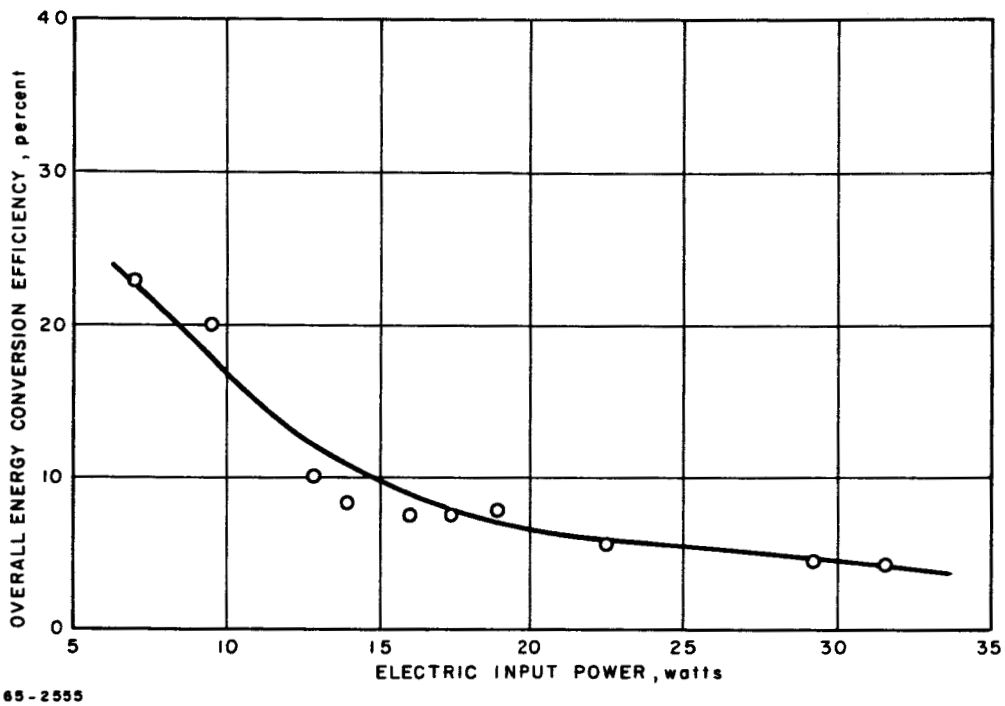

Figure 18 OVERALL ENERGY CONVERSION EFFICIENCY VERSUS POWER INPUT

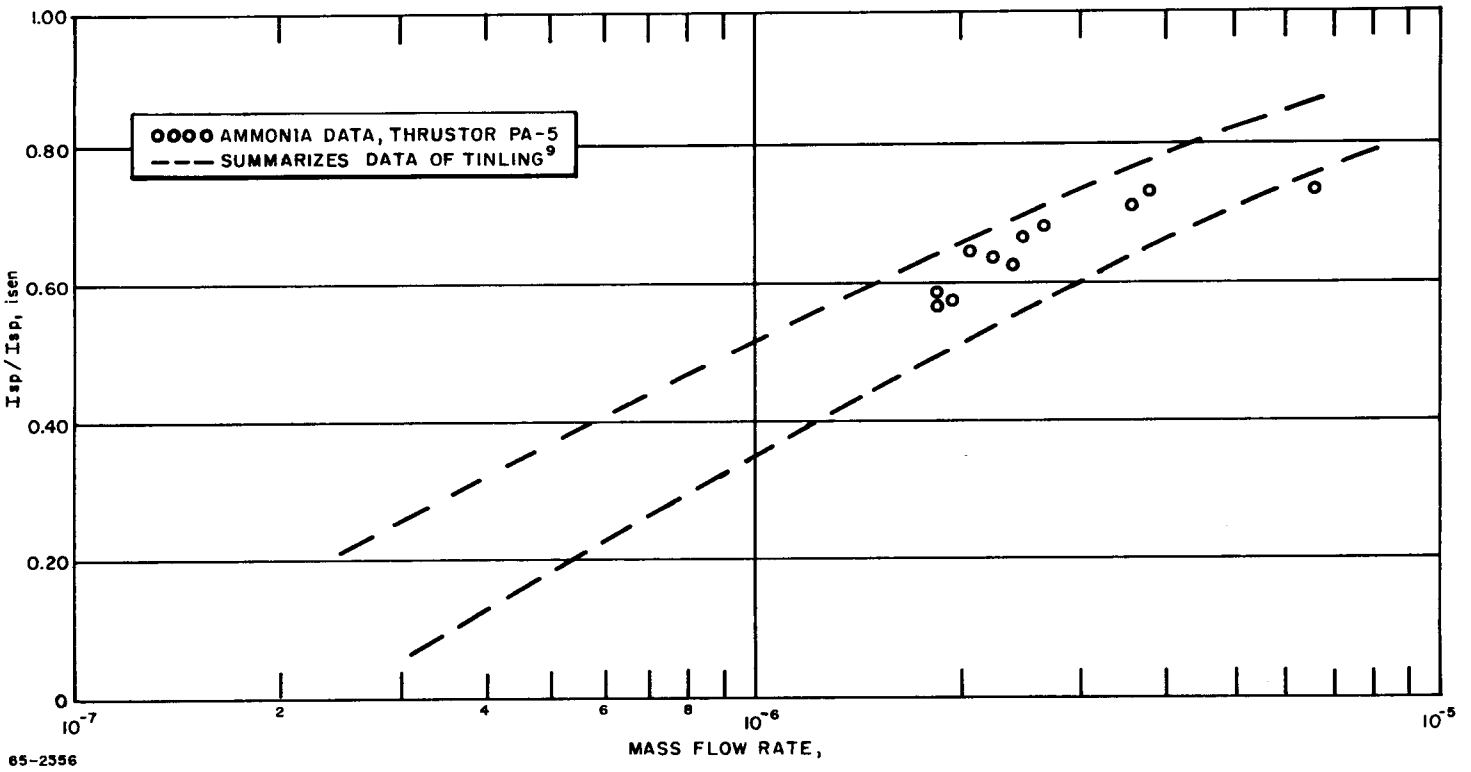

Figure 19 NORMALIZED SPECIFIC IMPULSE VERSUS MASS FLOW RATE

Recent results from Tinling[10] indicate that the normalized specific impulse may not fall off with mass flow rate as rapidly as indicated in the original results presented in figure 19, but remains essentially constant at I_{sp} / I_{sp} , isen = 0.60 to 0.70 at flow rates below 15 x 10^{-4} gm/sec (3.3 x 10^{-6} lbs/sec). Tinling and the NASA, Ames group suggest that the difference between their most recent results and the original can be attributed to the fact that their present experiments are being carried out at 1 micron back pressure, whereas, the original work was carried out at 30 microns back pressure. (The experiments in the present resistojet program are being carried out at 1 micron back pressure.) To summarize, in the flow range of the present resistojet results, i.e., 3 to 7 x 10^{-6} lbs/sec, the normalized resistojet specific impulse is between 0.60 to 0.70; this value is in agreement with the original[9] and most recent results[10] from NASA, Ames. At mass flows below 3 x 10^{-6} lbs/sec (0.30 x 10^{-3} lbs of thrust) NASA, Ames now finds, in contradiction to their earlier results, that the normalized specific impulse is constant at 0.60 to 0.70. The entire area is however still open, and experiments on micropound thrust nozzle performance are being continued both at this laboratory and NASA, Ames.

III. SINGLE AXIS LABORATORY ATTITUDE CONTROL SYSTEM

A. INTRODUCTION AND BACKGROUND

As part of the present program a series of resistojet system tests are planned on an attitude control system test bed which has been recently installed at the NASA, Lewis Research Center. The attitude control system test bed is shown in figure 20. The test bed is mounted on an air bearing in a vacuum chamber. During a typical attitude control system test, the test bed is completely isolated from the laboratory and is self-contained. Power is supplied from on-board batteries; propellant is supplied from an on board propellant supply; and, finally, communication to and from the test bed is accomplished by means of telemetry. The test set-up has been designed and developed by NASA, Lewis Research to simulate an actual space control mission as far as is possible in the laboratory. The test bed and test set-up are readily adaptable to the testing of a variety of three-axis attitude control systems based on gas and particle expulsion devices; these include both electrothermal plasma and ion electric propulsion engines, and cold gas, subliming solid, mono-and bi-propellant rockets. The air bearing test facility is thus ideally suited for comparing the overall performance of different attitude control systems.

The primary purpose of the intial resistojet attitude control system (ACS) test on the NASA, Lewis Research Center Air Bearing will be to demonstrate the feasibility of applying the resistojet concept to a complete satellite attitude control system, and to identify actual and potential interface problems. To simplify the control problem the initial air bearing test will be single rather than three axis. It is stressed that in the design and development of the resistojet attitude control system for the single-axis air bearing test emphasis has been placed on demonstrating hardware feasibility, rather than demonstrating optimum resistojet attitude control system performance.

For the initial air bearing resistojet attitude control system test, Avco RAD is responsible for the electrical and mechanical system components indicated in table V.

The control logic package includes a light source and sensor to establish test table position; basically, the control logic package signals the individual resistojet engines to turn-off and on in response to signals from the light sensor located on the test table. The basic electrical system is shown in figure 21.

The power conditioning package converts the regulated power obtained from the battery supply located on the test table into a form suitable for resistojet operation. It will be recalled from previous discussion that the power conditioner must be carefully matched to the resistojet engines because of their inherent low resistance.

TABLE V

RESISTOJET ACS SYSTEM COMPONENTS TO BE SUPPLIED BY AVCO RAD

- Control Logic Package
  - Light Source and Sensor
- Power Conditioning Package
- Resistojet Engine System
  - Resistojet Engine
  - Propellant Storage and Regulation
  - Engine Instrumentation
- Signal Conditioning Package
  - Check-out Console

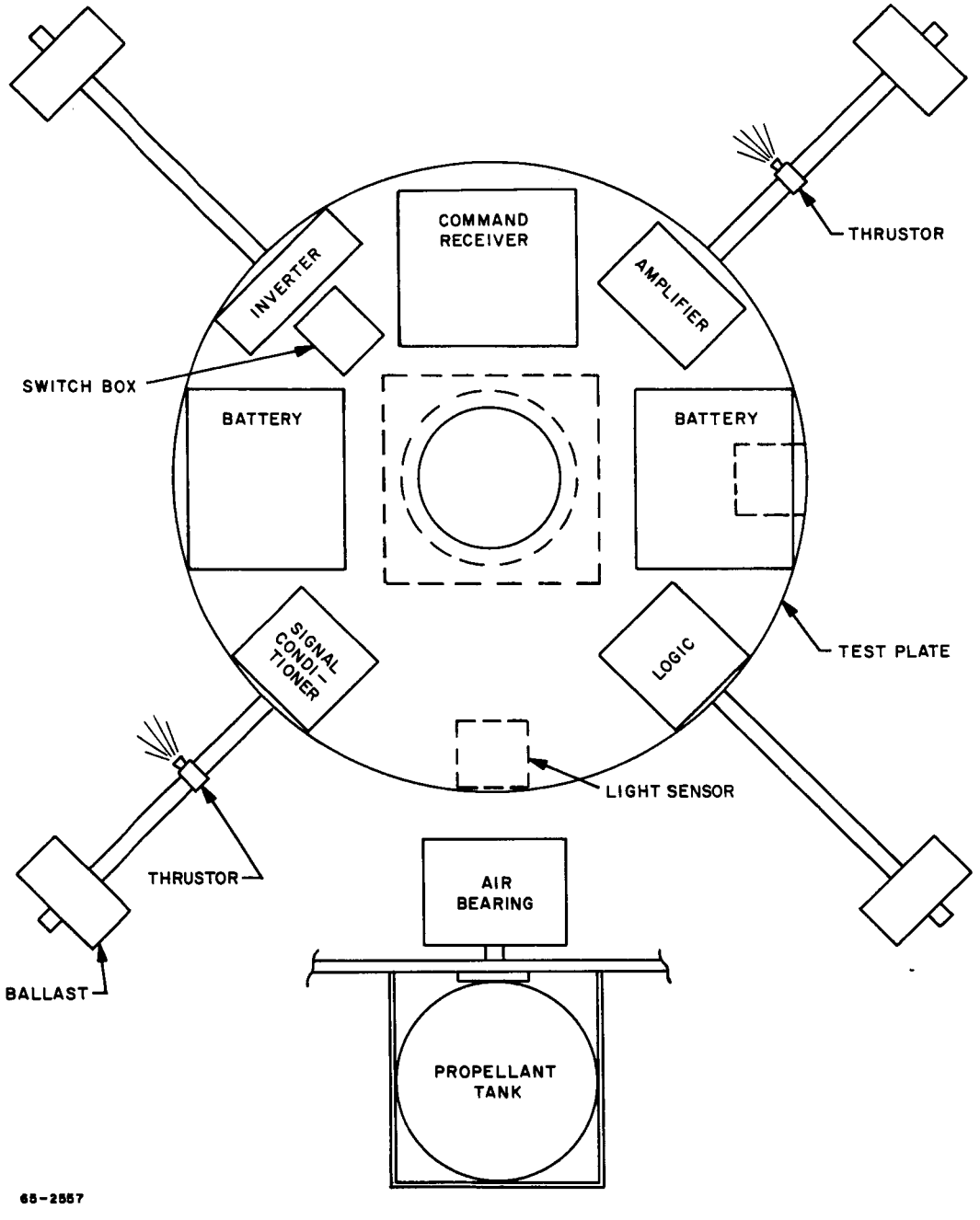

Figure 20 NASA LEWIS SINGLE AXIS AIR BEARING ATTITUDE CONTROL SYSTEM TEST BED

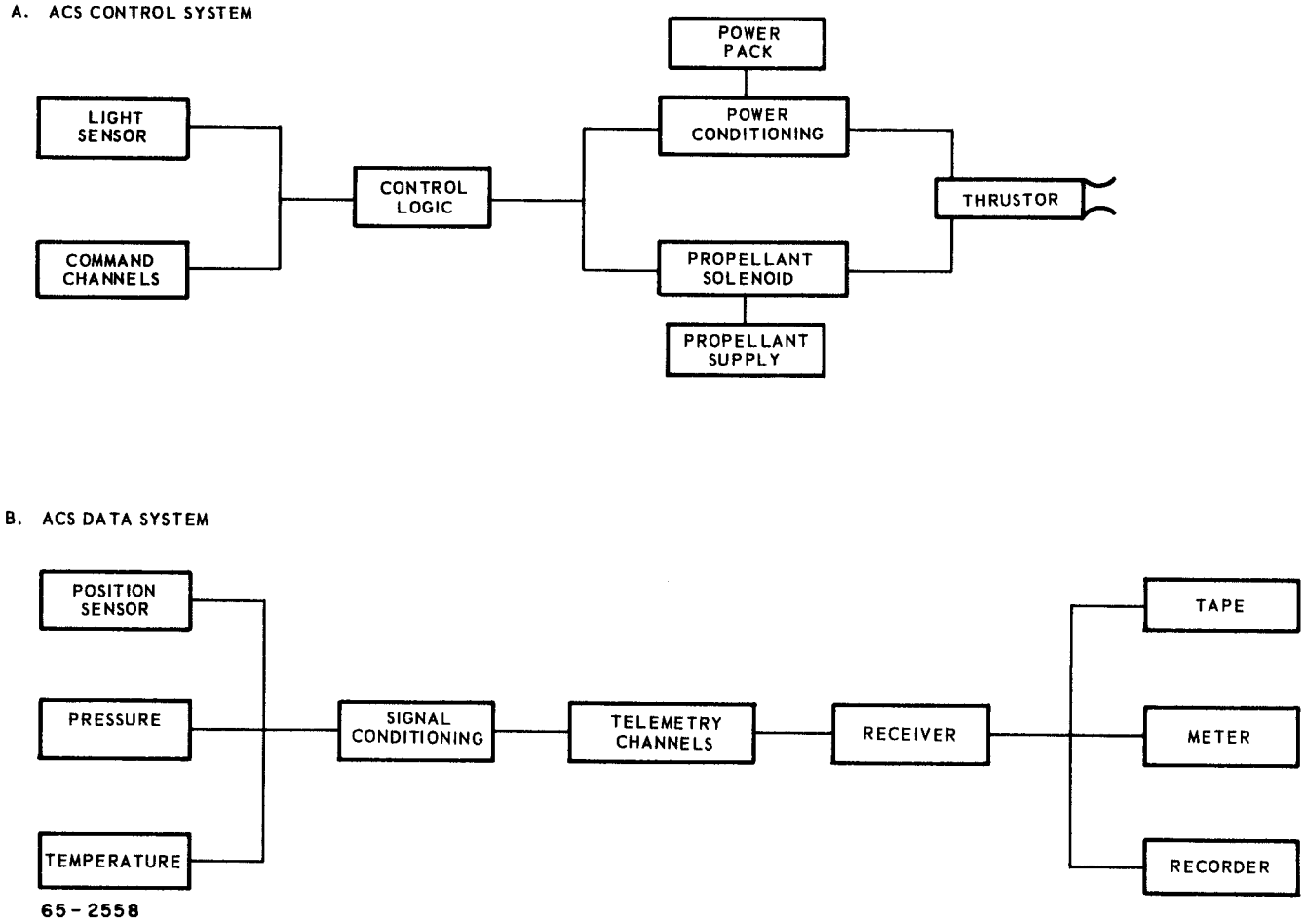

Figure 21 BLOCK DIAGRAM FOR THE ATTITUDE CONTROL ELECTRICAL SYSTEM

The resistojet engine system includes 3 resistojet engines, 2 for attitude control and 1 for station keeping. The engine system also includes liquid and gaseous ammonia reservoirs. A block diagram of the system is shown in figure 22. The propellant, ammonia, is stored as liquid in the ammonia reservoir. The liquid ammonia tank is connected to the gaseous ammonia reservoir by means of a solenoid valve operated by a pressure switch. The pressure switch opens the valve when the gas plenum pressure falls below a preset value and closes the valve when the pressure rises to another preset value. Referring to figure 22 instrumentation is supplied to measure the resistojet chamber pressure, heater temperature, gas inlet temperature, and gas flow rate.

The signal conditioning package amplifies the signals produced by the pressure, temperature, and error sensors preparatory to transmission by the telemetry package.

The basic purpose of the intital resistojet ACS test is to hold the position of the test bed around a single axis to within ± 1/2 degree. The position of the test bed with respect to the light beam is established by means of a light sensor located on the test bed. If the angular displacement of the test bed is outside the prescribed limits a signal is passed to the control logic package which in turn calls for power (from the power conditioner) and propellant (from the propellant gas reservoir) to be delivered to the proper thrustor. The test will include both acquisition and limit cycle operation.

Apart from the resistojet engine system, two physical electronic packages will be delivered to NASA, Lewis for attachment to the air bearing test bed. Package No. 1 will contain the control logic system and the power conditioning equipment for the two attitude control thrustors; Package No. 2 will contain the signal conditioning equipment and the power conditioning equipment for the station keeping control thrustor.

In the following sections detailed descriptions are presented of the individual components of the total resistojet ACS. These include:

1. Control Logic Package
2. Power Conditioning Package
3. Resistojet Engine System
4. Signal Conditioning Package

B. CONTROL LOGIC PACKAGE

The discussion of the control logic package is subdivided into four parts:
1. Single Axis Control Logic; 2. Estimated Performance of the Single Axis

Control Logic System; 3. Electronic Circuitry for the Control Logic System; 4. Description of the Light Sensor and Light Source.

1. Single Axis Control Logic

A control system has been selected for control of the two resistojet attitude control engines with the purpose of maintaining the attitude of the single axis table within the desired angular limits with a minimum of fuel consumption. The control method selected is based on the method proposed by Vaeth.[11] This method not only provides for effective damping of initial conditions (that is, acquisition), but minimizes fuel consumption and the valve cycling frequency. The Vaeth technique accomplishes the same degree of limit cycle optimization as obtained by the use of a number of different switching levels as originally proposed by Gaylord and Keller[12] and in addition provides for the rapid damping of initial conditions. Basically, the Vaeth method uses two sets of rate dependent control commands. Both sets are controlled by a function of both the angular divergence and the angular rate. Whenever the function exceeds the smaller of two preset values, the appropriate resistojet is pulsed on for a preset time producing an impulse bit which, if the angular rate is small enough, reverses the direction of rotation of the table. The system thus oscillates between two preset limits resulting in limit cycle control. If the rate of rotation is too large, however, the impulse bit will not be sufficiently large to reverse the rotation. With this condition, the function will reach and exceed the larger of the two preset values, above which the resistojet is turned on and remains on continuously until the function again drops below this preset value. This set of commands is used for acquisition and as a backup to the limit-cycle control lines.

The control logic can be explained in more detail by reference to figure 23. The bottom sketch illustrates schematically the control system and single axis table. A well-collimated light source is placed inside the vacuum tank containing the air bearing table to serve as the reference for orientation. On the table itself, a light sensor is placed which provides a signal proportional to the angular divergence, θ, of the table with the null at $\theta = 0$. This light sensor covers a maximum range of $\pm$ 8°. The signal from the light sensor goes to the control logic system which in turn controls the resistojet engine operation. The light source will be described subsequently.

The top sketch of figure 23 indicates the logic used in the control system. Lines A and B represent the acquisition control lines and also serve as backup lines to the inner lines. Whenever the combination of θ and $d\theta/dt = 0$ lies outside of these lines, the appropriate resistojet engine (R1 for line B and R2 for line A) is operated continuously until the table is rotated to a state within these lines. These lines are set at $\pm$ 0.4° with $d\theta/dt = 0$. Lines C and D represent the limit cycle control lines for control after acquisition. Whenever θ and $d\theta/dt$ change such that line D is crossed,

resistojet R1 is pulsed on for a preset short time period to provide an impulse bit. Whenever line C is crossed, resistojet R2 is pulsed on to provide an impulse bit in the opposite direction. Lines C and D are set at ± 0.2° with $d\theta/dt = 0$. It should be noticed that both sets of lines have a slope to the left and thus the operation of the resistojet control is not only dependent on the angular error, θ, but also on the rotation rate, $d\theta/dt$.

The operation of the logic in acquisition can now be explained by reference to figure 24 which is a plot of the acquisition lines only extending out to the limit of the optical sensor, ± 8°. Consider the case of the table initially at a large positive angle with zero rate of rotation. A telemetry command signal for counterclockwise rotation is given from the "ground" station and resistojet engine R1 turned on.

The resistojet operates continuously until line B is reached following the dotted line 1 to 2 in figure 24. This resistojet is then turned off and the system drifts from B to A. When line A is crossed, resistojet R2 is turned on automatically and operates continuously driving the table along the parabolic path 3 to 4 where line A is again intersected and resistojet R2 turned off; the table then drifts at constant rate between lines A and B where resistojet R1 is turned on automatically. The system again follows a parabolic path along the dotted line from 5 to 6 where resistojet R1 is turned off automatically as line B is crossed. It is seen that due to the slope of the control lines, a spiral-like path is followed which tends to reduce both θ and $d\theta/dt$. Continuation of this cycling thus reduces both θ and $d\theta/dt$ to very small values so that the inner control lines can take over the control. The dynamics of the control system and table have been simulated on an analogue computer. In figure 25, a typical plot from the computer is presented illustrating acquisition from an angle of +60° with an initially zero rate of rotation. For this particular case, the acquisition time for the table was 2090 seconds with a thrust torque of 10^{-3} ft lb and table moment of inertia of 27 slug ft^2.

Attention will now be turned to limit cycle operation between lines C and D of figure 23. During the acquisition phase, control lines C and D are active and the resistojets are actually pulsed on when these lines are crossed. The rate of rotation is high enough however so that lines A or B respectively are reached before the pulse period is over and the resistojets remain on. As the rate decreases, a value is eventually reached where the rate is small enough for the pulse from lines C or D to change the direction of rotation and to prevent lines A or B from being crossed. When this condition occurs, the system drops out of the acquisition phase into limit cycle control between lines C and D with lines A and B serving now as a backup in case the system should leave the limit control cycle due to some unusual disturbance.

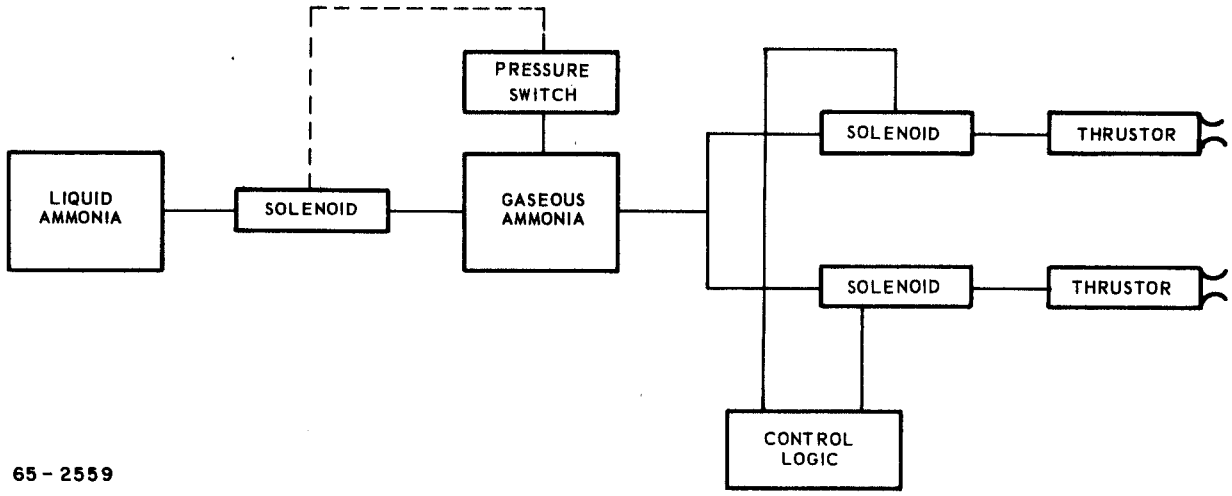

Figure 22 BLOCK DIAGRAM FOR THE ATTITUDE CONTROL FLOW SYSTEM

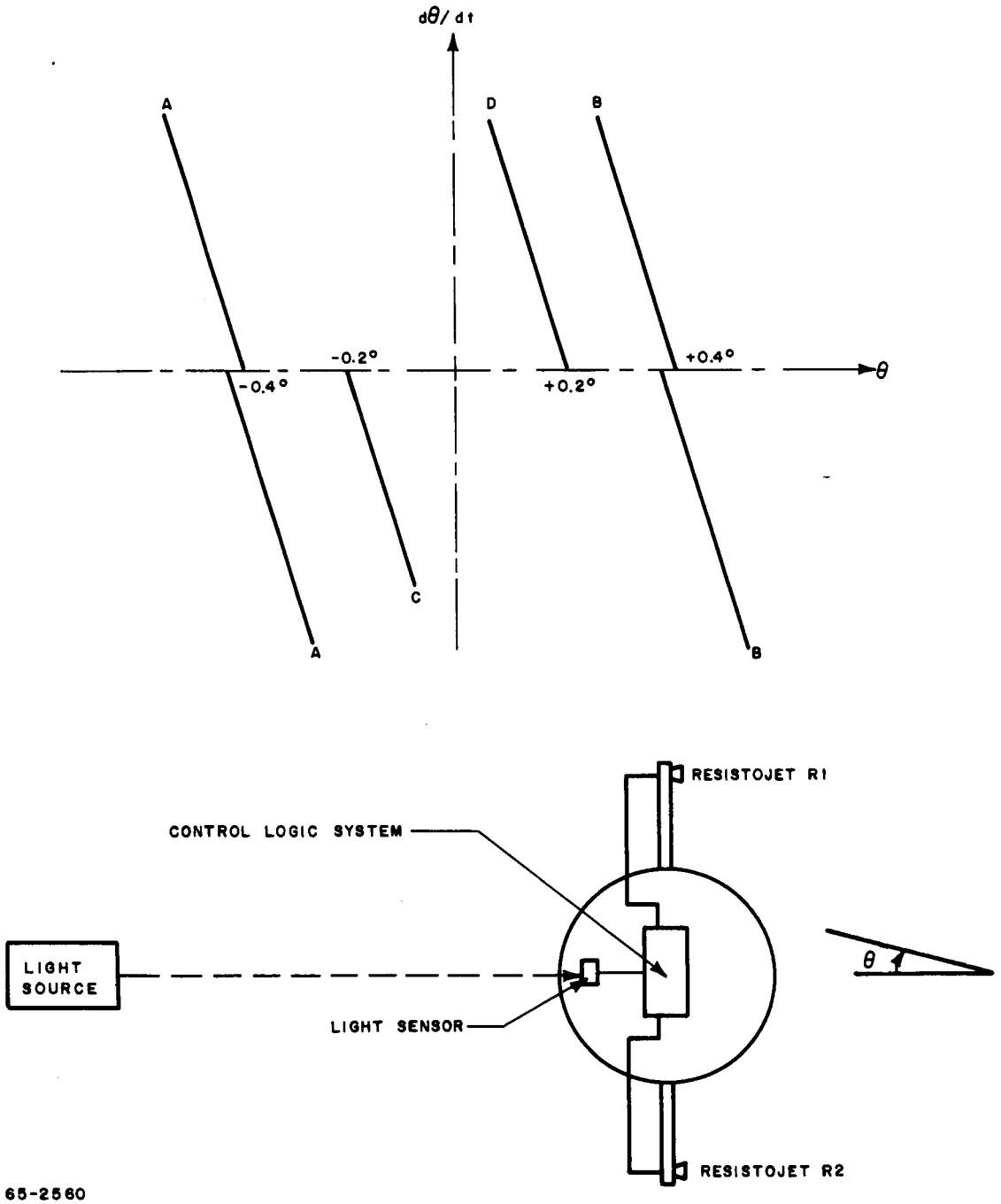

Figure 23 BASIC CONTROL LOGIC LINES FOR THE SINGLE AXIS RESISTOJET ATTITUDE CONTROL SYSTEM

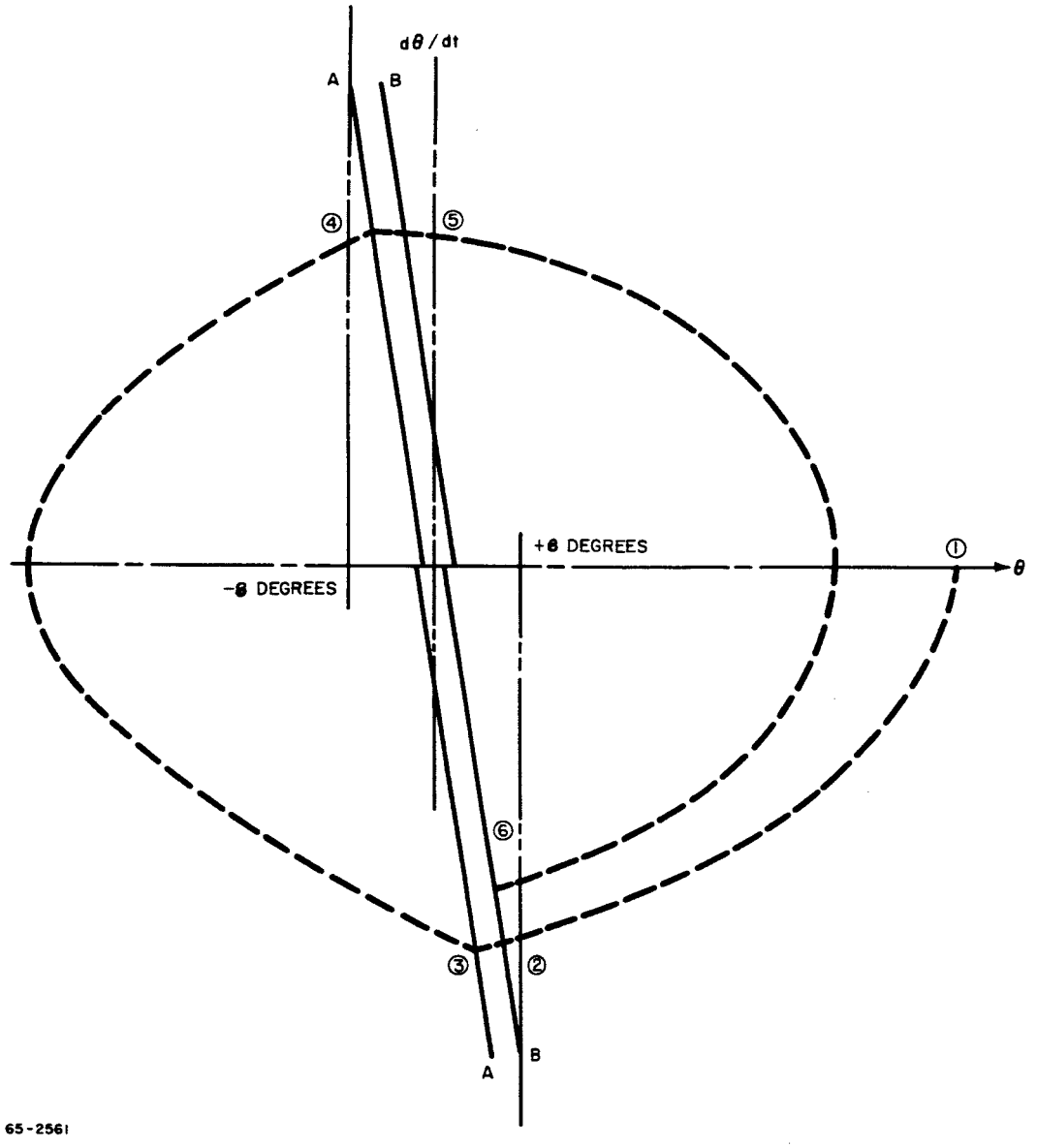

Figure 24 ILLUSTRATION OF LARGE ANGLE ACQUISITION

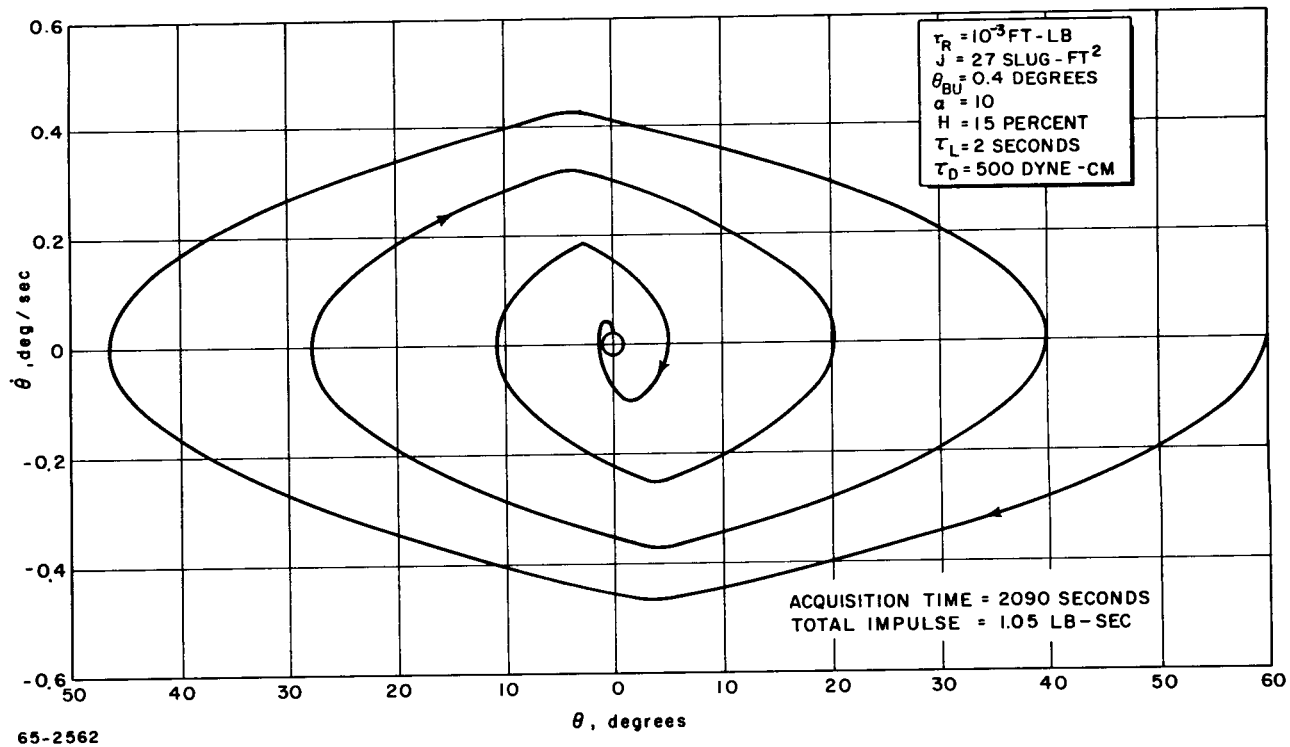

Figure 25 ANALOG COMPUTER SOLUTION FOR LARGE ANGLE ACQUISITION OF THE SINGLE AXIS TEST TABLE

The effect of disturbance torque on limit cycle operation is very strong. Operation can be either in a "hard" limit cycle or a "soft" limit cycle depending on the relative magnitude of the disturbance and control torques. The difference between these modes of operation can be explained by reference to figure 26. In this figure, it is assumed that the rate of rotation is small enough so that no change in θ occurs during the resistojet pulse, that is, the resistojet produces a step change in $d\theta/dt$. In the soft limit cycle as illustrated in the top sketch, the resistojet impulse produce by crossing line D is insufficient to drive the system to an intersection with line C ; instead, the disturbance torque changes the $d\theta/dt$, θ state along the dotted parabolic curve during the drift phase until line D is again crossed and the resistojet pulsed again. Thus, the resistojet is pulsed only once per cycle and the impulse from the distrubance torque is exactly balanced by the impulse from the resistojet. This mode of operation thus represents a minimum in fuel consumption and, for a given disturbance torque, the fuel consumption is independent of the thrust parameters (thrust, pulse length, moment arm length) so long as these parameters are such that operation in a soft limit cycle is maintained.

It should be noted here that a soft limit cycle need not be symmetrical as illustrated in figure 26. A. In figure 26. B a non-symmetrical soft limit cycle is illustrated; as is evident from this sketch, this type of cycle is non-repeating. The type of cycle encountered in any particular case depends on the acquisition or point of entry into the soft limit cycle. It should be emphasized again however that the fuel consumption and number of resistojet pulses is independent of the thrust parameters or the acquisition phase so long as soft cycle operation is maintained.

The dotted lines 1 and 2 on the symmetrical soft limit cycle sketch of figure 26 represent two different levels of disturbance torque for constant thrust parameters, line 1 representing the smaller disturbance torque. It is obvious that below some disturbance torque limit, the system will be over-driven and will cross control line C so that the resistojet in the opposite direction will be pulsed on. Thus, instead of exactly balancing the disturbance torque and having only one pulse per cycle, there will be two pulses per cycle and the two resistojets will be partially counterbalancing each other. This type of operation is called "hard" limit cycle operation and results in a significant increase in the fuel consumption relative to the soft limit cycle. If the disturbance torque is zero, it is apparent that the limit cycle must necessarily be "hard" and the operation will be as illustrated in parts C and D of figure 26; the drift phase here takes place at constant $d\theta/dt$ and the resistojet pulsing serves to reverse the rotation thus keeping the orientation within the desired limits. The path of the cycle repeats itself regardless of whether the cycle is symmetrical or non-symmetrical.

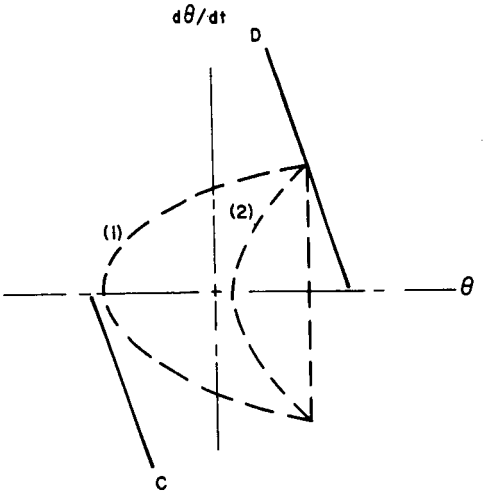

(a) SYMMETRICAL SOFT LIMIT CYCLE

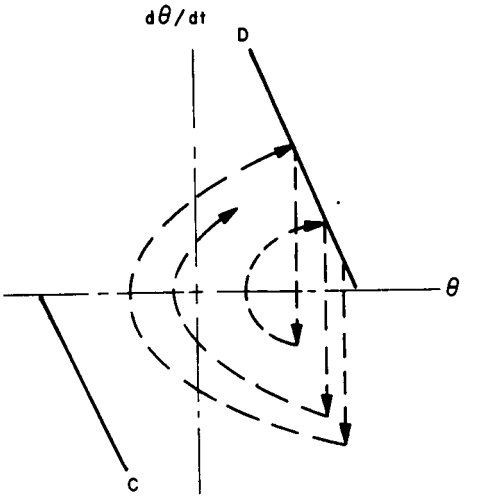

(b) NON-SYMMETRICAL SOFT LIMIT CYCLE

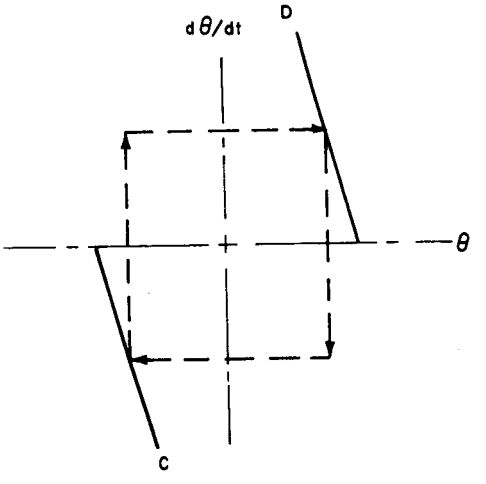

(c) SYMMETRICAL HARD LIMIT CYCLE – NO DISTURBANCE TORQUE

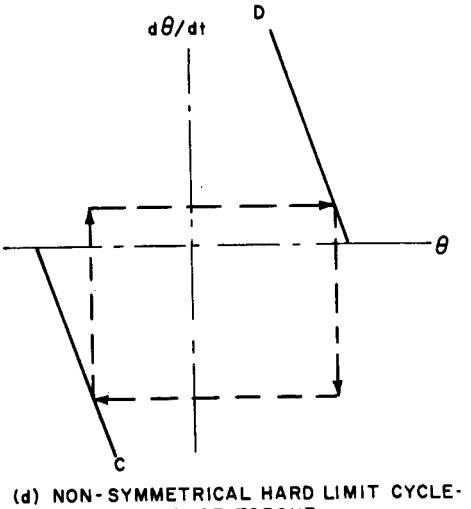

(d) NON-SYMMETRICAL HARD LIMIT CYCLE – NO DISTURBANCE TORQUE

65-2563

Figure 26 ILLUSTRATIONS OF HARD AND SOFT LIMIT CYCLE OPERATION

It should be noted that the slope (or rate dependence) of the control lines is necessary to provide stability to the control cycle. This is illustrated in figure 27 where the hard limit cycle with no disturbance torque is presented for the practical situation where the two resistojet pulses do not exactly balance each other. In these sketches, the pulse controlled by line C is assumed to be 1-1/2 times as large as that controlled by line D. In the top sketch with rate dependent control lines the path starting from point 1 returns to that point after two cycles and the control system is basically stable. In the bottom sketch with control lines dependent only on θ, the imbalance in impulse from the two opposing resistojets results in the system "jumping out" of the limit cycle control as shown; this system is thus basically unstable and requires backup lines.

The case of a hard limit cycle with a disturbance torque is illustrated in figure 28. In the coast phase, the rate of rotation, $d\theta/dt$, changes due to the disturbance torque. The exact path followed by the hard limit cycle operation with a disturbance torque is strongly dependent on the state of entry into the cycle, that is, on the acquisition phase. A non-repeating type of cycle can be obtained as illustrated in figure 28. A. Under certain conditions of entry into the cycle, a combination soft and hard limit cycle can be produced as is illustrated in the three pulse repeating cycle of figure 28. The soft limit cycle results when the control torque changes the rate to a small negative value so that the disturbance torque can change $d\theta/dt$ to a positive value before the opposite control line is reached. The occurrence of these soft limit cycles will increase in frequency as the disturbance torque is increased for constant thrust parameters. At zero disturbance torque, no soft limit cycles will occur; as the disturbance torque is increased, more and more soft limit cycles will occur until the disturbance reaches or exceeds a limiting value where the operation will be completely in the soft limit cycle.

2. Estimated Performance of the Single Axis Control Logic System

The basic goals in optimizing the attitude control system performance for a mission are: (i) To minimize fuel consumption, (ii) to minimize the pulsing frequency for reliability reasons.

The test to be performed on the NASA, Lewis air bearing table will eventually permit study and comparison of various control systems as well as a test of the resistojet itself and the associated mechanical equipment. The first test to be performed will be primarily a test of the control logic and system.

This section presents the calculated performance which might be expected from the system as a function of the air bearing disturbance torque level. At this time the disturbance torque level characteristic of the NASA, Lewis

air bearing has not been completely established; however, it is probably less than 1000 dyne-cm. The nominal characteristics of the first resistojet single axis attitude control system, which will be referred to as Avco Resistojet Attitude Control System - Model 1, are presented in Table VI.

a. Soft Limit Cycle Operation

The fuel consumption as mentioned previously is a minimum for soft limit cycle operation and, for a given disturbance torque should be independent of the thrustor characteristics as long as their magnitude is in the range to maintain soft limit cycle operation. The fuel consumption for operation in this mode can be written as:

$$m_s = \frac{\tau_D T}{980\, I_{sp} L} \tag{4}$$

where

m_s = total mass of propellant required for soft limit cycle operation, gmm

τ_D = disturbance torque, dyne-cm

T = total time period of control, sec

I_{sp} = specific impulse of propellant, $\frac{\text{gmf sec}}{\text{gmm}}$

L = moment arm length, cm

The number of resistojet pulses or of soft limit cycles can be written as:

$$N = \frac{\tau_D T}{980\, F L t_R} \tag{5}$$

where

N = number of required resistojet pulses

F = thrust force from resistojet, gmf

t_R = thrust time per pulse, sec.

The duty cycle or ratio of time of thrust on to total time is given by

$$f = \frac{\tau_D}{980\, F L} = \frac{\tau_D}{\tau_R} \tag{6}$$

where τ_R is the torque generated by the resistojet in dyne-cm. Thus, very simple relations suffice to describe the performance of a system controlling in a "soft" limit cycle with a constant disturbance torque. The quantities m_s, N, and f are presented in figure 29 as a function of disturbance torque for the conditions expected in the NASA, Lewis test. As indicated in the following discussion, the limiting disturbance torque above which soft limit cycle operation is postitively obtained is 575 dyne cm for the nominal operating conditions.

b. Maximum Thrust Force for Soft Limit Cycle Operation

The question now arises as to when the limiting value of disturbance torque is reached for soft cycle operation. This occurs when the control impulse bit is just sufficient to rotate the table to the opposite control line as discussed in the preceding section. A quantitative relation will now be derived for this limit. Consider the following sketch.

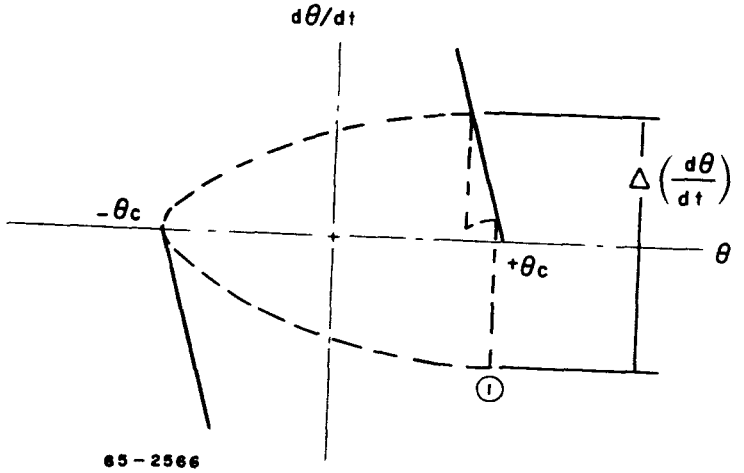

It is desired to determine the magnitude of the thrust force below which soft limit cycle operation will definitely occur. The worst possible case must be considered and is illustrated in the above sketch. This worst case occurs when the limit cycle is entered so that the control pulse decreases the rate very close to zero. When this occurs, the same control line is again crossed producing a second pulse in the cycle. Thus, the control pulse in this case is two pulses from the resistojet instead of one. In the following discussion, the small change in orientation between the two pulses will be assumed to be negligible.

The relation describing the table motion in the absence of the control torque is:

TABLE VI

AVCO SINGLE AXIS RESISTOJET ATTITUDE CONTROL SYSTEM - MODEL 1
NOMINAL PERFORMANCE CHARACTERISTICS

Engine Thrust Level	5×10^{-4} lbs
Engine Specific Impulse	120 sec
Power Level	5 to 10 watts
Engine Chamber Pressure	30 psia
Ammonia Flow Rate	4.2×10^{-6} lbs/sec
Heat-up Period (No Propellant Flow)	1 second
Fixed Pulse Length (Inner Lines)	4 seconds
One-Half Deadband (Inner Lines)	0.2 deg
One-Half Deadband (Outer Lines)	0.4 deg
Table Moment of Inertia	27 slug-ft^2
Initial Attitude	2.25°

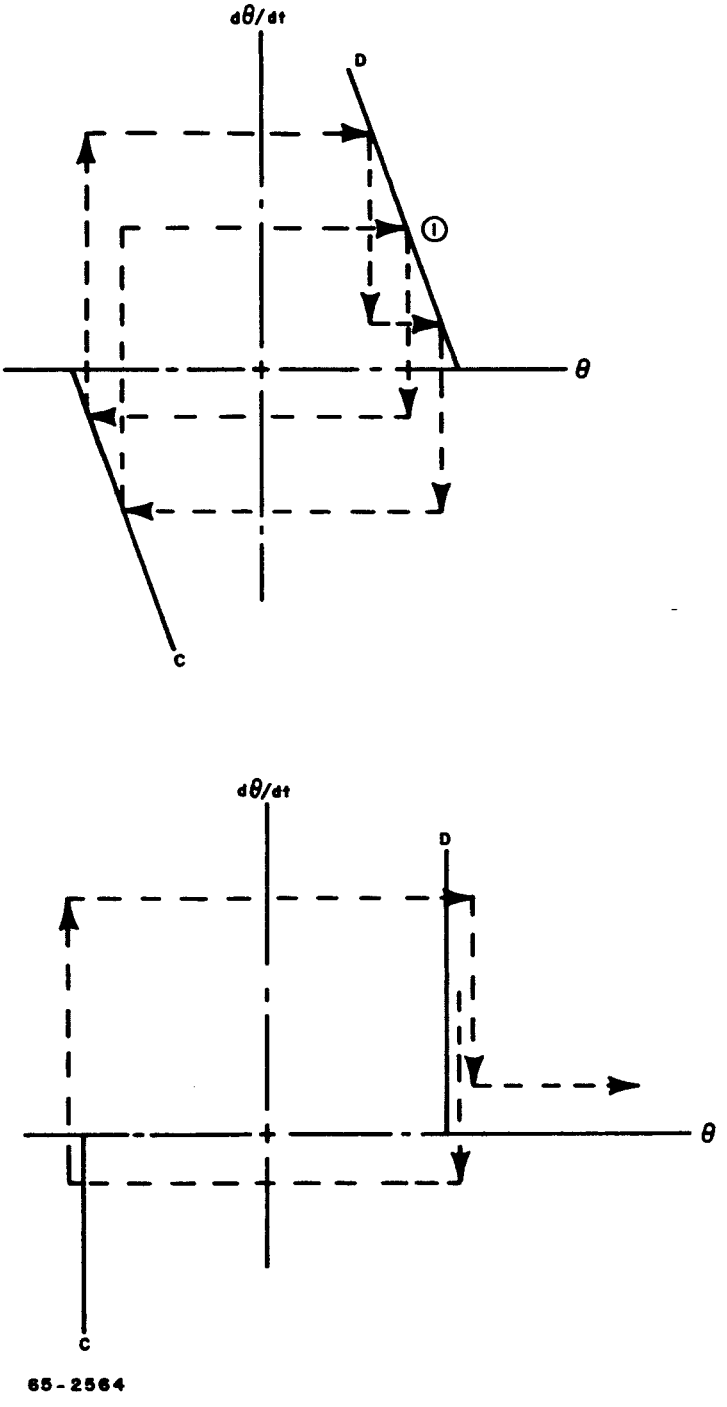

Figure 27 ILLUSTRATION OF CONTROL LOGIC STABILITY DUE TO RATE DEPENDENCE OF CONTROL LINES

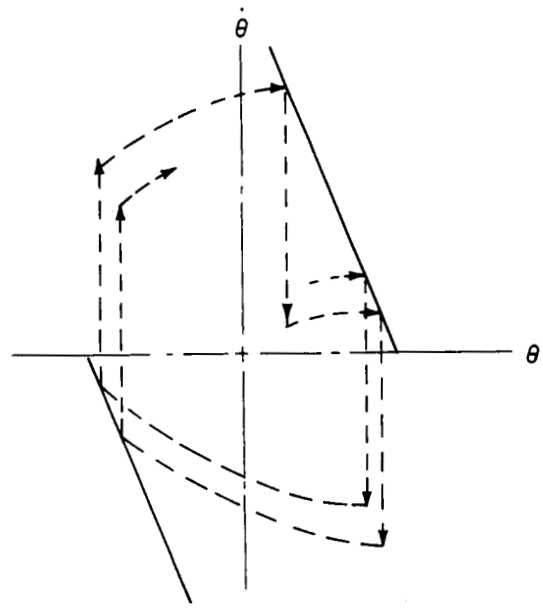

a) HARD LIMIT CYCLE WITH DISTURBANCE TORQUE

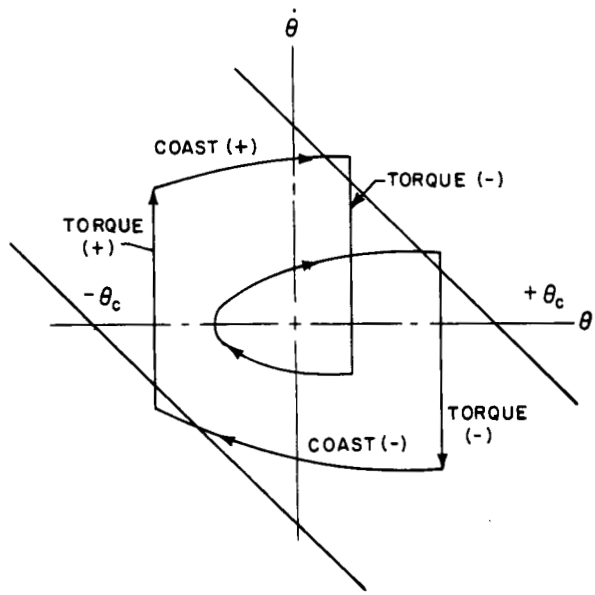

b) THREE PULSE COMBINATION HARD-SOFT LIMIT CYCLE

65-2565

Figure 28 ILLUSTRATIONS OF HARD LIMIT CYCLE WITH DISTURBANCE TORQUE

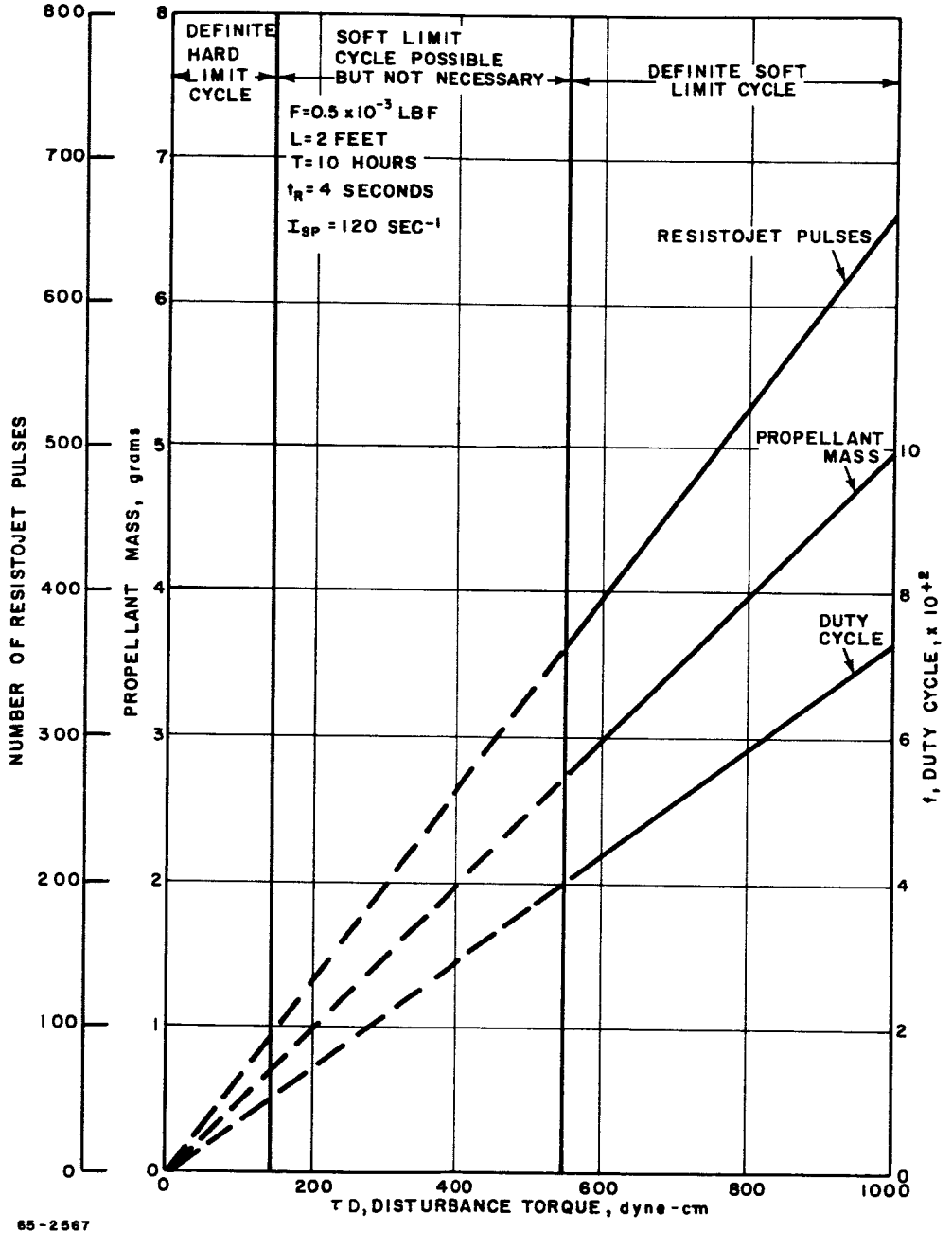

Figure 29 TOTAL PROPELLANT CONSUMPTION, TOTAL NUMBER OF RESISTOJET PULSES AND RESISTOJET DUTY CYCLE VERSUS DISTURBANCE TORQUE FOR SOFT LIMIT CYCLE OPERATION OF THE NASA LEWIS ACS TEST BED

$$\frac{d^2\theta}{dt^2} = \frac{\tau_D}{J} \tag{7}$$

where J is the table moment of inertia. Let condition (1) represent $t = 0$ where $\theta = \theta_o$ and $\frac{d\theta}{dt} = \left(\frac{d\theta}{dt}\right)_o$.

Integration thus gives with these initial conditions:

$$\left(\frac{d\theta}{dt}\right)^2 - \left(\frac{d\theta}{dt}\right)_o^2 = 2\frac{\tau_D}{J}(\theta - \theta_o) \tag{8}$$

Assuming that the control pulse width is short relative to the total cycle time, the two control pulses produce a step change in $d\theta/dt$. Thus,

$$\Delta\left(\frac{d\theta}{dt}\right) = 2t_R \frac{\tau_R}{J} \tag{9}$$

where t_R is the pulse time of the resistojet. Also, at position (1), $(d\theta/dt)_o = -1/2\ \Delta\left(\frac{d\theta}{dt}\right)$. Now, assuming that the slope of the control line is small and can be neglected, $\theta_o = \theta_c$. Substitution of these quantities gives

$$\left(\frac{d\theta}{dt}\right)^2 = \left(\frac{t_R \tau_R}{J}\right)^2 + 2\frac{\tau_D}{J}(\theta - \theta_c) \tag{10}$$

The limit for soft cycle operation occurs where $d\theta/dt = 0$ at $\theta = -\theta_c$ or

$$t_R \tau_R \leq 2\sqrt{\tau_D \theta_c J} \tag{11}$$

Letting $\tau_R = F_1 L$, where F_1 is the limiting thrust force and L the moment arm, gives

$$F_1 \leq \frac{2}{L t_R}\sqrt{\tau_D \theta_c J} \tag{12}$$

Thus, for a given disturbance torque and pulse time, any force greater than F_1 may or may not result in hard limit cycle operation depending on the entry point into the cycle; any force smaller than F_1 will always result in soft limit cycle operation, however.

Another limiting case can be derived which gives the maximum thrust force, F_2, with which soft limit cycle operation can be obtained. Soft limit cycle operation cannot be guaranteed in the region $F_1 \leq F \leq F_2$, however, and the mode of operation will depend on the entry point into the cycle. Whenever the thrust force is greater than F_2, the limit cycle will always be hard, although soft limit branches may occur in the cycle. The limiting force, F_2, is given by the cycle with only one pulse rather than two as was the case for determining F_1. In this case

$$\Delta \left(\frac{d\theta}{dt}\right) = t_R \frac{\tau_R}{J} \tag{13}$$

and

$$F_2 = \frac{4}{Lt_R} \sqrt{\tau_D \theta_c J} \tag{14}$$

Thus,

$$F_2 = 2F_1 \tag{15}$$

In figure 30, a plot of F_1 and F_2 as a function of disturbance torque is given and the areas of definite soft limit cycle, possible but not necessary soft limit cycle, and definite hard limit cycle operation are indicated for the nominal conditions of the NASA, Lewis test. It is seen that at a thrust level of 0.5×10^{-3} lbf, a disturbance torque greater than 575 dyne cm will definitely insure soft limit cycle operation while one less than 144 dyne cm will definitely insure hard limit cycle operation. For disturbance torques between these two values, the operation may be in either a soft or hard limit cycle, depending on the entry point into the cycle. The type of control operation to be experienced in the NASA, Lewis test will thus depend on the disturbance torque of the table.

c. Hard Limit Cycle Operation

The performance of the system when operating in a hard limit cycle is difficult to determine analytically and reliance must be placed primarily on the analogue computer calculations. The situation is further complicated by the fact that the cycle of operation, and hence the fuel consumption, is strongly dependent on the entry point into the cycle and also on the disturbance torque. The only case which permits limited study analytically is the zero disturbance torque case. Consider the following non-symmetrical hard limit cycle with zero disturbance torque.

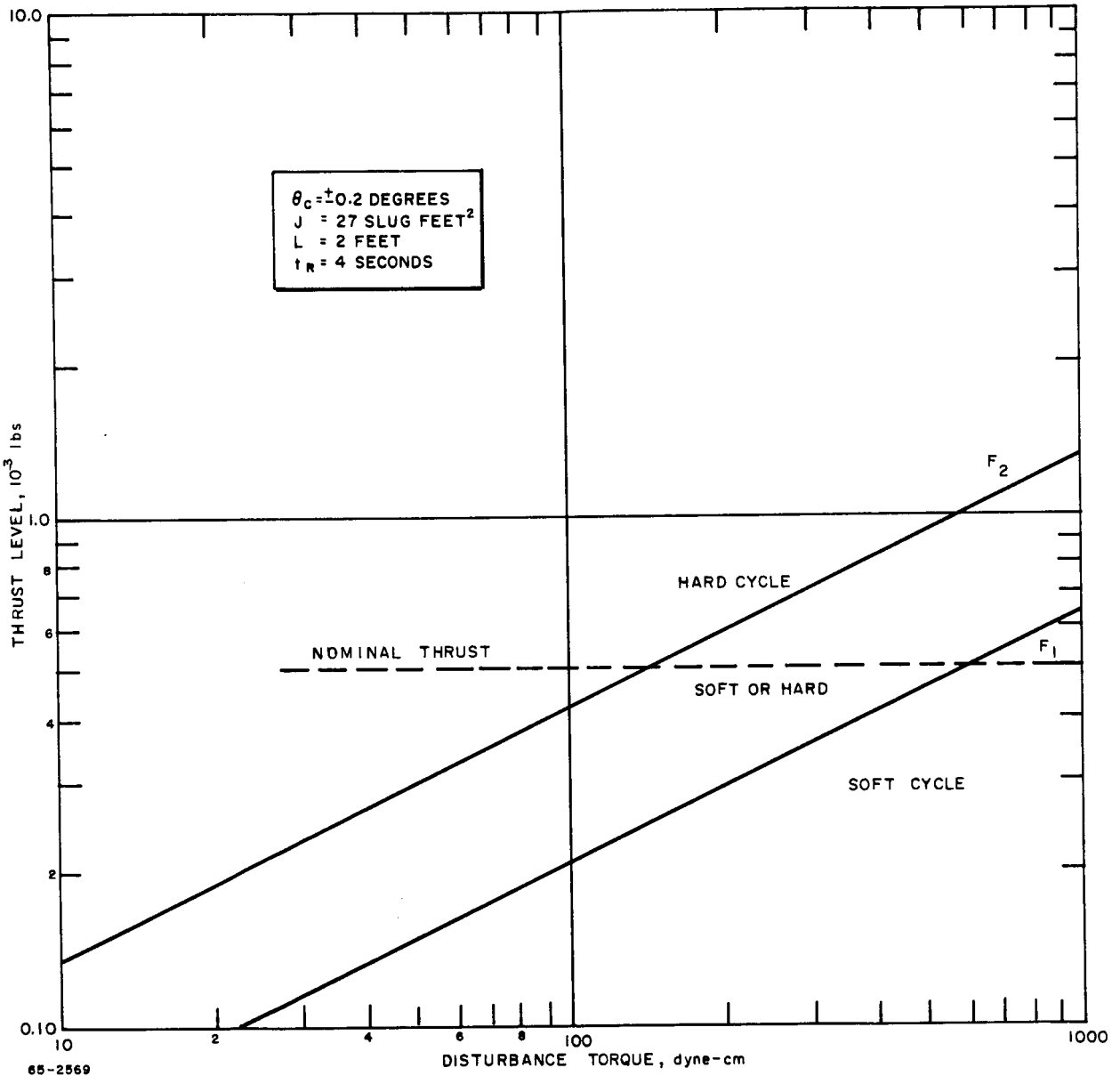

Figure 30 THRUST FORCE LIMITS FOR SOFT CYCLE OPERATION VERSUS APPLIED DISTURBANCE TORQUE

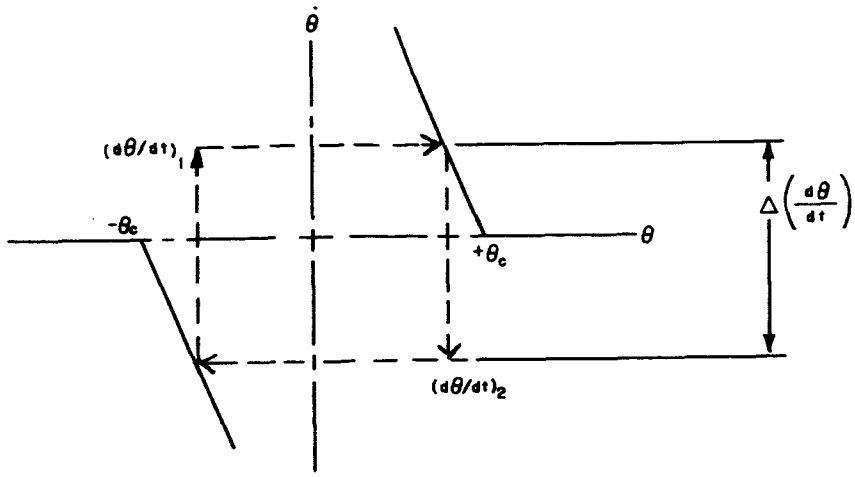

65-2568

The effect of the slope in the control lines will be neglected and it will be assumed that the pulse duration relative to the total cycle duration is negligible. Then, the time per cycle is

$$t_c = \frac{2\theta_c}{(d\theta/dt)_1} - \frac{2\theta_c}{(d\theta/dt)_2} = 2\theta_c \left[\frac{1}{\dot{\theta}_1} - \frac{1}{\dot{\theta}_2}\right] \tag{16}$$

Now,

$$\dot{\theta}_2 = \dot{\theta}_1 - \Delta\dot{\theta}$$

Substitution gives

$$t_c = 2\theta_c \frac{\Delta\dot{\theta}}{\dot{\theta}_1(\Delta\dot{\theta} - \dot{\theta}_1} \tag{17}$$

The cycle time thus depends not only on the $\Delta\dot{\theta}$ value but also on whether the control cycle is symmetrical or unsymmetrical and how unsymmetrical.

The values of $\dot{\theta}_1$ which gives a maximum and a minimum in t_c are:

Minimum t_c : $\dot{\theta}_1 = \frac{\Delta\dot{\theta}}{2}$, that is, a symmetrical cycle.

Maximum t_c : $\dot{\theta}_1 = \Delta\dot{\theta}$, that is, one leg of the cycle falls on the zero rate line giving an infinite cycle time.

For a symmetrical cycle, which gives the maximum fuel consumption, substitution of $\dot{\theta}_1 = \frac{\Delta\dot{\theta}}{2}$ gives:

$$t_c = 8\frac{\theta_c}{\Delta\dot{\theta}} \tag{18}$$

Now,

$$\Delta\dot{\theta} = \frac{r_R t_R}{J} \tag{19}$$

Substitution gives

$$(t_c)_{min} = 8\frac{\theta_c J}{r_R t_R} \tag{20}$$

There are two pulses per cycle; the duty cycle can thus be written as:

$$f = \frac{2t_R}{t_c} = 1/4\ \frac{r_R t_R^2}{\theta_c J} \tag{21}$$

The fuel consumption can be written as

$$m_s = f\frac{F}{I_{sp}}\ T = 1/4\ \frac{(F t_R)^2 L T}{\theta_c J I_{sp}} \tag{22}$$

For the nominal parameters of the NASA, Lewis test, the calculated values are (for the zero disturbance torque case):

$(m_s)_{max} = 2.90$ grams

$(t_c)_{min} = 314$ sec

$(f)_{max} = 2.55 \times 10^{-2}$

The above analysis represents the limit of simple analysis of the hard limit cycle case. Analogue simulation of the system has been performed however and the results are presented in figure 31 in terms of duty cycle versus disturbance torque. The plots are for pulse times, t_R, of 2, 3, and 4 seconds. In addition, the curve is given for the case of control between the outer backup lines only (pulse time t_R, = 0) moved into $\theta_c = 0.2°$. These curves are for acquisition from an attitude of 2.25°. For the $t_R = 3$ sec and $t_R = 4$ sec cases, the duty cycle (or fuel consumption) first rises rapidly with increasing disturbance torque reaching a maximum in both cases at 100 dyne cm. The duty cycle then decreases rapidly with increasing disturbance torque and approaches

soft limit cycle operation as represented by the solid line. For the t_R = 4 sec case, soft limit cycle occurs for disturbance torques above 300 dyne cm and for the t_R = 3 sec case, above about 200 dyne cm. For the t_R = 2 sec case, the duty cycle is very close to the soft limit cycle case above a disturbance torque of 50 dyne cm. It is apparent from this plot that for this particular acquisition angle, a pulse length of 2 sec would be the most desirable operating condition. It is also apparent that control without the inner control lines is better than operation with the control lines and pulse lengths of three or four seconds.

In figure 32, a plot is given of the limit cycle period as a function of the duty cycle with pulse duration and disturbance torque as parameters. This plot is based on the results of analogue computer calculations, including those presented in figure 31, to determine the soft limit cycle boundary. This boundary as given is thus applicable only for an acquisition angle of 2.25°. As discussed earlier, the fuel consumption for soft limit cycle operation is dependent only on the disturbance torque and the constant disturbance torque lines are thus vertical lines on this plot (constant duty cycle).

d. Acquisition Performance

The acquisition performance of the system has been determined using results from the analogue simulation. In figure 33, the acquisition performance is given in terms of the time and impulse required for acquisition as a function of the initial acquisition angle.

3. Electronic Circuitry for the Control Logic System

a. Circuit Description

The functional diagram of the control system is illustrated in figure 34. An attitude sensor provides a signal linearly proportional to the angle of divergence, θ, with a null at θ = zero and with a maximum range of ± 8° for the single axis test. This signal is amplified by a preamplifier and an absolute magnitude amplifier whose output amplitude is proportional to the magnitude of the error signal and is always positive in polarity. The output of the absolute magnitude amplifier goes to the lead network, the purpose of which is to provide a rate dependent signal for operation of the switching logic. The gain of the lead network can be represented as:

$$F(p) = \frac{1 + a\tau_L p}{1 + \tau_L p} \qquad (23)$$

where

$F(p)$ = gain factor for lead network

$p = \frac{d}{dt}$

a = constant in network

τ_L = constant in network, sec.

The significance of this gain factor can be seen by expanding $F(p)$ in a power series about $p = 0$ and neglecting terms higher than first order:

$$F(p) = 1 + (a - 1)\tau_L p \tag{24}$$

The output signal from the lead network, Z, is thus given (with θ as the input to the network) as:

$$Z = \theta[1 + (a - 1)\tau_L p]$$

$$= \theta + (a - 1)\tau_L \frac{d\theta}{dt} = \theta + (a - 1)\tau_L \dot{\theta} \tag{25}$$

This output which depends on both θ and $d\theta/dt$ then goes to the Schmitt triggers which provide switching signals when Z reaches either of two fixed values set in the Schmitt trigger circuitry. Thus, at the point where switching occurs, which represents the control line in the phase plot, Z is a fixed value, Z_{sw}. The equation of the control line on the phase plane is thus:

$$Z_{sw} = \theta_c + (a - 1)\tau_L \dot{\theta}_c \tag{26}$$

or

$$\dot{\theta}_c = \frac{Z_{sw}}{(a - 1)\tau_L} - \frac{1}{(a - 1)\tau_L}\theta_c \tag{27}$$

$$\dot{\theta}_c = \text{constant} - \frac{1}{(a - 1)\tau_L}\theta_c \tag{28}$$

Thus, in the phase plane plot, the slope of the control line is $-\frac{1}{(a - 1)\tau_L}$ as illustrated below:

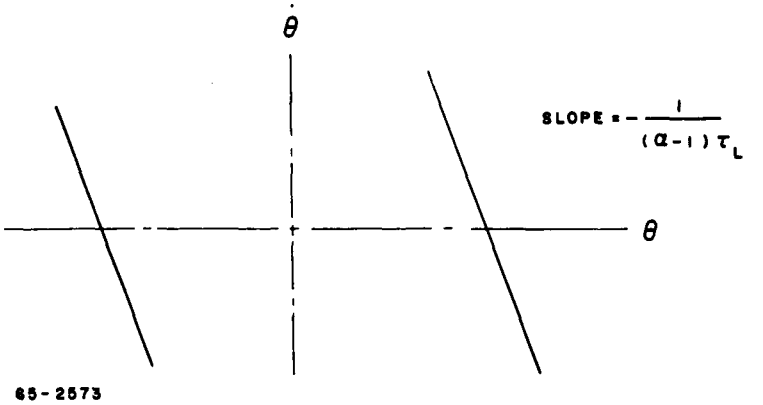

65-2573

Referring back to the signal output from the lead network of figure 34 now, this output goes to two Schmitt trigger circuits. The two Schmitt triggers are set to trigger at different signal levels and the sequence of events resulting in the operation of a resistojet is different depending upon which Schmitt is triggered. For the lower signal level Schmitt, which is triggered when the error angle of the light sensor is 0.2° at $\dot{\theta} = 0$ (inner control lines), the sequence is as follows:

The error signal energizes the Schmitt trigger which in turn energizes the first monostable multivibrator. Trigger of the multivibrator turns on the power supply for the resistojet heaters; the polarity detector determines which resistojet heater is turned on by means of an "and" circuit requiring two simultaneous signals (from heater power supply and polarity detector) before power is passed. The multivibrator operates for a preset time to provide time for the resistojet to be heated to the operating temperature without propellant flow. For the initial tests the heat-up time has been set at 1 second. At the end of the one second heat-up period, the monostable multivibrator returns to its stable state and triggers the second monostable multivibrator. The second multivibrator triggers the heater power supply thus maintaining power to the resistojet heater and, at the same time, supplies a signal to the valve "and" circuits. The "and" circuit receiving a signal from both the polarity detector and second multivibrator then passes the signal to the valve solenoid allowing propellant to flow through the heated resistojet providing thrust. The heater and valve remain energized through the delay period of the second monostable multivibrator and become deenergized when the multivibrator returns to its stable state. For the initial tests (Resistojet Single Axis Attitude Control System-Model 1) the propellant pulse length has been preset at 4 seconds.

The above sequence is used for the low level signals to give a "fixed duration pulse". The second Schmitt trigger is used for higher level signals and over-rides the effect of the first Schmitt trigger. The sequence for the second Schmitt, which is triggered at an error angle of 0.4° (backup or acquisition control lines) is as follows.

The error signal triggers the Schmitt which turns on the heater supply and the first monostable multivibrator; the resistojet heater receiving a signal from the polarity detector as well is the one turned on. At the end of the one second heating period, the multivibrator returns to its stable state and supplies a signal to an "and" circuit. If the Schmitt trigger is supplying a signal to the "and" circuit also, a signal is passed to the "and" circuits controlling the valves. The "and" circuit also receiving the polarity detector signal then passes a signal to the proper valve solenoid opening that valve. The valve and heater remain energized continuously until the error signal drops to the level at which the Schmitt trigger returns to its untriggered state.

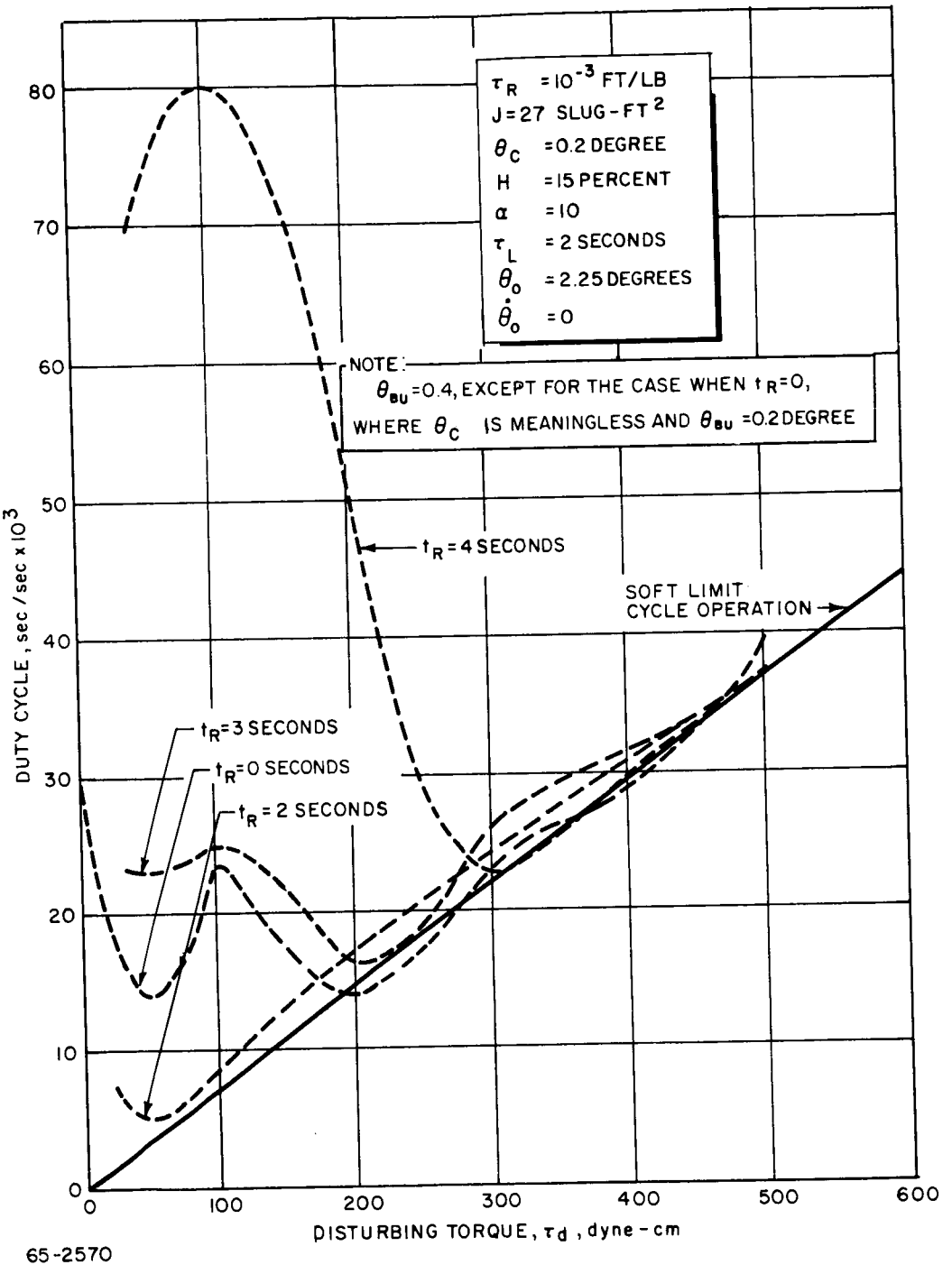

Figure 31 DUTY CYCLE VERSUS DISTRUBANCE TORQUE FOR DIFFERENT INNER LINE FIXED PULSE WIDTHS

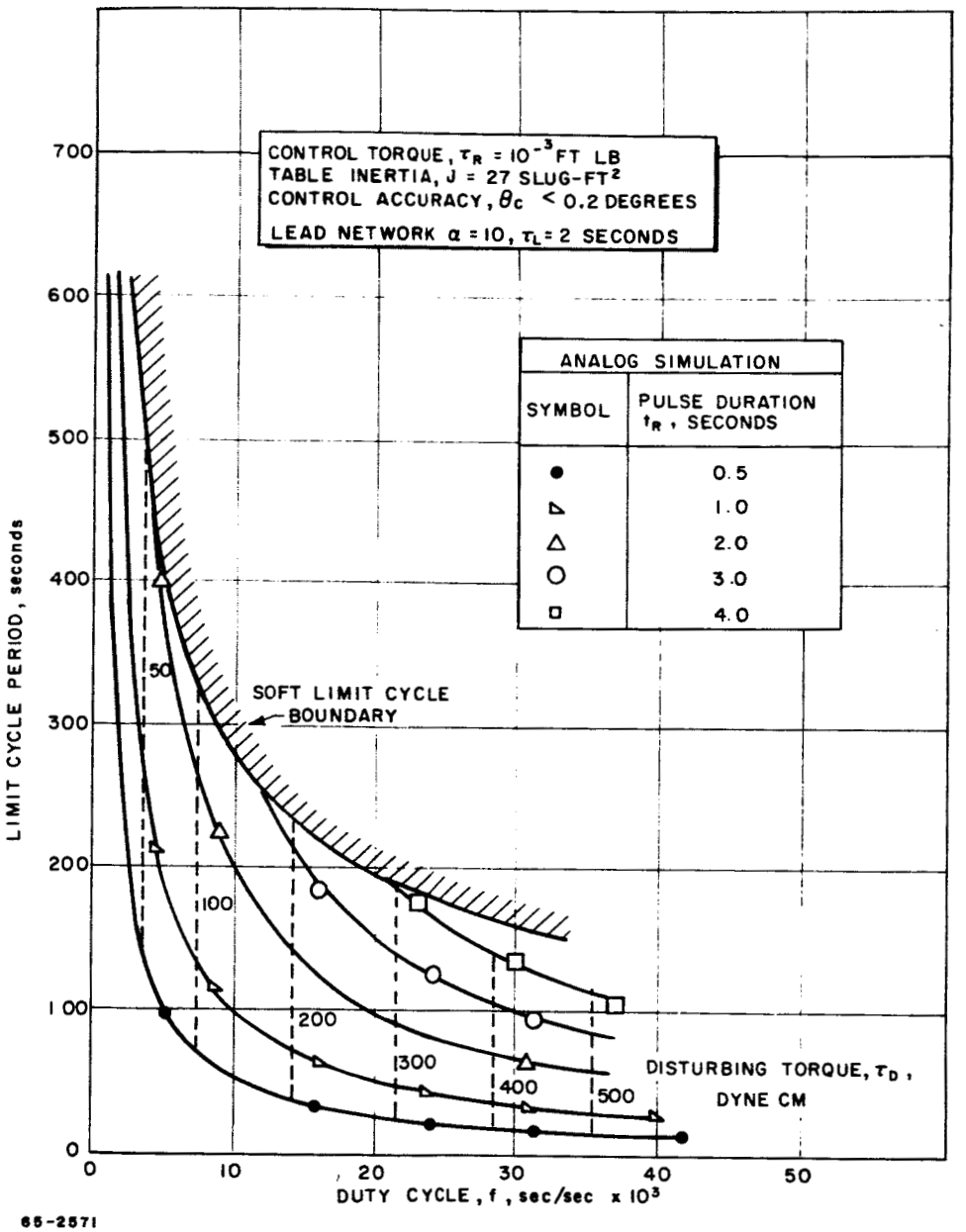

Figure 32 LIMIT CYCLE PERIOD VERSUS DUTY CYCLE FOR DIFFERENT INNER LINE FIXED PULSE WIDTHS

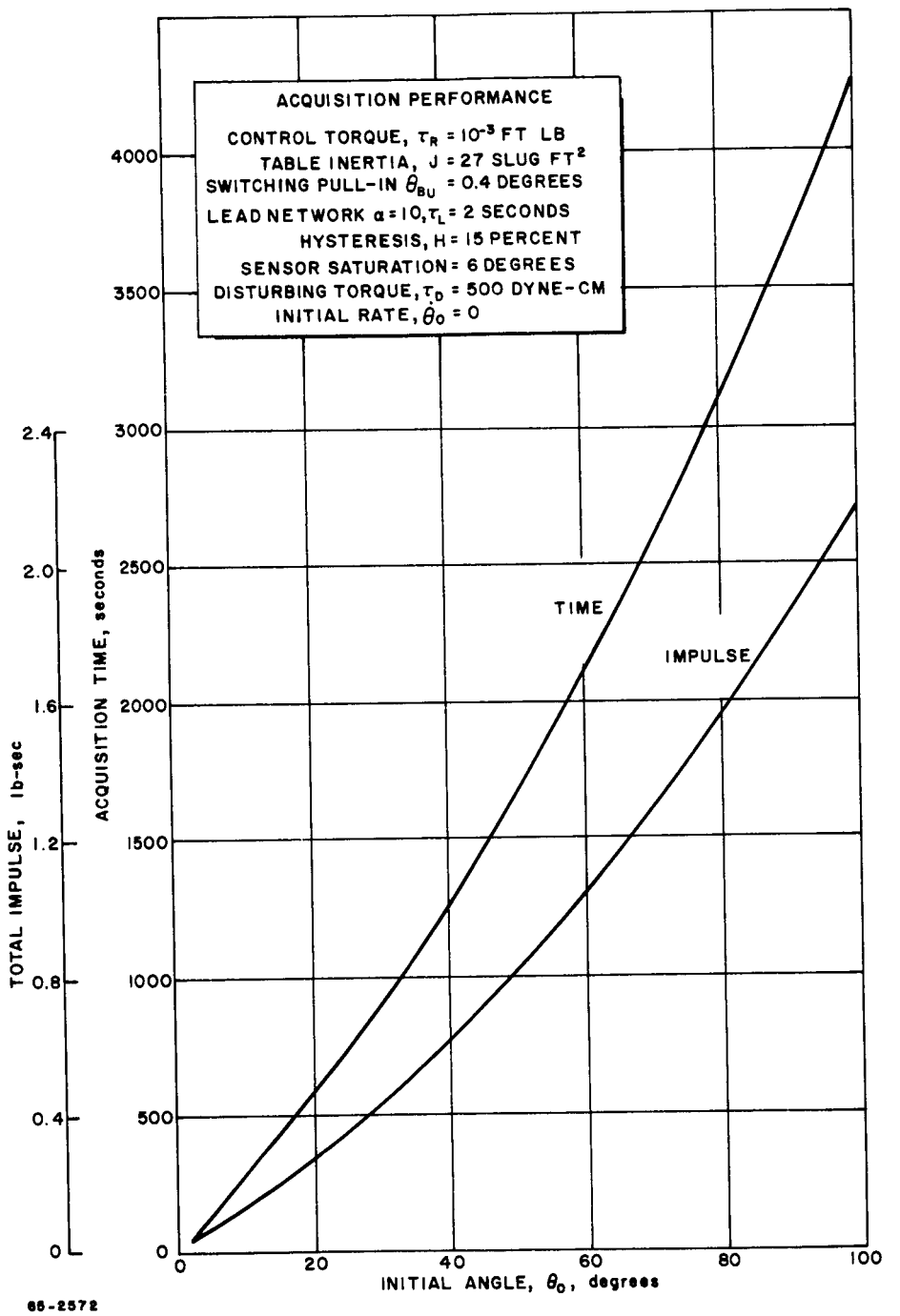

Figure 33 ACQUISITION TIME AND TOTAL ACQUISITION IMPULSE VERSUS ACQUISITION ANGLE

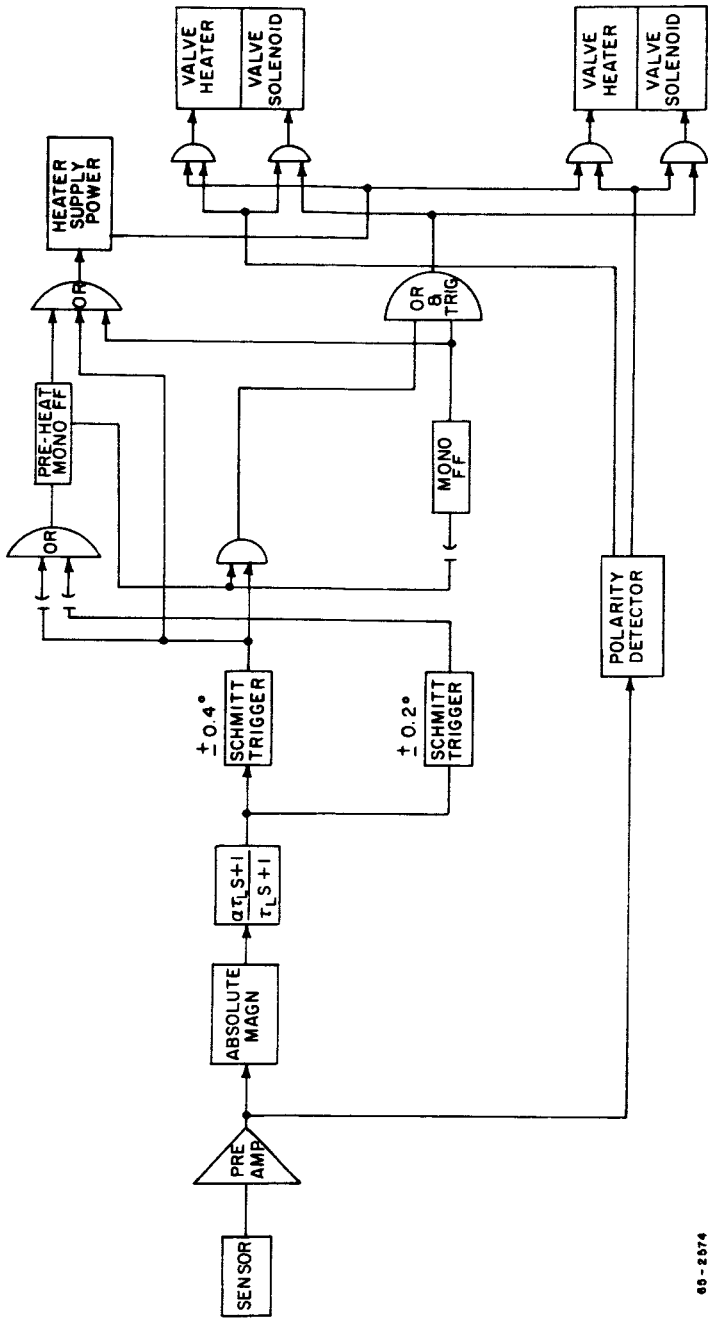

Figure 34 FUNCTIONAL DIAGRAM OF THE CONTROL LOGIC SYSTEM

The polarity detector is necessary since the output of the absolute magnitude amplifier is always positive regardless of whether the signal polarity is positive or negative. The polarity detector detects the polarity of the error signal and provides outputs to the "and" circuits controlling the resistojet heaters and valve solenoids so that the proper heater and valve are energized. The polarity detector also serves the purpose of eliminating separate positive and negative channels, thereby reducing the number of components in the system.

The control electronics as described above have been fabricated and tested. Results of the breadboard testing have shown that the system operates as desired. The physical system will now be described.

b. Control Logic Circuit Hardware

The control logic circuit test package for installation on the single axis air bearing contains the control logic circuitry for both the attitude control and station keeping resistojet thrustors and the power conditioning equipment for the attitude control resistojet thrustors. A circuit diagram for the control logic circuit is presented in figure 35.

A sectional view of the control logic test package is shown in figure 36. The package is approximately 6 1/2 inches long, 5 inches wide, and 4 1/4 inches high. The package is subdivided into three shelves. The bottom shelf, which is shown in figure 37 contains the resistojet attitude control engine power conditioning equipment; the middle and top shelves, shown in figures 38 and 39, contain the control logic circuitry for the resistojet attitude control and station keeping engines. A photograph of the control logic test package is presented in figure 40.

The station keeping resistojet heater and control valve are operated by telemetered commands. The logic circuit for this purpose is illustrated schematically in figure 41. The circuit consists of a monostable multivibrator, diode logic, and a power stage. This circuitry is also contained in the logic package.

4. Light Source and Sensor

The single axis resistojet attitude control optical system consists of an angle sensor and a collimated light source. The collimated light source will be structurally attached to the vacuum chamber in which the single axis tests are to be made and will project a collimated light beam toward the axis of the air bearing test table. The sensor will be mounted on the test table and will use the light source as an angular reference detecting angular error of the air bearing table position. The electrical error signal generated by the sensor is used as an input to the air bearing table control system commanding resistojet thrustor operation to reduce table position error to zero.

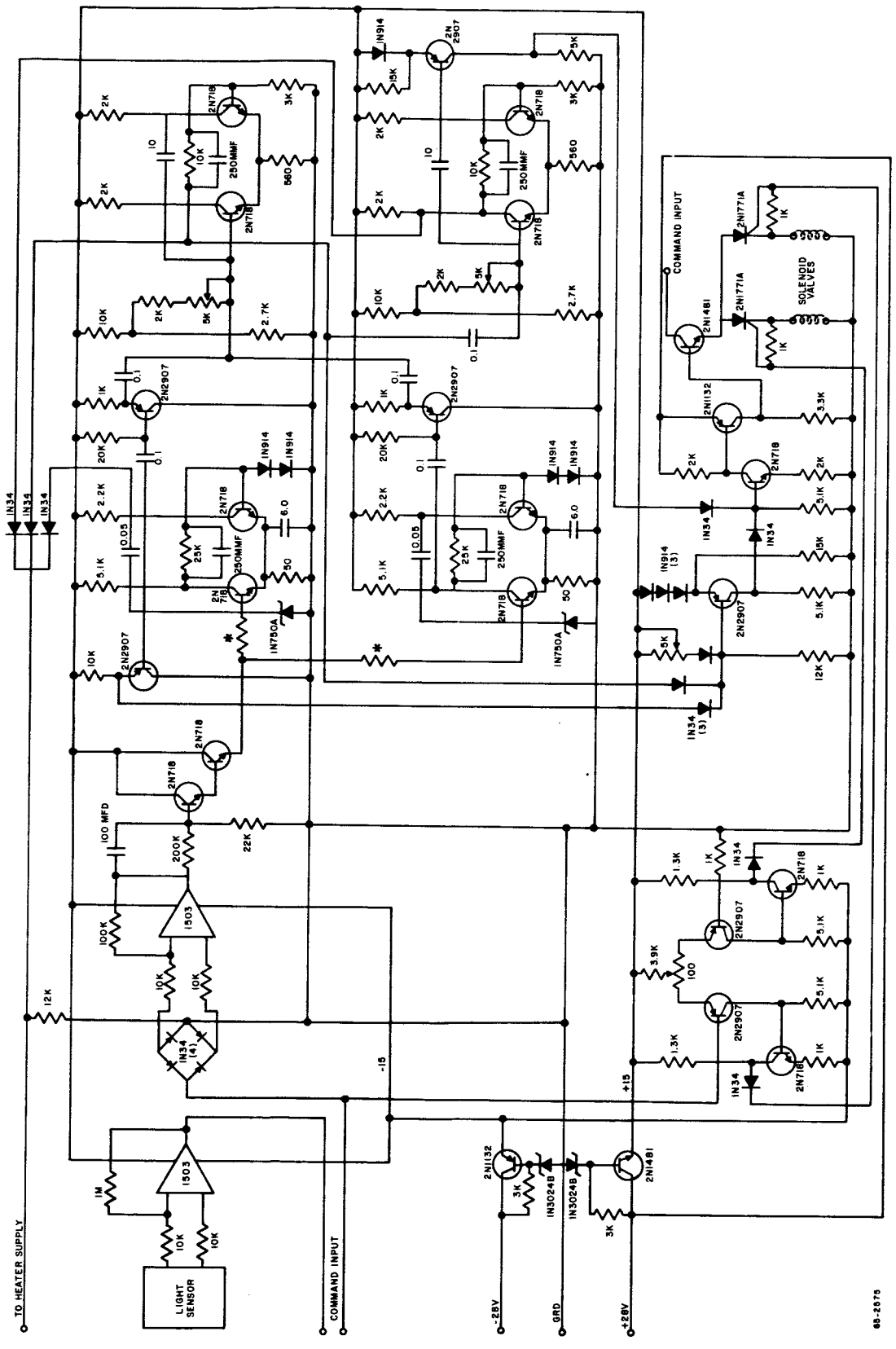

Figure 35 DIAGRAM FOR THE ATTITUDE CONTROL THRUSTORS CONTROL LOGIC CIRCUIT

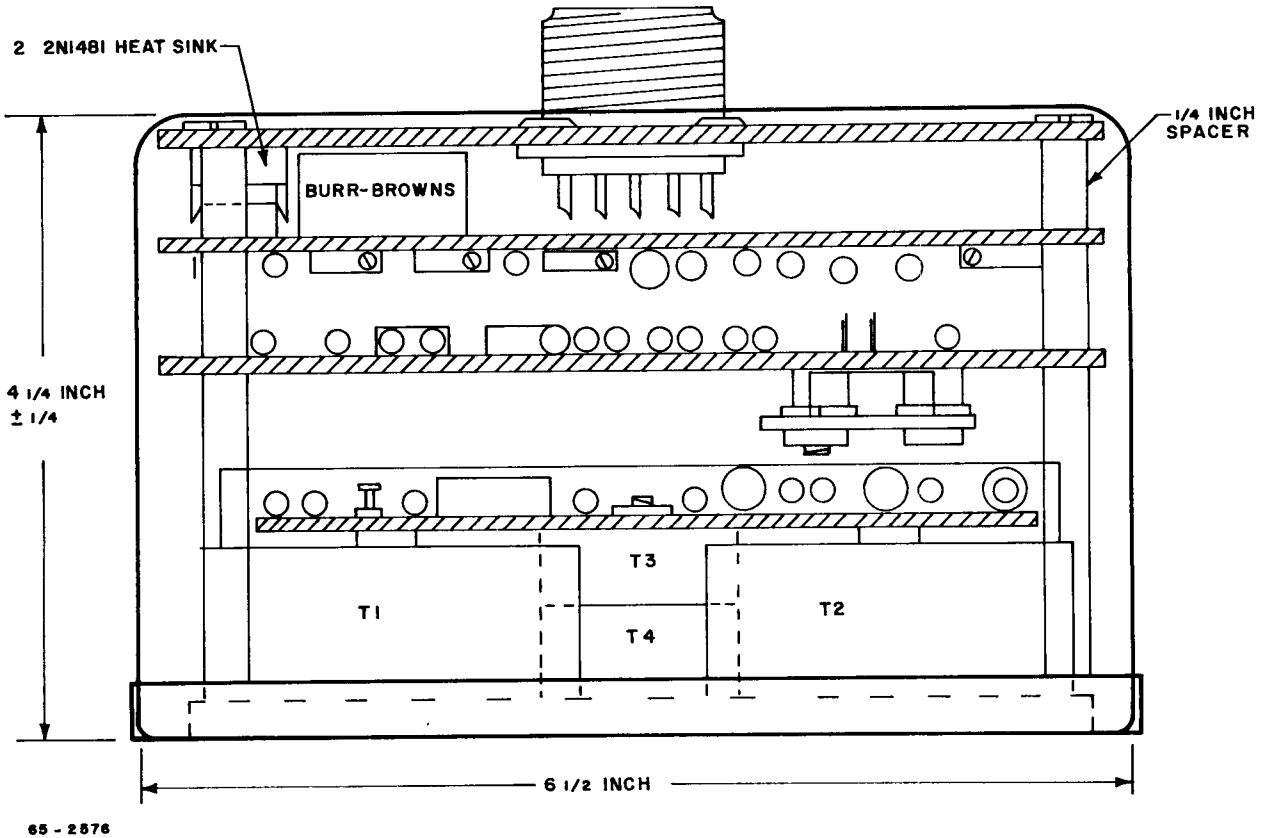

Figure 36 SECTIONED VIEW OF THE CONTROL LOGIC TEST PACKAGE

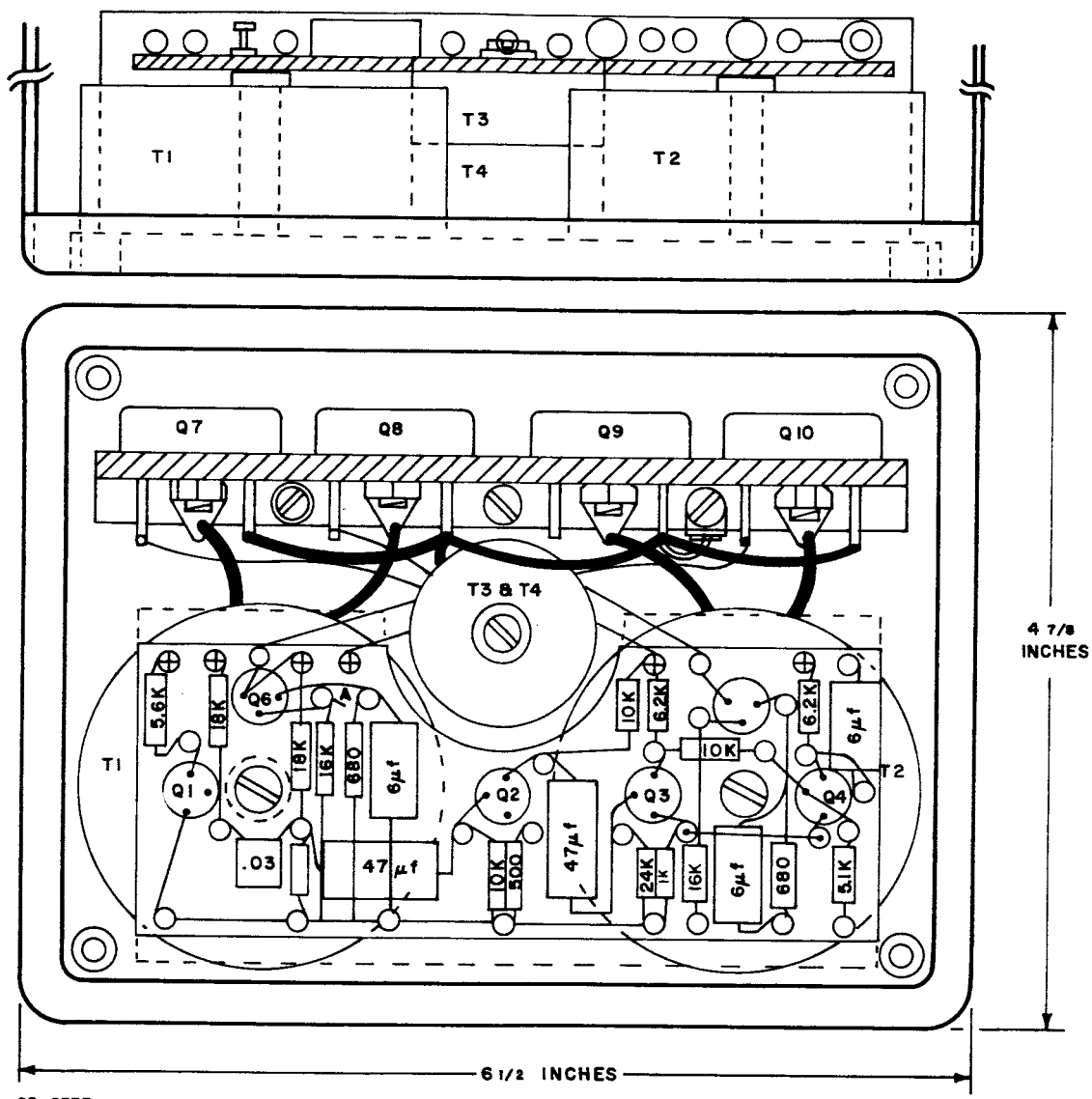

Figure 37 SECTIONED VIEW OF THE BOTTOM SHELF OF THE CONTROL LOGIC TEST PACKAGE

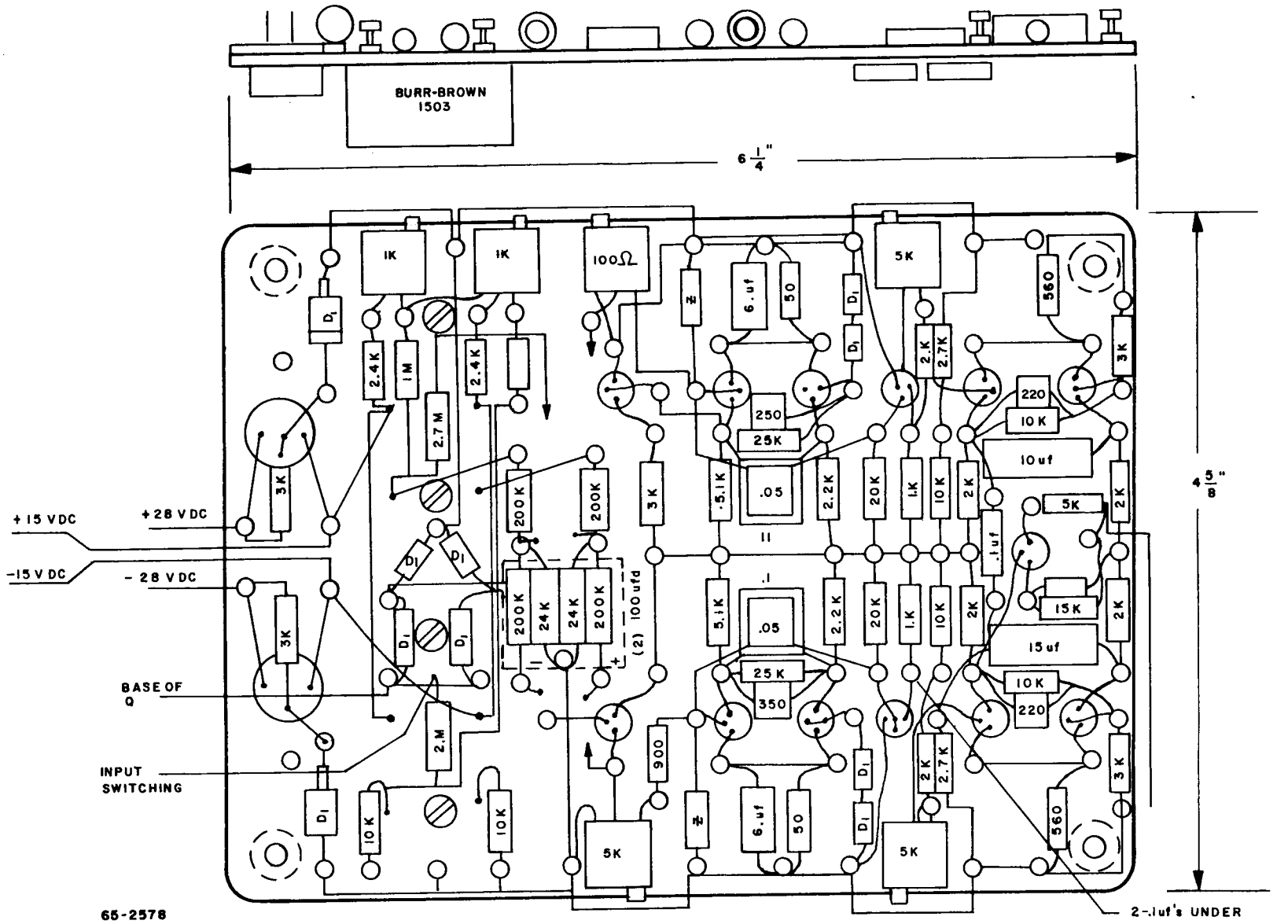

Figure 38 SECTIONED VIEW OF THE TOP SHELF OF THE CONTROL LOGIC TEST PACKAGE

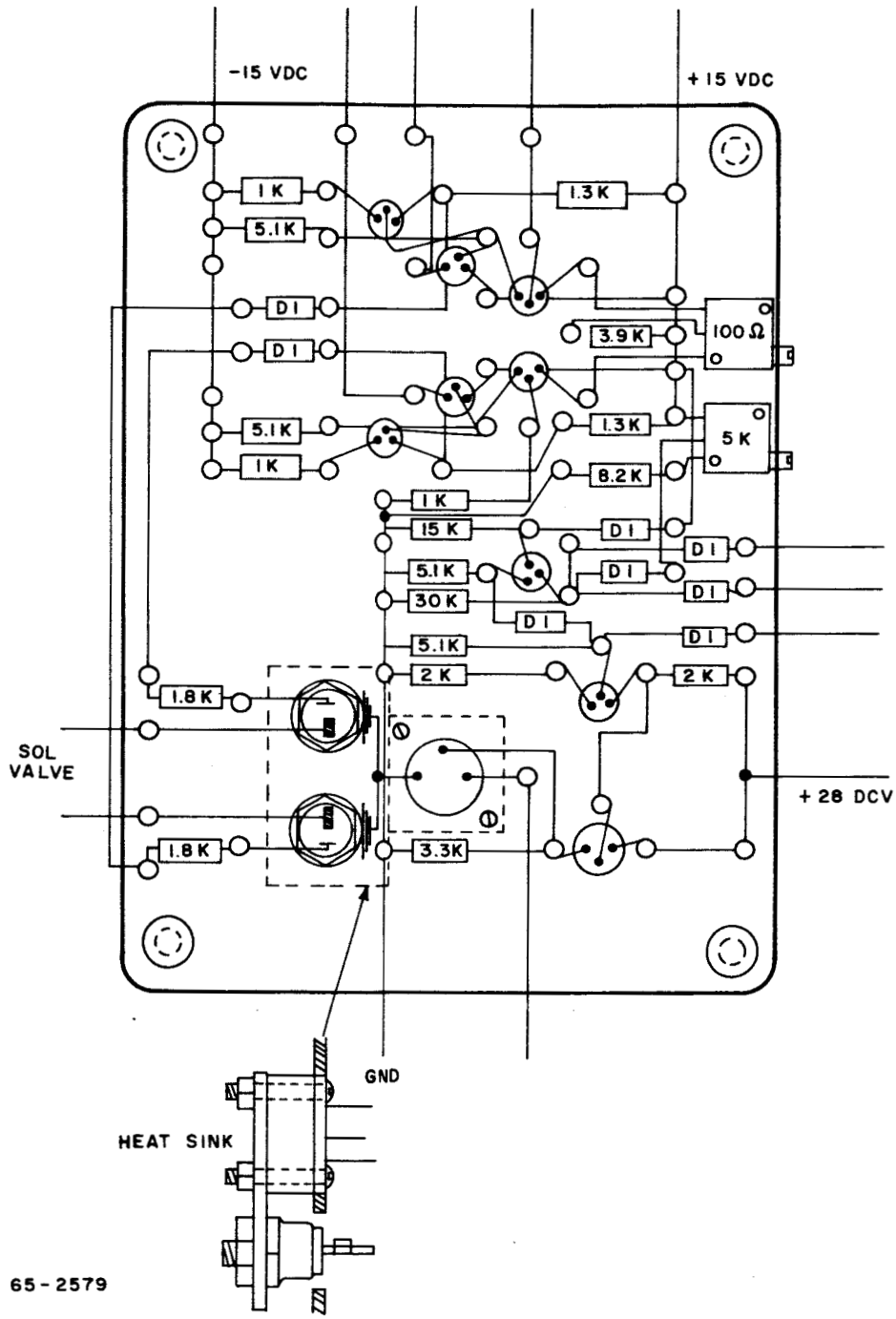

Figure 39 SECTIONED VIEW OF THE MIDDLE SHELF OF THE CONTROL LOGIC TEST PACKAGE

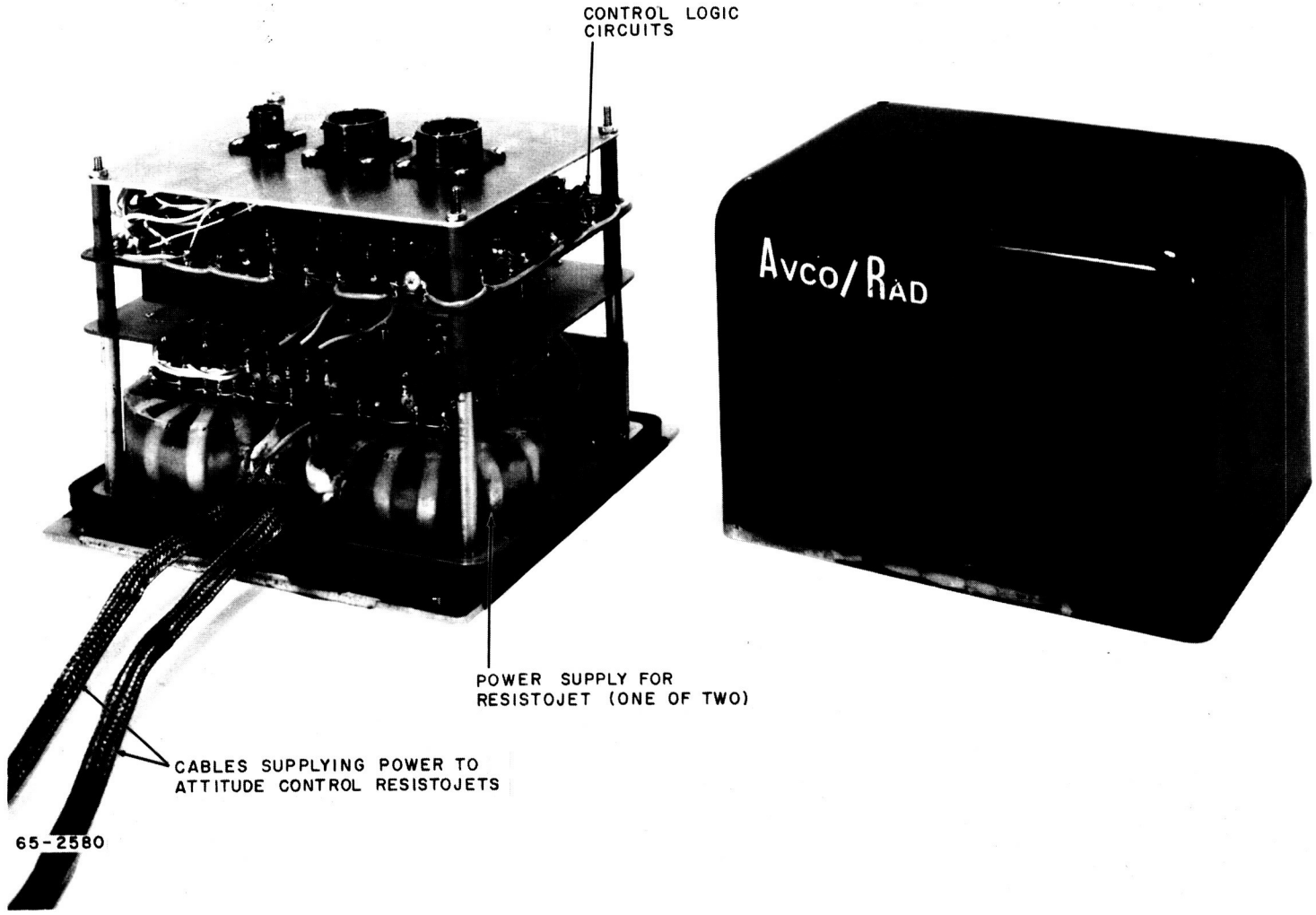

Figure 40 PHOTOGRAPH OF THE CONTROL LOGIC TEST PACKAGE

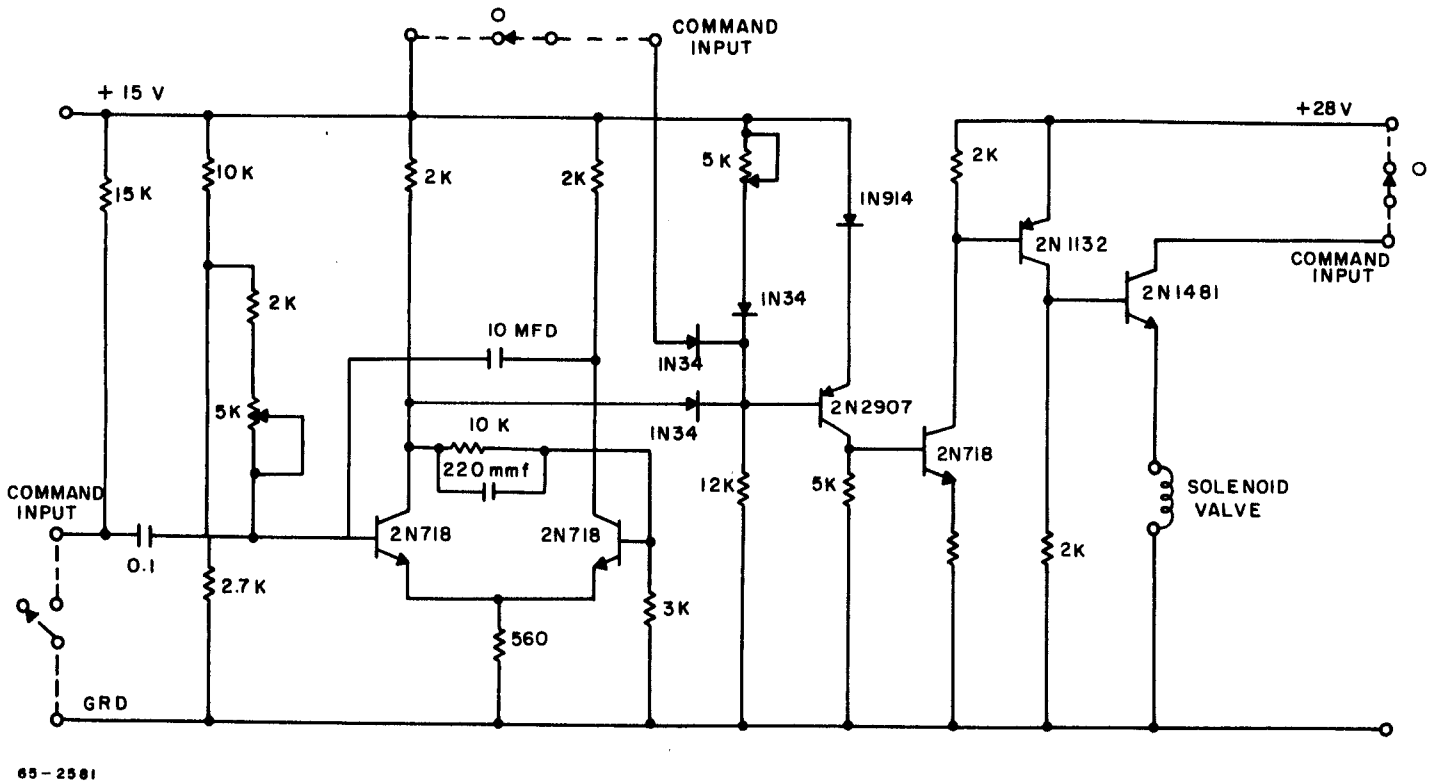

Figure 41 DIAGRAM FOR THE STATION KEEPING THRUSTOR CONTROL LOGIC CIRCUIT

a. Light Source

The light source uses a straight line filament incandescent lamp. The filament is spring loaded so that straightness is constantly assured. This lamp filament is located at the focal point of an Aero Elector lens, having a focal length of seven inches and an aperture of F:2.5.

The light source projects a collimated beam of light onto the angle sensor. Due to the collimated characteristic of the light beam, distance between the sensor and the light source is not critical. The lens diameter of the light source has been made larger than that of the sensor permitting small lateral displacements between the two units with full illumination of the sensor.

b. Angle Sensor

The optical angle sensor consists of a silicon photo voltaic semiconductor sensing element and a small lens system used to focus the light source reference on the sensing element. Operation of the sensor can be explained if we consider the sensing element to be made up of a pair of triangular shaped silicon photo voltaic cells as shown below.

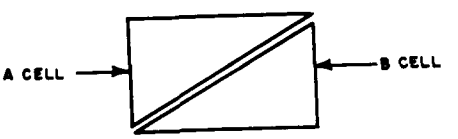

Project (optically) an image of a straight line filament on to this pair of cells as shown below.

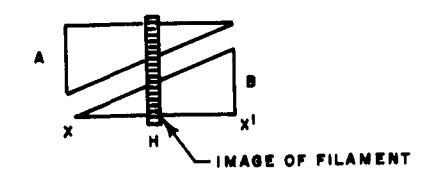

65-2582

When the filament is centered between X and X' the cells will receive equal amounts of illumination and therefore the voltage output of each cell will be identical. A displacement of the image in the X X' axis will cause the illumination on one cell to increase with a corresponding decrease on the other. The summation of the two cells will then produce a dc signal with magnitude and sign determined by the location of the image. Sensor null will occur when the image is centered on the cells.

The image of the filament is longer than the width of the cells so that a displacement in the vertical direction does not effect the output voltage. If the image is rotated about an axis perpendicular to the plane of the cells (about the optical axis) then, because of symmetry there will be no change in the null signal. The optical element of the angle sensor consists of a 3.5 inch focal length F:2 lens system. Therefore the image displacement is 0.06 inch per degree. The performance characteristics of the position sensor are summarized in table VII. Figure 42 is a photograph of the light source and light sensor.

C. POWER CONDITIONING PACKAGE

The basic power supply system will be furnished by NASA, Lewis. The system consists of a battery bank capable of supplying 60 amp hours at 24 vdc. The battery bank is connected to three voltage regulators, two of which supply a regulated voltage of + 28 vdc at a maximum rating of 2.13 amps; the other supplies a regulated voltage of -28 vdc at a maximum rating of 1.0 amps. In table VIII the power requirements for the 10 hour test are given for each regulated supply indicating that the power supply is ample for this test. The basic ± 28 vdc supply is conditioned by Avco RAD equipment to the desired levels required for the test; the power conditioning equipment will now be described.

Power is required for the resistojet heaters, for the solenoid-operated valves, and for the transducers and signal conditioning equipment. The solenoid valves all operate on 28 vdc and can be connected directly to the NASA power supply through the appropriate control system.

1. Power Supply for Attitude Control Resistojet Heaters

The resistojet engine has a resistance of approximately 0.1 ohms at operating temperature. For the desired power of about 10 watts for the test of the Resistojet Attitude Control System, Model 1, a voltage of 1 volt and current of 10 amps is required for heating the resistojet. To convert the 28 vdc supply to this level with a reasonable overall efficiency, the inverter circuit illustrated in figure 43 is used. The DC supply is converted to 10K cps AC with a square wave shape. This AC signal is then transformed to the desired voltage level. The high frequency results in a high efficiency and reduced output transformer size. In table IX the measured characteristics of the resistojet power supply to be used for the initial test are presented. The power output as well as the overall efficiency from the system is seen to be a strong function of load resistance.

TABLE VII

PERFORMANCE OF POSITION SENSOR

Scale Factor	30 m.v./degree
Linear Range ± 2%	± 3 degrees
Maximum Output	± 8 degrees
Null Stability (one week)	1 minute of arc

TABLE VIII

POWER AND TOTAL ENERGY REQUIREMENTS FOR A TEN HOUR SINGLE AXIS TEST OF THE RESISTOJET ATTITUDE CONTROL SYSTEM

A. Peak Current Drain from Regulated Power Supplies

Power Supply Number	Power Supplied to:	Maximum Current Drawn, amps	Power Required:
1	Attitude Control Resistojets	0.8	Intermittent
+28vdc, 2.7 amps	Station Keeping Resistojet	0.8	
	TOTAL	1.6	
2	Control Logic Package	0.16	Continuous
+28vdc, 2.7	Signal Condition Package	0.11	Continuous
amps	Pressure Regulating Valve	0.30	Intermittent
	TOTAL	0.57	
3	Sensor Excitation	0.580	Continuous
-28vdc, 1.0	Control Logic Package	0.050	Continuous
amps	Signal Condition Package	0.110	Continuous
	TOTAL	0.740	

B. Battery Drain for 10 Hour Test Period

1. Continuous Operation

Supply No. 2		0.270 amps
Supply No. 3		0.740 amps
	TOTAL	1.010 amps

Power = (28)(1.01) = 28.28 (watts)
Energy = 282.8 (watt hours)

2. Intermittent Operation

Acquisition - It is assumed that 0.5 hours is required for acquisition.

Resistojet Operation

Power = (0.8)(28) = 22.4 (watts)
Energy = (22.4)(0.5) = 11.2 (watt hours)

TABLE VIII (Concl'd)

Control Valve Operation

Power = (0.300)(28) = 8.4 (watts)
Energy = $(8.4)(\frac{1}{60})(0.5)$ = 0.07 (watt hours)

TOTAL Energy = 11.3 watt hours

Limit Cycle Control - It is assumed that limit cycle control occurs for 9.5 hours with a duty cycle of 5%.

Resistojet Operation

Energy = (22.4)(9.5)(0.05) = 10.6 (watt hours)

Control Valve Operation

Energy = $(8.4)(\frac{1}{60})(9.5)(0.05)$ = 0.07 (watt hours)

TOTAL Energy = 10.7 watt hours

3. Total Battery Drain = 316 watt hours

TABLE IX

OUTPUT CHARACTERISTICS OF THE HEATER POWER SUPPLY FOR RESISTOJET ATTITUDE CONTROL SYSTEM - MODEL 1

Load Resistance Ohms	RMS Voltage	Power, Watts Input	Output	Efficiency
0.052	0.40	12.60	3.08	24.4
0.104	0.76	11.48	5.55	48.4
0.215	1.27	8.40	7.50	89.3

12989-A

A. SOURCE (13.42 INCHES)

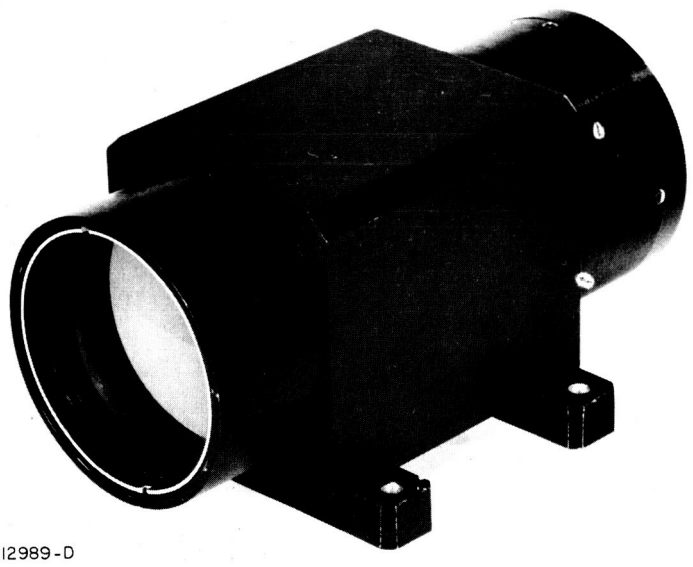

12989-D

B. LENGTHS SENSOR (4.81 INCHES)

Figure 42 PHOTOGRAPH OF LIGHT SOURCE AND POSITION SENSOR

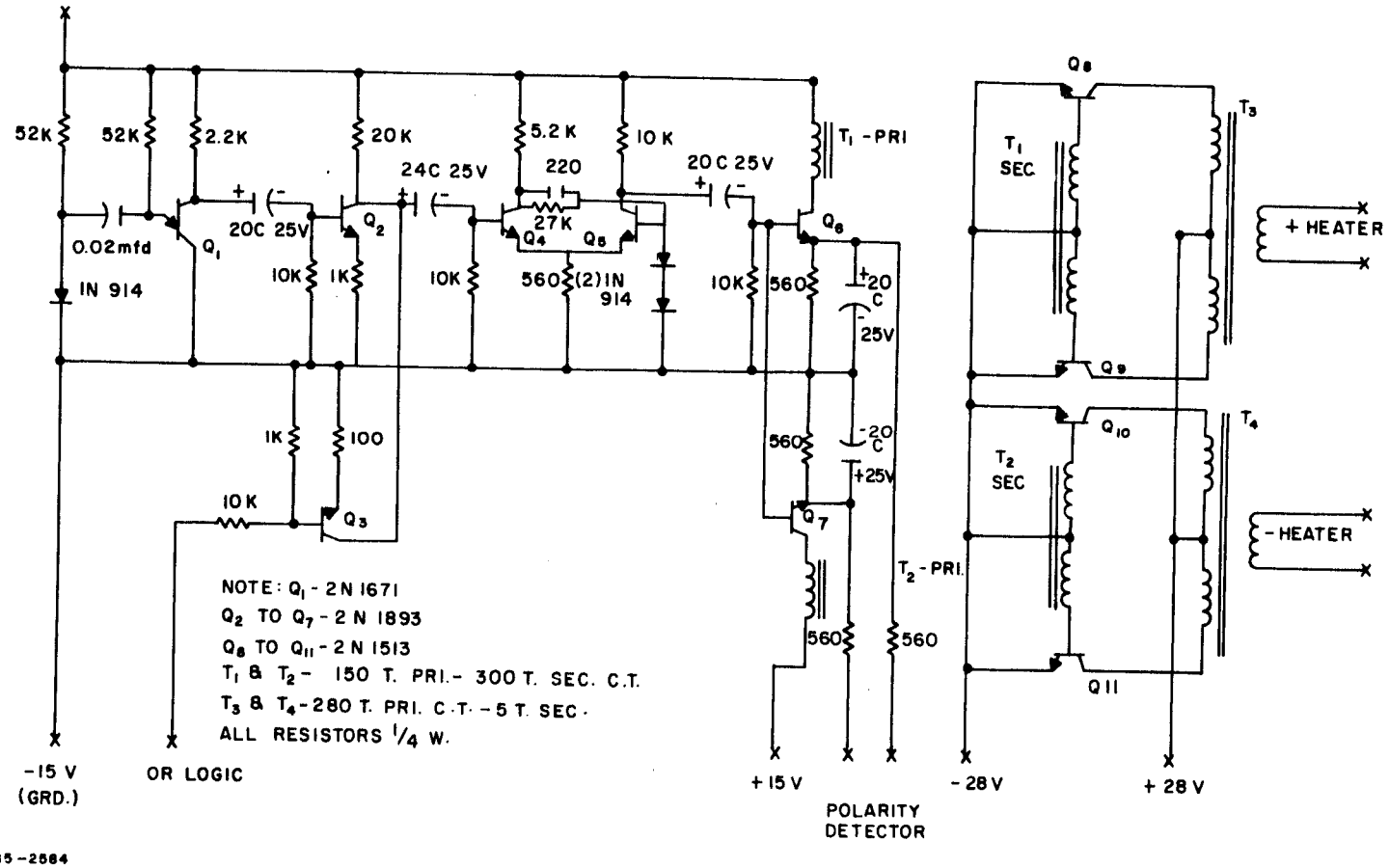

Figure 43 INVERTER CIRCUIT FOR THE ATTITUDE CONTROL RESISTOJET HEATERS

Work is presently underway aimed at improving the efficiency characteristics of the power conditioning equipment. A new power conditioning package has been designed which will provide a variable power level adjustable between 5 and 35 watts. This new power system will be compatible with existing electrical harness connections.

The power supply described above for the two attitude control resistojet thrustors is physically located in the Control Logic Test Package described previously.

2. Power Supply for the Station Keeping Resistojet Thrustor

The circuit schematic of the station-keeping resistojet heater power supply is shown in figure 44. Operation of the power supply is identical to that used with the attitude control resistojet heaters except that the operating signal is derived from "ground" command through telemetry rather than from the attitude control logic system. The station keeping power supply is physically located in the Signal Conditioning Test Package.

3. Signal Conditioning Power Supply Circuitry

The signal conditioning power supply provides regulated voltages necessary for the signal conditioning circuits for the various transducers and for the transducers themselves. This sytem converts + 28 vdc to regulated + 15 vdc and - 28 vdc to - 15 vdc. The - 15 vdc is further attenuated by resistive divider networks to the - 7 vdc, - 5 vdc, and - 4 vdc levels necessary to power the transducers. This power supply is located in the Signal Conditioning Test Package.

D. RESISTOJET ENGINE SYSTEM

A flow diagram of the resistojet engine system is given in figure 45; also shown in table X are the manufacturer and model number of the major components. As indicated previously, three identical resistojets will be used for the test, two for attitude control (clockwise and counterclockwise rotation of the table in the horizontal plane) and one for station keeping.

1. Resistojet Assembly

Referring to figure 45 each of the three resistojet assemblies consists of a control valve for pulsing the ammonia flow, a pressure transducer, a resistojet heater element and exit nozzle, and a photocell for resistojet temperature measurement.

A resistojet assembly drawing is presented in figure 5 and a photograph of the resistojet engine is shown in figure 6 of Section II. Referring to figure 5

the volume between the propellant control valve and the heater element has been held to a minimum to increase the transient response of the resistojet. The propellant valve, pressure transducer, and heater tube are all connected to the main thrustor body. The heater element is surrounded by a concentric heater support. The heater support serves to provide a stable surface to which the resistojet leads at the end of the nozzle can be connected, and also serves to protect the relatively fragile heater tube against misalignment. The support tube is electrically insulated from the main thrustor body by a ceramic insulator. One electrical connection can thus be made to the heater support tube and the other to the main thrustor body.

The Eckel solenoid valve weighs only 0.017 pound and requires only 1.92 watts (0.08 amp at 24 volts dc) input power. The leakage rate of the valves as received is being measured using a helium leak detector. The leakage rate of the two valves which have been delivered is quite low with a typical value being 10^{-6} cm^3/hr for a 35 psi pressure differential across the valve. For comparison, a leakage of 1 gram of ammonia over a three year period is equivalent to 1.75×10^{-4} cm^3/hr.

A photo-diode is used to monitor the resistojet heater element temperature. Figure 46 shows a plot of detector response at a fixed bias voltage as a function of distance from the thrustor. The heater element is observed by the photo-diode through a 3/16 inch hole located in the heater support.

2. Ammonia Supply System

The ammonia supply system is illustrated in figure 47; a photograph of the complete assembly is shown in figure 48. The supply system, which will be mounted beneath the NASA, Lewis test bed, consists of a liquid ammonia tank and a gas reservoir. The pressure in the plenum or gas reservoir is controlled by means of a pressure switch and solenoid operated valve.

The ammonia liquid storage tank which has a volume of 775 ml has an ammonia capacity of about 1 pound of liquid ammonia at 70° F. Continuous operation of a resistojet engine for 10 hours at a nominal flow rate of 5×10^{-6} lbs/sec consumes only 0.18 lbs of fuel so that the storage tank provides a more than ample fuel reserve for the single axis test. The gas reservoir volume of 775 ml minimizes the number of cycles of operation required of the pressure switch and solenoid valve. For example, assuming the pressure switch operates between 24 and 26 psia, the resistojet engine can be pulsed about 15 times (4 second pulse) before the pressure drops from 26 to 24 psia and the pressure regulating switch and valve operate.

TABLE X

MANUFACTURE AND MODEL NUMBER OF MAJOR PURCHASED COMPONENTS

Symbol	Description	Source
P1	Pressure Transducer, PA208TC, Range 0-250 psia	Statham Instr. Inc. Los Angeles 64, Calif.
P2	Pressure Transducer, PA208TC, Range 0-50 psia	Statham Instr. Inc. Los Angeles 64, Calif.
P3, P4, P5	Pressure Transducer, PA222TC, Range 0-50 psia	Statham Instr. Inc. Los Angeles 64, Calif.
V1	Pressure Regulating Valve, No. B2DA9175 Two-way Solenoid Valve	Skinner Electric Valve Div. New Britain, Conn.
V2, V3, V4	Solenoid Operated Valve, No. AF70C-37 Norm. Closed Type "E" Ends	Eckel Valve Co. San Fernando, Calif.
T1,T2,T3,T4	4K 1SO Curve Bead Thermistor Assembly	Fenwal Electronics, Inc. Framingham, Mass.
DP1,DP2,DP3	Differential Pressure Transducer, PL283TC, Range 0-1 psia	Statham Instr. Inc. Los Angeles 64, Calif.
RT1, RT2, RT3,	Type IN2175 N-P-N Diffused Silicon Photo-Duo-Diode	Texas Instr. Inc. Dallas 22, Texas

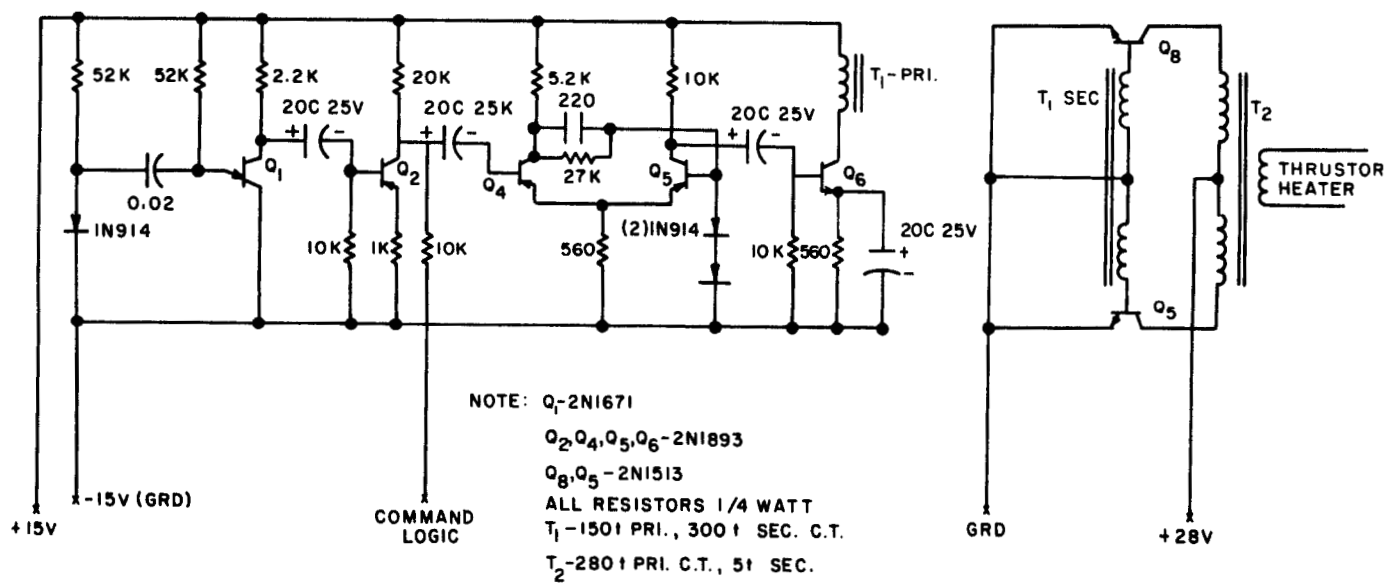

65-2585

Figure 44 INVERTER CIRCUIT FOR THE STATION KEEPING RESISTOJET HEATERS

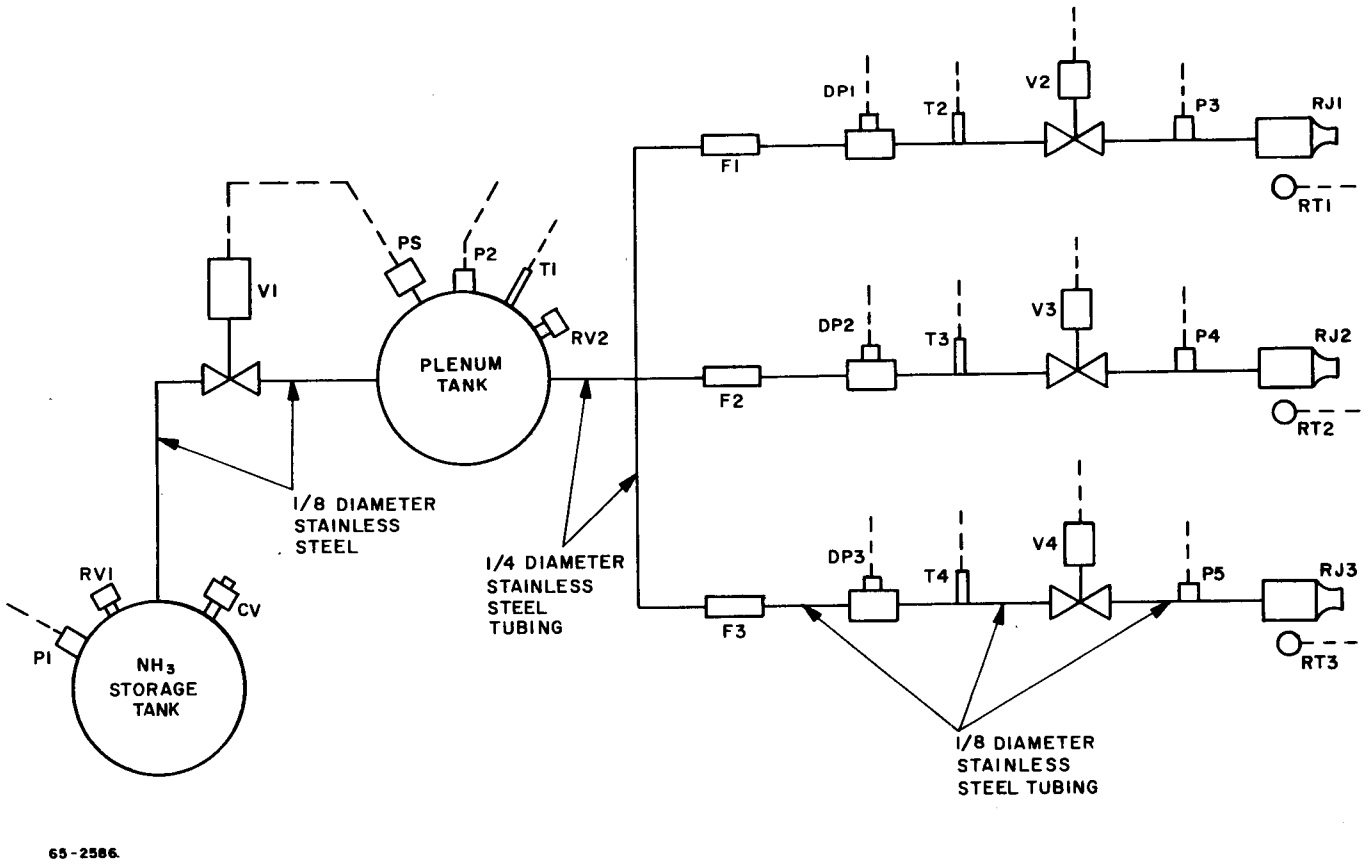

Figure 45 SCHEMATIC DIAGRAM OF THE RESISTOJET AMMONIA FLOW SYSTEM

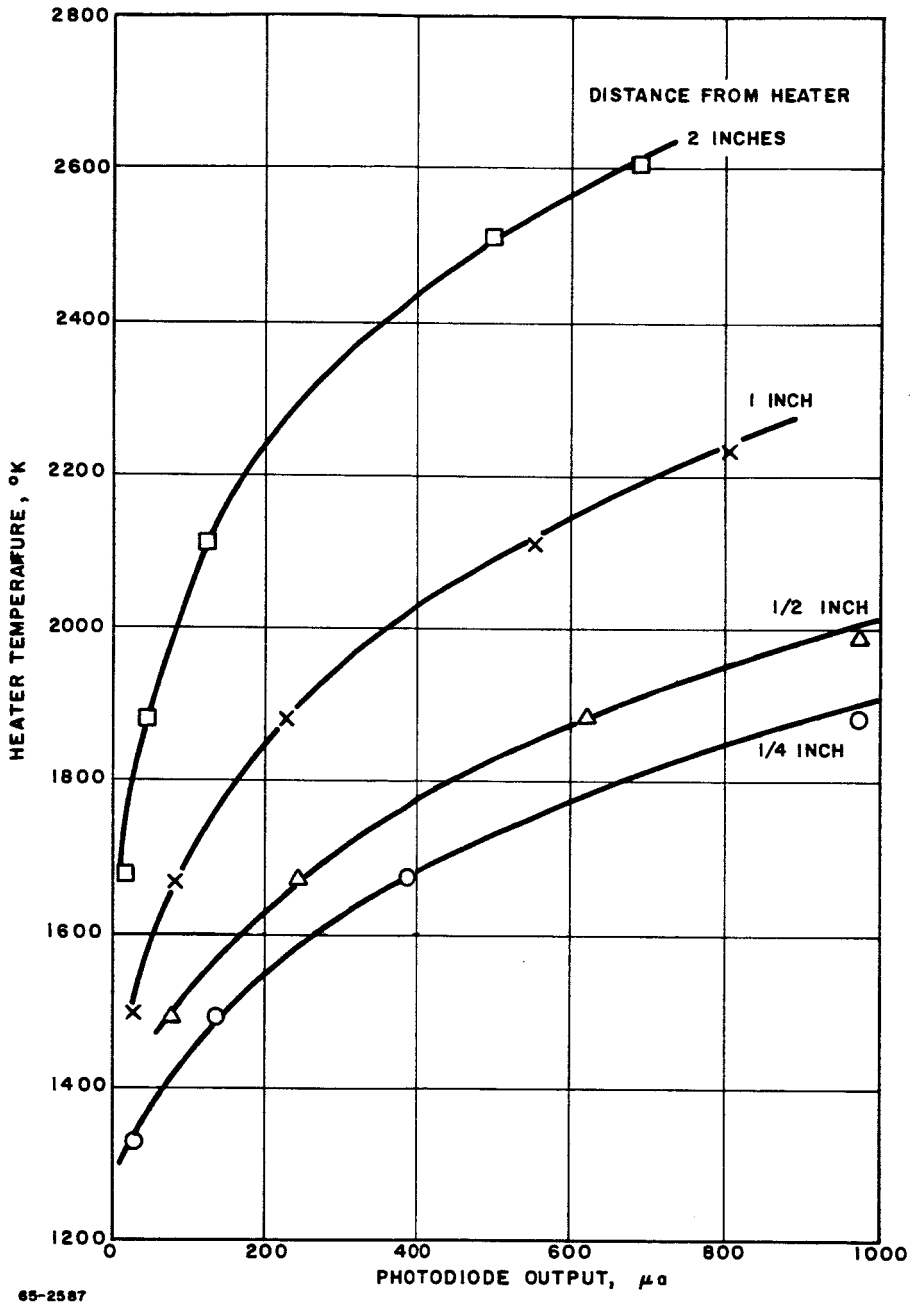

Figure 46 PHOTODIODE RESPONSE VERSUS RESISTOJET HEATER TEMPERATURE

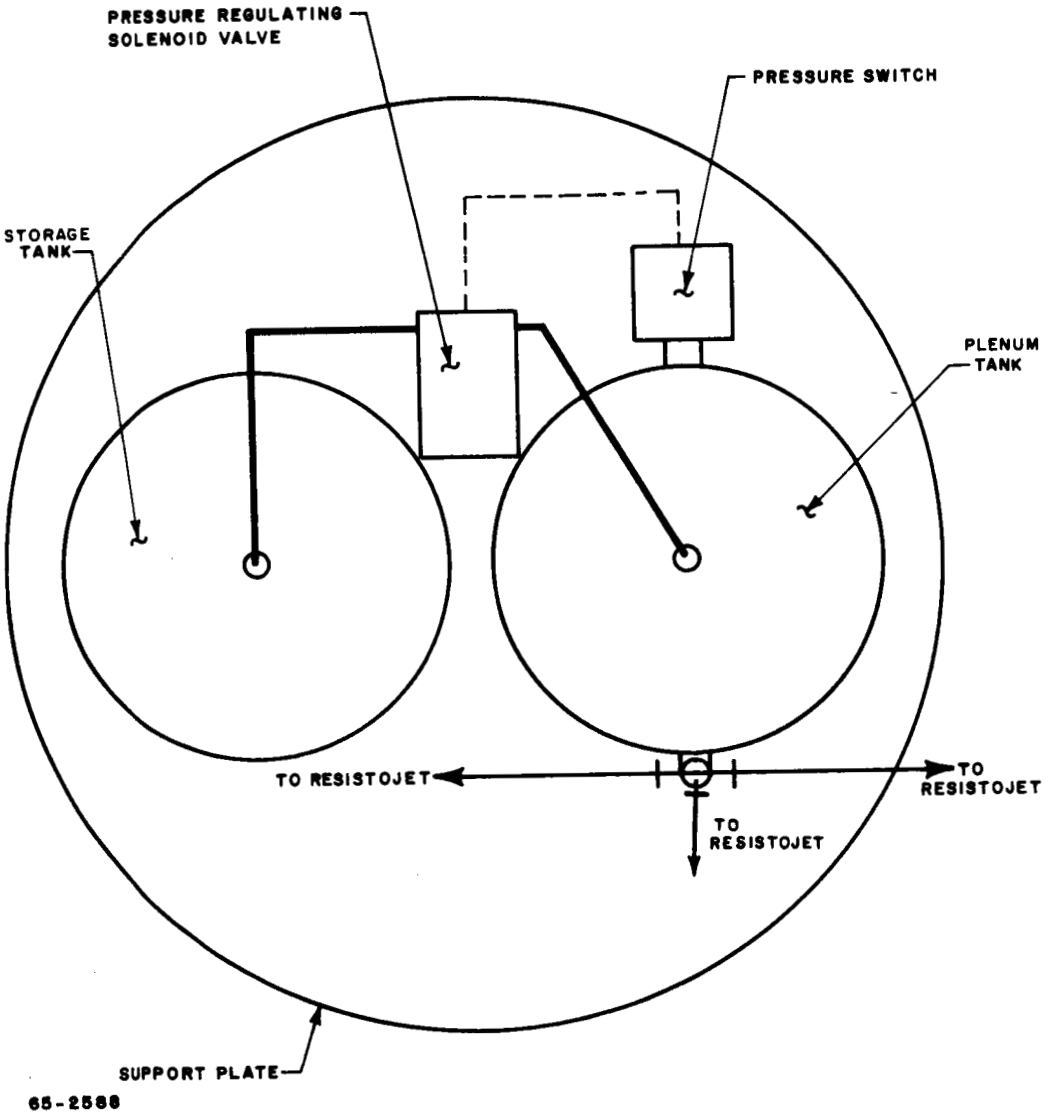

Figure 47 AMMONIA SUPPLY SYSTEM ASSEMBLY

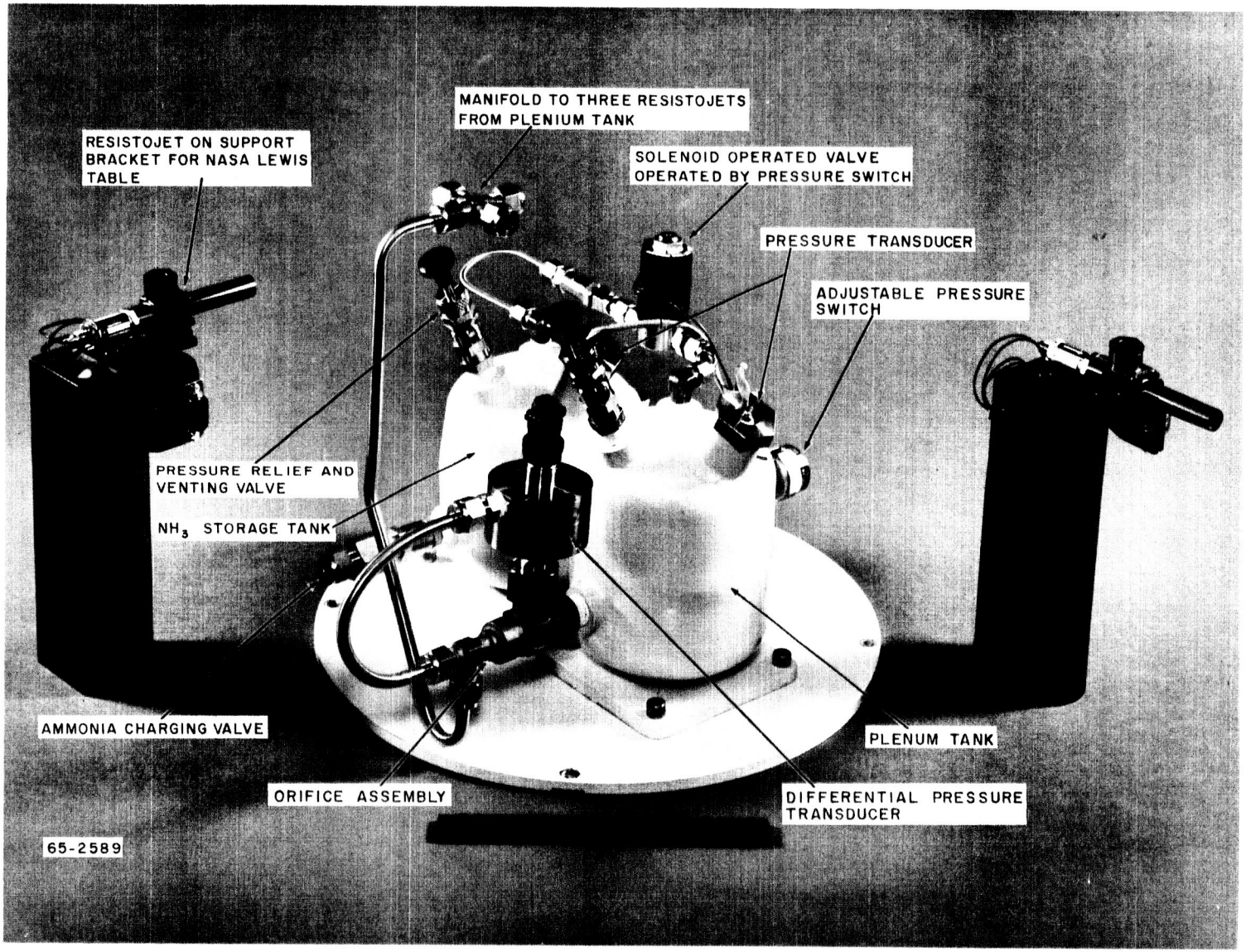

Figure 48 PHOTOGRAPH OF AMMONIA SUPPLY SYSTEM

Both the liquid and gas storage tanks have a combination pressure relief and venting valve; the liquid ammonia storage tank has a check valve for ease in tank charging. The stainless steel tubing between the ammonia gas reservoir and the filter flowmeter assembly is 1/4 inch diameter.

The filter-flowmeter assembly is illustrated in figure 49. The filter, a sintered stainless steel plug, is located upstream of the flowmeter to prevent plugging of the system downstream of this point. The filter will stop any particulates with a size larger than about 10 microns.

The flowmeter consists of a 10 mil diameter sharp-edged orifice located immediately downstream of the filter. The pressure drop is measured with a differential pressure transducer. The orifice size has been selected so that the pressure drop across the orifice is small e.g. 0 to 1 psia, relative to the plenum pressure, and so that the ammonia flow is choked across the exit nozzle rather than across the orifice. A thermistor is located immediately upstream of the flow orifice in order to measure the ammonia inlet temperature.

E. SIGNAL CONDITIONING PACKAGE

The signal conditioner test package is connected to the NASA telemetry package. Both the signal conditioner test package and the NASA telemetry package are located on the air bearing test bed. The NASA telemetry package, which is located on the test bed, receives command signals from a transmitter and transmits data signals from the test bed to a receiver. Both the command transmitter and signal receiver are located away from the proximity of the test tank. In this manner actual space flight test conditions are thus simulated as closely as possible in the laboratory.

For convenience the power conditioning unit for the station-keeping resistojet thrustor has been included in the signal conditioning test package.

1. Telemetry Command Channels

Eight telemetry command on-off channels will be used for the single axis resistojet attitude control system test. When a command channel on-off switch is turned on at the telemetry transmitter console (located outside the tank) a signal is transmitted to the test bed telemetry receiver. The test bed receiver passes this signal to the signal conditioner test package to which it is connected. The test bed receiver delivers 24 volt on-off command signals to the signal test package.

The functions of the 8 individual on-off command channels are indicated in Table XI.

TABLE XI

COMMAND CONTROL CHANNELS FOR THE RESISTOJET SINGLE AXIS TEST

	*	
Command Channel No. 1	(4)	Table Power On
Command Channel No. 2	(5)	Table Power Off
Command Channel No. 3	(1)	Table Clockwise Slew
Command Channel No. 4	(2)	Table Counterclockwise Slew
Command Channel No. 5	(7)	Station Keeping Thrustor On
Command Channel No. 6	(8)	Station Keeping Thrustor Off
Command Channel No. 7	(6)	Close Three Propellant Valves
Command Channel No. 8	(3)	Table on Automatic Control

*Actual pin numbers in plug number 206 J-1DD50S are indicated in parentheses.

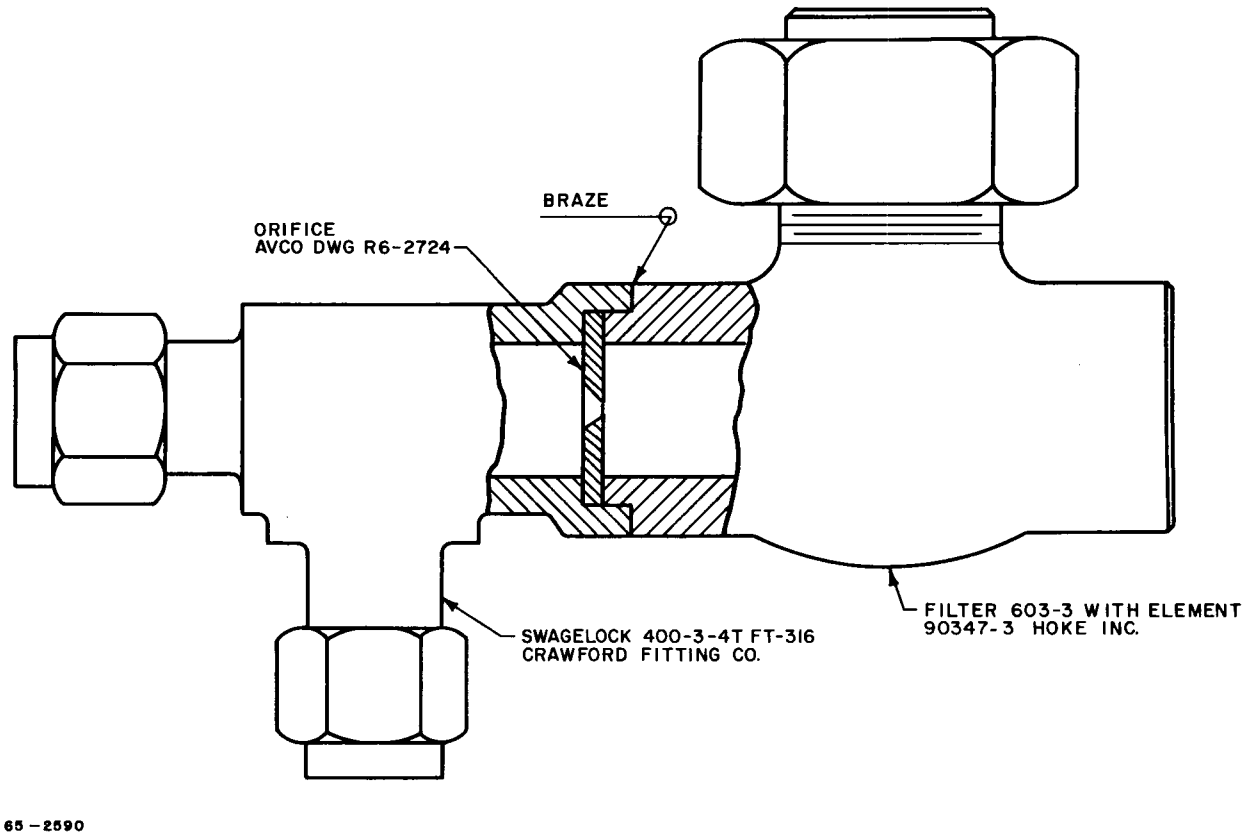

Figure 49 SCHEMATIC DIAGRAM OF FILTER FLOWMETER ASSEMBLY

The clockwise slew (channel no. 3), counterclockwise slew (channel no. 4), the close three propellant valves (channel no. 7) and table on automatic control (channel no. 8) are interconnected and operate in the following fashion.

The clockwise (channel no. 3) and counterclockwise (channel no. 4) slew commands remove the optical sensor and preamp from the control logic circuit and replace the preamp output with a 1.5 volt or a -1.5 volt signal depending on the desired direction of rotation.

The automatic control command (channel no. 8) connects the optical sensor and preamp to the logic circuitry and applies power to the valve solenoid and resistojet heater control portion of the control logic circuit. The table power on-off commands (channel no. 1 and channel no. 2) operate a latching relay which controls all table power.

The station keeping thrustor on-off commands (channel no. 5 and channel no. 6) operate a latching relay which provides a voltage sufficient to start and stop the thrustor operation.

2. Telemetry Data Transmission Channels

The on-board telemetry transmitter provides 9 continuous telemetry channels. The input to one of the continuous channels is a 43 channel commutator manufactured by Fifth Dimension, Inc. and supplied by NASA, Lewis. The commutator sends a signal from each of its 43 input channels every 1/2 second; thus, the commutator permits sampling of each of the input signals at 1/2 second intervals.

During the initial resistojet single axis attitude control system test use will be made of 8 continuous channels and 16 intermittent or commutated channels. The signals passing into the commutated channels, as indicated above, will be sampled every 1/2 second.

A basic instrumentation diagram is shown in figure 50, and a list of the telemetry data transmission channels is presented in table XII. Briefly, each of the individual engines is monitored by 6 data channels (or a total of 18 channels for the engines), the propellant supply is monitored by 3 channels, and the angular position and rate of the vehicle are monitored by 3 channels. Thus, a total of 24 channels of information will be transmitted from the vehicle; 8 of these channels will be continuous and 16 will be intermittent.

As indicated in table XII all the signals received at the laboratory telemetry receiver are recorded on tape (T). Some of the signals can also be immediately read out on a panel meter (M), or on a pen recorder (R) for possible diagnostics during a test.

TABLE XII

TELEMETRY DATA TRANSMISSION CHANNELS

Channel No.	Commutated Channel No.	Channel Identification	Description	Channel	Range	Telemetry Output	Instrumentation
1		V_1	Sensor Preamplifier Output (Fine)	C	0-0.5°	-2.5V to +2.5V	T, R
2		V_3	Total Error Signal	C	0-0.05/sec	0-5V	T, R
3		V_4	Valve Actuation Signal (Clockwise Rotation)	C	28 VDC	0-5V	T
4		V_5	Valve Actuation Signal (C-Clockwise Rotation)	C	28 VDC	0-5V	T
5		P_3	Nozzle Box Pressure (Clockwise Rotation)	C	0-50 psi	0-5V	T, R
6		P_4	Nozzle Box Pressure (C-Clockwise Rotation)	C	0-50 psi	0-5V	T, R
7		DP_1	ACS Clockwise Rotation Differential Pressure (Flow)	C	0-1 psi	0-5V	T, M
8		DP_2	ACS Counterclockwise Rotational Differential Pressure (Flow)	C	0-1 psi	0-5V	T, M
9	38	P_1	Ammonia Tank Pressure	I	0-250 psi	0-5V	T, M
10	39	P_2	Plenum Pressure	I	0-50 psi	0-5V	T, M
11	33	T_1	Plenum Temperature	I	0-100°F	0-5V	T, M
12	43	DP_3	ACS Station Keeping Differential Pressure (Flow)	I	0-1 psi	0-5V	T

TABLE XII (Concl'd)

Channel No.	Commutated Channel No.	Channel Identification	Description	Channel	Range	Telemetry Output	Instrumentation
13	34	T_2	Ammonia Line Temperature (Clockwise Rotation)	I	0-100°F	0-5V	T
14	35	T_3	Ammonia Line Temperature (C-Clockwise Rotation)	I	0-100°F	0-5V	T
15	36	T_4	Ammonia Line Temperature (Station Keeping)	I	0-100°F	0-5V	T
16	40	P_5	Nozzle Box Pressure (Station Keeping)	I	0-50 psi	0-5V	T, R
17	41	RT_1	Resistojet Temperature (Clockwise Rotation)	I	1000-1700°K	0-5V	T, M
18	42	RT_2	Resistojet Temperature (C-Clockwise Rotation)	I	1000-1700°K	0-5V	T, M
19	31	RT_3	Resistojet Temperature (Station Keeping)	I	1000-1700°K	0-5V	T
20	4	V_2	Sensor Preamplifier Output (Coarse)	I	0-5°	-2.5V to+2.5V	T, R
21	8	V_6	Valve Actuation Signal (Station Keeping)	I	28 VDC	0-5V	T
22	7	V_7	Resistojet Heater Voltage CW	I	2 VDC	0-5V	T, M
23	6	V_8	Resistojet Heater Voltage CCW	I	2 VDC	0-5V	T, M
24	5	V_9	Resistojet Heater Voltage Station Keeping	I	2 VDC	0-5V	T

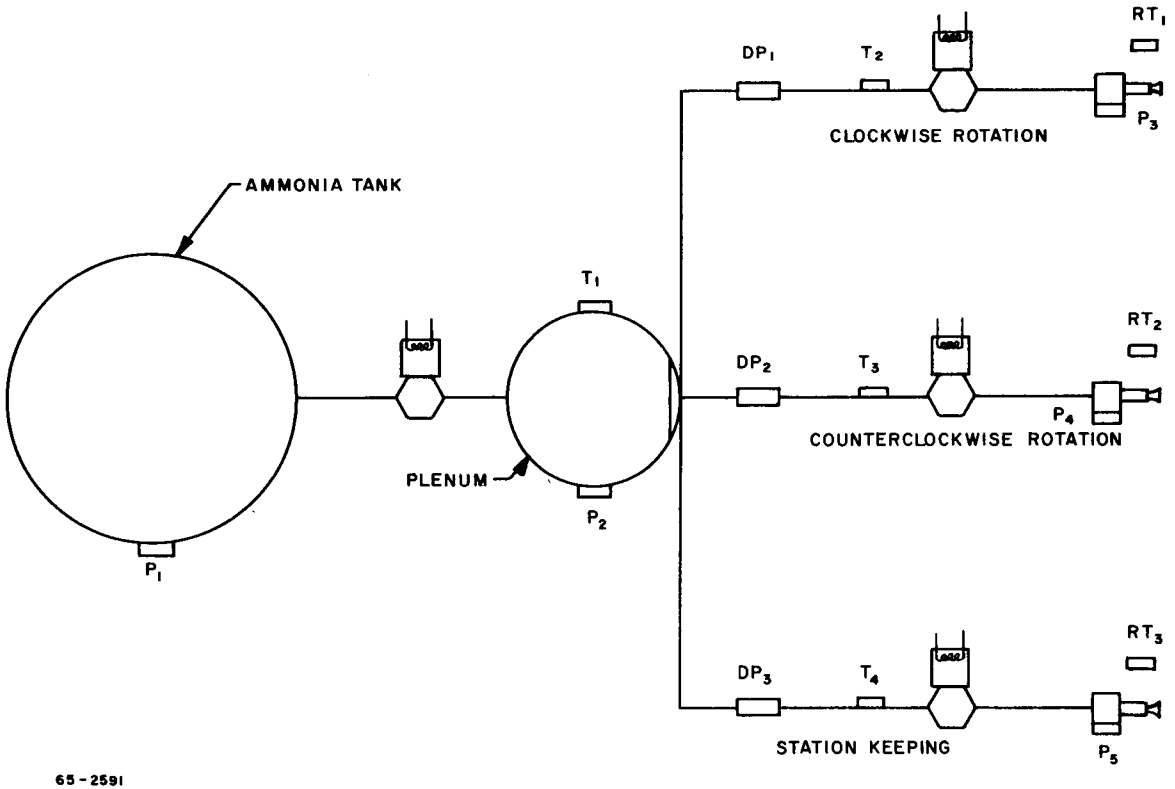

Figure 50 BASIC INSTRUMENTATION DIAGRAM

The eight continuous (C) channels are used to measure the following quantities: 1 - the sensor pre-amplifier output indicating the test bed position (fine control); 2 - the control logic output indicating the test bed total error; 3, 4 - the valve actuation signals for the attitude control engines; 5, 6 - the nozzle box pressure for the attitude control engines; 7, 8 - the mass flow rate for the attitude control engines.

The sixteen intermittent channels are used to measure the following quantities: 9 - ammonia liquid reservoir pressure; 10, 11 - ammonia gas plenum pressure and temperature; 12 - the mass flow rate for the station keeping thrustor; 13, 14, 15 - ammonia line temperatures for the three resistojet engines; 16 - nozzle box pressure for the station keeping thrustor; 17, 18, 19 - heater temperature for the resistojet engines; 20 - the sensor preamplifier output indicating the test bed position (coarse control); 21 - valve actuation signal for the station keeping thrustor; 22, 23, 24 - heater voltages for the three resistojet engines.

Signal conditioning circuitry is provided to convert the transducer, position sensor and rate sensor signals into voltage signals in the 0 to 5 volt range suitable for transmission by the test bed telemetry package. Five voltage dividers are used to provide the 0 to 5 volt actuation signals from the three (3) solenoid valves and the coarse and fine position sensors. Three (3) ac amplifiers are provided to amplify the heater voltage signals, and finally, sixteen dc amplifiers are provided to amplify the engine pressure transducer signals (3), the engine temperature sensor signals (3), the engine line temperature sensor signals (3), the engine flow rate sensor signals (3), the ammonia liquid storage pressure sensor (1), the ammonia gas pressure and temperature sensors (2), and the total table error signal (1).

A photograph of the signal conditioner test package is shown in figure 51.

3. Check-out Console

A check-out console has been designed and built to provide a means for determining whether or not the control logic and instrumentation electronic circuitry is functioning properly before the attitude control system is placed on the air bearing in the test tank. A manual describing the operation of the check-out console will be forwarded separately to NASA, Lewis.

F. DESCRIPTION OF THE SINGLE AXIS RESISTOJET ATTITUDE CONTROL SYSTEM - MODEL II

As indicated previously the basic purpose underlying the initial single axis resistojet attitude control system test has been to demonstrate the feasibility of

applying the resistojet concept to the attitude control and station keeping of satellites. Electrical and mechanical interfaces involved in utilization of a resistojet attitude control system on the NASA, Lewis air bearing test bed have been resolved. During the course of development and construction of the Model I Resistojet Single Axis Attitude Control System, a number of small modifications which will make the Model I system more flexible for test purposes have become apparent. The modifications to the Model I system are of such a nature that no changes are required in the physical dimensions of either the control logic test package or the signal conditioner test package; and only minor changes (involving the utilization of presently unused pin connections) are involved in the electrical harness. The changes which will be incorporated into the Model II system are indicated below:

1. The resistojet heater power supplies will be modified so that for a given test the input power can be manually varied to different settings between 5 and 35 watts. This modification will permit operation of different power level thrustors.

2. A manually adjustable pressure control valve will be placed on the gas reservoir tank so that the engine pressure can be varied over the range from 2 to 30 psia. This adjustment will permit operation of a specific resistojet engine over more than an order of magnitude range in thrust level.

3. Provision will be made in the control logic circuit so that the heater warm-up time, (defined as the time period between power-on time and propellant-on time), can be manually varied before a run to time periods of from 0 to 10 seconds.

4. Provision will be made in the control logic package to manually adjust before a run the constant pulse length associated with the inner control lines to time periods of from 1 to 5 seconds.

5. Minor changes will be made to the light sensor electronics so that the system can acquire automatically from angles greater than the present 8 degree limit.

It is important to note that items 1 through 5 involve no changes in the electrical harness connections, but only involve internal electrical changes within the signal conditioning and control logic test packages.

6. Provision will be made to measure the ac current into two (2) resistojet attitude control engines, and the dc voltage and dc current inputs to the power conditioner. Data signals from these measurements will be transmitted on the commutator channel, and will involve wire connections to three presently unused commutator pin connections.

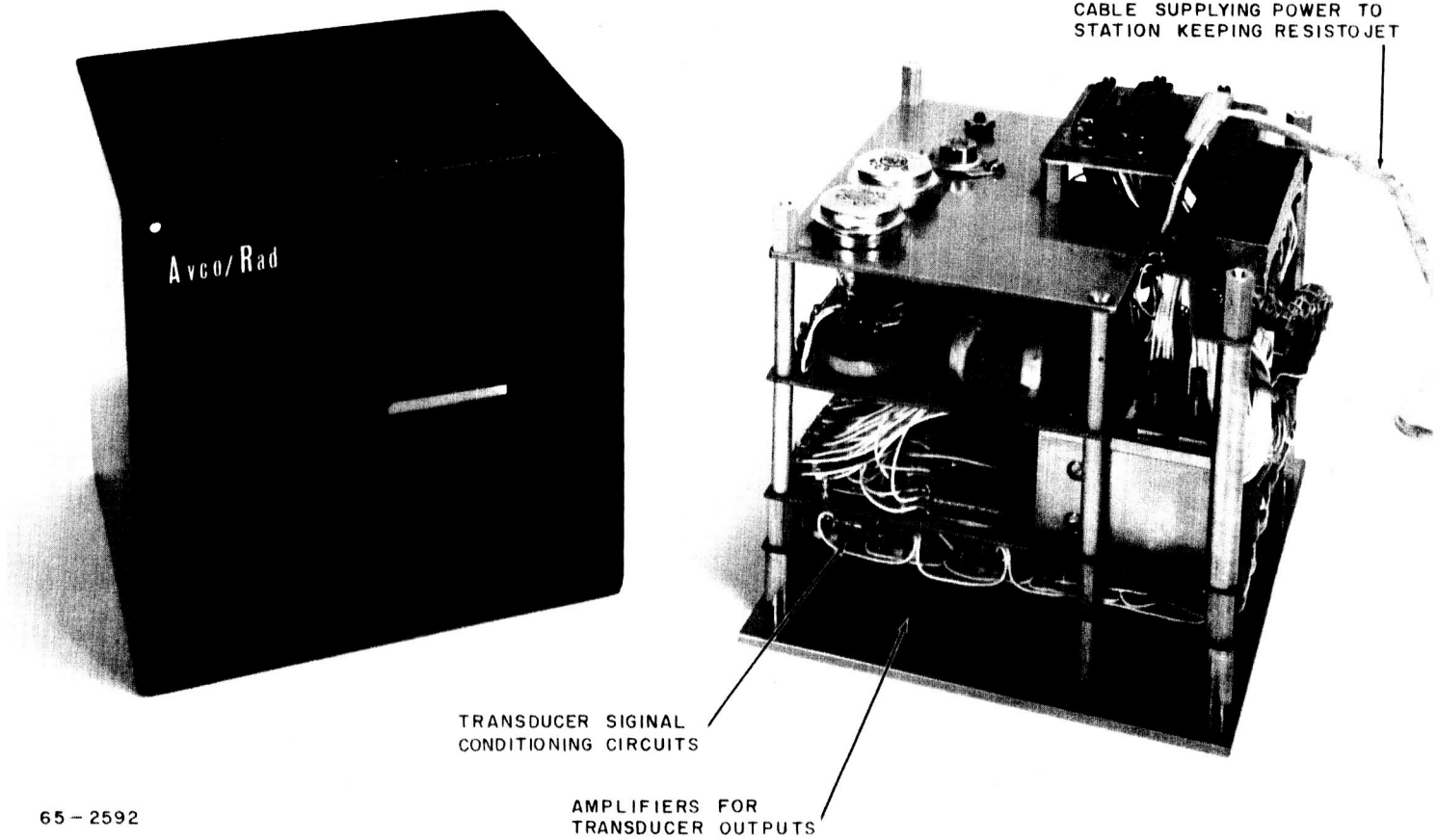

Figure 51 PHOTOGRAPH OF THE SIGNAL CONDITIONER TEST PACKAGE

IV. WEIGHT ESTIMATES FOR A FLYABLE ATTITUDE AND ORBIT CONTROL SYSTEM

Work on the preliminary design of a resistojet attitude control and station keeping system for a 500 lb synchronous satellite is continuing. The characteristics of this vehicle have been described previously.[7] Emphasis is at present being placed on the conceptual design and weight estimates of the power conditioning equipment necessary to convert the power delivered from the solar panels into a form suitable for operation of the resistojet engines. Consideration is being given to the advantages and disadvantages of the inclusion of batteries in the power conditioning package. A study is also being made of possible control logic systems for satellite attitude control and the compatibility of these systems with the resistojet engine.

V. DIRECTION FOR FUTURE RESEARCH AND DEVELOPMENT

A. THRUST MEASUREMENT SYSTEM

The lower thrust measurement limit of the open loop string-in-tension thrust stand will be reduced to 10^{-5} pounds by further isolation of the thrust measurement system from low frequency background vibration. Installation of a 32 inch diffusion pump will permit semi-continuous engine operation at pressures less than 1 micron of Hg. A study will be completed on a comparison of a closed-loop and open-loop low thrust measurement systems.

B. RESISTOJET THRUSTOR DEVELOPMENT

1. Nozzle Performance

An experimental study will be carried out on the performance characteristics of hot and cold nozzles which operate in the thrust range from 10^{-5} to 10^{-3} pounds. The only systematic performance data in this thrust regime is the work of Tinling.[9] The study will involve an experimental comparison of actual and ideal nozzle performance as a function of the following parameters: a) nozzle throat diameter (5 to 25 x 10^{-3} inches); b) nozzle area ratio (1 to 1, 10 to 1, and 100 to 1); c) nozzle chamber pressure (1 to 50 psia) and back pressure (1 to 100 x 10^{-3} mm of Hg); and d) nozzle temperature. Measurements will be made of nozzle thrust, chamber pressure, and mass flow rate.

2. Heater Performance

A systematic experimental study will be made on the effect of the length and diameter of fast heat-up heaters on the main heat transfer coefficient and the efficiency of energy conversion from electric input power to gas power. The experimental study will include measurement of the time for heat-up and measurement of heater resistance as a function of temperature and geometry. The heater warm-up time and heater resistance are, as indicated previously, important parameters in the design of the control logic circuitry and power conditioning equipment.

Thermal cycling experiments will be continued on potential heater materials. Emphasis will be placed on the fabrication of the individual heater elements out of vapor-deposited tungsten. Experiments will be carried out on the effect of wall thickness on thrustor life.

3. Engine Design

Studies will be continued on an investigation of possible engine configurations for the fast heat-up resistojet. Emphasis will be placed on the development of low power loss current connections.

4. Resistojet Engine Concepts

The basic fast heat-up resistojet concept will be reviewed; the thrust, specific impulse and electric to thrust power conversion efficiency limitations of the fast heat-up engine will be established. Exploratory studies will be carried out on other resistojet concepts, and studies will be carried out on propellants other than ammonia for possible application to other thrust regimes.

C. SINGLE AXIS ATTITUDE CONTROL SYSTEM

The initial single axis resistojet attitude control system (Model I) will be evaluated on the air bearing at the NASA, Lewis Electric Propulsion Test Facility.

A modified resistojet attitude control system (Model II), which has provision for manually adjusting the tank pressure, heater power level, heater warm-up period, and pulse length, will be delivered to NASA, Lewis by 1 May. The Model II resistojet attitude control system is identical to the Model I system in terms of electrical and mechanical interfaces; therefore, the Model II system can be used on the air bearing table with a minimum set-up period. The Model II system will make it possible to check out a variety of resistojet engine designs and resistojet control logic concepts.

D. DESIGN OF A THREE AXIS PROTOTYPE STATION KEEPING AND ATTITUDE CONTROL SYSTEM

Preliminary layouts for a three axis attitude control and station keeping system will be initiated. Emphasis will be placed on the establishment of power requirements and on estimating the weight of the necessary power conditioning equipment. A study will be made of possible control logic circuitry and the compatibility of the control logic circuitry with the resistojet concept.

VI. REFERENCES

1. Tobias, I., and R. Kosson, Application of Electrothermal Arc Jets to a Manned Orbiting Research Laboratory, 1st AIAA Annual Meeting, June 29-July 2, 1964, AIAA Preprint No. 64-499.

2. Geideman, W., Muller, K., and J.W. Rosenbery, Development Status of Low Power Arc Jet Engines and Their Applicability to Near Future Space Missions 1st AIAA Annual Meeting, June 29 - July 2, 1964 AIAA Preprint No. 64-502.

3. Boucher, R.A., Electrical Propulsion for Control of Stationary Satellites, Journal of Spacecraft and Rockets, March-April, 1964 Vol. 1, Number 2, p. 164-169.

4. Molitor, J.H., Ion Propulsion System for Stationary-Satellite Control, Journal of Spacecraft and Rockets, March-April, 1964 Vol. 1, Number 2, p. 170-175.

5. Bennett, S., Connors, J.F., and K.E., Clark, Development of a 3-Kilowatt Resistojet, AIAA Fourth Electric Propulsion Conference, Philadelphia, Penn. August 31 - September 2, 1964, AIAA Preprint No. 64-672.

6. Jack, J., and E. Spisz, "NASA Research on Resistance Heated Hydrogen Jets," AIAA Electric Propulsion Conference, AIAA Preprint 63-023 (March 1963).

7. Resistojet Research and Development - Phase II, First Quarterly Progress Report, Avco RAD SR-64-290, November 25, 1964.

8. Summerfield, M., The Liquid Propellant Rocket Engine in High Speed Aerodynamics and Jet Propulsion, Vol. XII, Jet Propulsion Engines, Princeton University Press, Princeton, New Jersey. 195 p. 446-447.

9. Tinling, B.E., Measure Steady-State Performance of Water Vapor Jets for Use in Space Vehicle Attitude Control Systems, NASA Technical Note D-1302. May 1962, Ames Research Center.

10. NASA, Ames, Personal Communication, February, 1965.

11. Vaeth, James E., "Vapor Jet Control of Space Vehicles," IRE Transactions on Automatic Control, 1962.

12. Gaylord, R.S. and Keller, W.H., "Attitude Control System Using Logically Controlled Pulses." ARS Preprint No. 1921-61.

DISTRIBUTION

Addressee	No. of Copies
NASA-Lewis Research Center 21000 Brookpark Road Cleveland, Ohio 44135	
Attention: J. H. Childs	1
R. J. Rulis	3
H. Gold	1
R. Cybulski	1
NASA Headquarters FOB - 10B 600 Independence Avenue, Northwest Washington, D. C. 20546	
Attention: RNT/J. Lazar	1
RNT/J. Mullen	1
NASA-Lewis Research Center 21000 Brookpark Road Cleveland, Ohio 44135	
Attention: J. H. DeFord	1
H. R. Hunczak	2
J. Jack	1
N. Musial	1
Reports Control Office	1
Technology Utilization Office	1
Library	1
NASA Scientific and Technical Information Facility Box 5700 Bethesda, Maryland 20014	
Attention: RQT-2448/NASA Representative	6
NASA Marshall Space Flight Center Huntsville, Alabama 35812	
Attention: Library	1
R-RP-DIR/G. Heller/Bldg. 4481	1
R-RP-DIR/Dr. E. Stuhlinger	1
R-RP-T/W. Jones/Bldg. 4488	1
MS-T/Dan Gates/Bldg. 4488	1
NASA-Ames Research Center Moffett Field, California 94035	
Attention: Library	1
DR. G. Goodwin	1